

LEGIBILITY NOTICE

A major purpose of the Technical Information Center is to provide the broadest dissemination possible of information contained in DOE's Research and Development Reports to business, industry, the academic community, and federal, state and local governments.

Although a small portion of this report is not reproducible, it is being made available to expedite the availability of information on the research discussed herein.

BNL--52204

DE90 000886

OPTIMIZATION OF THE FACTORS THAT ACCELERATE LEACHING

TOPICAL REPORT

**M. Fuhrmann, R.F. Pietrzak, E.M. Franz,
J.H. Heiser III, and P. Colombo**

March 1989

**NUCLEAR WASTE RESEARCH GROUP
DEPARTMENT OF NUCLEAR ENERGY
BROOKHAVEN NATIONAL LABORATORY
ASSOCIATED UNIVERSITIES, INC.
UPTON, LONG ISLAND, NEW YORK 11973**

**Prepared for the
UNITED STATES DEPARTMENT OF ENERGY
NATIONAL LOW-LEVEL WASTE MANAGEMENT PROGRAM
UNDER CONTRACT NO. DE-AC02-76CH00016**

MASTER

DISTRIBUTION OF THIS DOCUMENT IS UNLIMITED

EB

DISCLAIMER

This report was prepared as an account of work sponsored by an agency of the United States Government. Neither the United States Government nor any agency thereof, nor any of their employees, nor any of their contractors, subcontractors, or their employees, makes any warranty, express or implied, or assumes any legal liability or responsibility for the accuracy, completeness, or usefulness of any information, apparatus, product, or process disclosed, or represents that its use would not infringe privately owned rights. Reference herein to any specific commercial product, process, or service by trade name, trademark, manufacturer, or otherwise, does not necessarily constitute or imply its endorsement, recommendation, or favoring by the United States Government or any agency, contractor or subcontractor thereof. The views and opinions of authors expressed herein do not necessarily state or reflect those of the United States Government or any agency, contractor or subcontractor thereof.

Printed in the United States of America
Available from
National Technical Information Service
U.S. Department of Commerce
5285 Port Royal Road
Springfield, VA 22161

NTIS price codes:
Printed Copy: A08; Microfiche Copy: A01

TABLE OF CONTENTS

	Page
EXECUTIVE SUMMARY	xvii
1. INTRODUCTION	1
2. MATERIALS AND METHODS	3
2.1 Waste Form Types	7
2.1.1 Portland I Cement Containing Sodium Sulfate as Simulated Waste	7
2.1.2 Portland I Cement Containing Incinerator Ash as Simulated Waste	7
2.1.3 Vinyl Ester-Styrene Containing Sodium Sulfate as Simulated Waste	7
2.1.4 Bitumen Containing Sodium Tetraborate as Simulated Waste	8
2.2 Preparation of Samples	8
2.3 Leaching Tests	9
2.4 Analytical Methods	9
2.4.1 Radiochemical Analysis	10
2.4.2 Elemental Leachate Analysis	10
2.4.3 Alkalinity Measurements	10
2.4.4 pH Measurements	10
2.4.5 SEM/EDS	10
3. LEACHING MECHANISMS AND MODELS	11
3.1 Introduction	11
3.2 Methods of Presenting Leaching Data as a Function of Time	11
3.2.1 Tabular and Graphical Methods	11
3.2.2 Empirical Equations	13
3.2.3 Mathematical Solutions to Mass Transport Equations	13
3.2.3.1 Analytical Solutions for Diffusion	14
3.2.3.2 Concentration Dependent Diffusion	16
3.2.3.3 Skin Effects of Sample Surface	17
3.2.3.4 Diffusion + Reaction (K_d)	17
3.2.3.5 Anomalous Transport	18
3.2.4 Numerical Solutions to the Transport Equations	19
3.2.5 Temperature Effects and the Arrhenius Equation	20
3.3 Application of Modeling Techniques	21
3.3.1 Modeling Releases from Cement	21
3.3.1.1 Diffusion Coefficient (D_e) Calculated from the Semi-Infinite Model	21

TABLE OF CONTENTS - continued

	Page
3.3.1.2 The Finite Cylinder Model	22
3.3.1.3 Effects of Leaching Conditions	23
3.3.2 Vinyl Ester-Styrene + Sodium Sulfate	30
3.3.3 Bitumen	31
3.4 Summary	31
4. PORTLAND CEMENT CONTAINING SODIUM SULFATE AS SIMULATED WASTE	35
4.1 Introduction	35
4.2 Modeling and Mechanisms of Leaching	36
4.3 Single Factors that Accelerate Leaching	42
4.3.1 Temperature	42
4.3.1.1 Portland Cement Paste	43
4.3.1.2 Portland Cement Plus 5 wt% Sodium Sulfate	45
4.3.2 Specimen Size	49
4.3.3 Volume of the Leachant	49
4.4 Combined Acceleration Factors for Portland Cement Containing Sodium Sulfate	50
4.4.1 Cs-137 Results	50
4.4.2 Sr-85 Results	60
4.5 Conclusions	67
5. PORTLAND CEMENT CONTAINING INCINERATOR ASH	69
5.1 Introduction	69
5.2 Modeling and Mechanisms of Leaching	69
5.3 Single Factors that Accelerate Leaching	76
5.3.1 Temperature	76
5.3.2 Size	79
5.3.3 The Volume of Leachant	80
5.4 Combined Acceleration Factors	80
5.4.1 Cs-137 Results	81
5.4.2 Sr-85 Results	87

TABLE OF CONTENTS - continued

	Page
5.5 Conclusions	95
6. ASPHALT (BITUMEN)	97
6.1 Introduction	97
6.2 Effect of Single Factors on the Leaching of the Bitumen	97
6.3 Waste Loading	100
6.4 Mechanisms of Leaching	106
6.5 Modeling	114
6.6 Conclusions	115
7. VINYL ESTER-STYRENE CONTAINING SODIUM SULFATE SALT	117
7.1 Introduction	117
7.2 Modeling and Mechanisms of Leaching	117
7.3 Single Factors that Accelerate Leaching	121
7.3.1 Temperature	121
7.3.2 Size	122
7.3.3 Volume of Leachant	122
7.4 Combined Acceleration Factors	123
7.5 Conclusions	129
8. CONCLUSIONS	131
8.1 Leaching Cement Containing Sodium Sulfate	131
8.2 Portland Cement Containing Incinerator Ash	131
8.3 Bitumen Containing Sodium Tetraborate	132
8.4 Vinyl Ester-Styrene Containing Sodium Sulfate	132
REFERENCES	135

LIST OF FIGURES

		Page
Figure 3.1	A comparison of characteristic leach curves: Fickian, Sigmoid, Two-staged. After Crank [15]	19
Figure 3.2	Cs-137 CFL versus $t^{1/2}$ (in days ^{1/2}) from cement containing sodium sulfate leached in deionized water at 20°C	22
Figure 3.3	CFL of Sr-85 and Cs-137 versus time leached from cement containing 5 wt% sodium sulfate in deionized water at 20°C. The leachant was changed daily. Releases were modeled using the finite cylinder model	23
Figure 3.4	A comparison of some basic leaching techniques: Static, Semidynamic, and Flow tests	24
Figure 3.5	CFL of Sr-85 leached from cement containing 5 wt% sodium sulfate in deionized water at 20°C. A comparison of the effect of change in the leachant replacement schedule is shown	25
Figure 3.6	Cs-137 CFL versus time for cement containing 15 wt% incinerator ash at 20°C. The solid lines represent the finite cylinder model prediction with $D_e=6.0 \times 10^{-8}$ cm ² /s for the early results of 0 to 20 days and $D_e=1.0 \times 10^{-9}$ for the long-term results	26
Figure 3.7	CFL of Sr-85 versus time from cement containing 5 wt% sodium sulfate leached in deionized water at 20°C. A comparison of results was made between results for leachant volume to sample surface area ratios of 10/1, 30/1 and 50/1	27
Figure 3.8	Log (CFL x V/S) versus log t for Cs-137 from cement containing ion-exchange resin. Six sizes of cylindrical waste forms are compared after correction with V/S	28
Figure 3.9	Arrhenius plot of Log D_e versus 1/T for Cs-137 and Sr-85 leached from neat cement in deionized water	29
Figure 3.10	CFL versus time for Co-57 from vinyl ester-styrene containing 20 wt% sodium sulfate leached in deionized water at 20°C. The solid line represents the finite cylinder calculation	30
Figure 3.11	CFL versus time for Cs-137 leached from bitumen containing 0, 20, 30, and 40 wt% sodium tetraborate in deionized water at 20°C	31

LIST OF FIGURES - continued

		Page
Figure 4.1	Averages of triplicate data for three types of leach tests: ANS 16.1, semidynamic with daily leachant replacements, and flow-through tests. These data are plotted against the square root of time which produces a linear plot up to CFL=0.2 if diffusion is the leaching mechanism	36
Figure 4.2	The finite cylinder model fails to follow the Cs-137 release data for the semidynamic ANS 16.1 test (1), but does accurately model the data from the flow test (2)	38
Figure 4.3	Experimental data and model results for Cs-137 from experiments with daily leachant replacements and with the ANS 16.1 schedule of leachant replacement	39
Figure 4.4	Triplicate baseline data for Sr-85 are plotted against the square root of time. There is a change in leach rate after the first week of an ANS 16.1 test . . .	40
Figure 4.5	Modeling Sr-85 releases required two diffusion coefficients, one for the early portion of the experiment and one for long-term leaching. For the experiment with daily leachant replacements, the model fits with one diffusion coefficient	40
Figure 4.6	Data from three types of leach tests: ANS 16.1, semidynamic with daily leachant replacements, and flow-through tests. These data are plotted against the square root of time which produces a linear plot if diffusion is the leaching mechanism	41
Figure 4.7	CFL of Cs-137 from portland type I cement paste specimens leached at 20°, 30°, 40°, 50°, and 70°C	43
Figure 4.8	Arrhenius plot of the diffusion coefficients from portland cement paste containing Cs-137 and Sr-85, leached at 20°, 30°, 40°, 50°, and 70°C	44
Figure 4.9	CFL for Sr-85 from portland cement paste containing radioactive tracers at temperatures ranging from 20°C to 70°C	45
Figure 4.10	CFL for Cs-137 vs time from portland I cement containing 5 wt% sodium sulfate at 20°, 40°, 50°, and 60°C	46
Figure 4.11	Arrhenius plot of Cs-137 leached from cement containing 5 wt% sodium sulfate showing diffusion coefficients as a function of the reciprocal temperature in Kelvins. Experiments were conducted at 20°, 40°, 50°, and 60°C	47

LIST OF FIGURES - continued

		Page
Figure 4.12	Sr-85 cumulative fraction leached vs time from portland I cement containing 5 wt% sodium sulfate at 20°, 40°, and 50°C leached in deionized water . .	48
Figure 4.13	Arrhenius plot of Sr-85 showing diffusion coefficients as a function of the reciprocal temperature in Kelvins	48
Figure 4.14	Cs-137 cumulative fraction leached vs time from portland I cement containing 5 wt% sodium sulfate at waste form volume to surface area (V/S) ratios of 0.42, 0.85, and 1.85. Samples were leached in deionized water at 20°C	49
Figure 4.15	Curves are calculated from the finite cylinder model, using selected diffusion coefficients from Table 4.1 to show ranges of leaching obtained under different test conditions. Also shown are data points for the baseline leaching experiment run at 20°C in 1.3 liters of water	52
Figure 4.16	Data from the two experiments that gave the greatest amount of acceleration for Cs-137 are compared to the baseline data. Each point represents the average value of triplicate specimens	53
Figure 4.17	Average cumulative fraction release curves for Cs-137 show that leaching at 60°C is substantially lower than at 50°C during a semidynamic leach test . .	54
Figure 4.18	Leaching of Cs-137 is lower at 60°C than it is at 50°C in static leach tests of cement/sulfate waste forms	55
Figure 4.19	Leaching of sodium from cement/sulfate specimens is lower at 60°C than at 50°C in static leach tests	55
Figure 4.20	Leaching of potassium is lower at 60°C than at 50°C in static leach tests . . .	56
Figure 4.21	Data for Cs-137 from cement/sulfate specimens during static and semi-dynamic leach tests at 50° and 60°C. The solid lines are calculated from the finite cylinder model	57
Figure 4.22	Comparison of Cs-137 releases from small cement/sulfate specimens (2.5 x 2.5 cm) leached at 20°C and at 50°C in different leachant volumes. Cs-137 releases are relatively insensitive to leachant volumes	58
Figure 4.23	Data from a leach test using 2.5 x 2.5 cm cement/sulfate specimens at 50°C in 3 liters of water with daily leachant replacement. The finite cylinder model may be overestimating releases after CFL=0.65	59

LIST OF FIGURES - continued

		Page
Figure 4.24	Cs-137 results from the optimized accelerated leach test for cement/sulfate specimens are compared to results from the baseline test. The acceleration factor is approximately 18	59
Figure 4.25	Data from two sets of portland cement specimens containing 5 wt% sodium sulfate. The optimized accelerated test is indicated by the filled squares and has an acceleration factor of about 17 compared to the baseline data. The finite cylinder model result is shown as the line through the optimized test data	62
Figure 4.26	Releases of Sr-85 from cement/sulfate waste forms during two semidynamic experiments run at 60°C but having different leachant volumes. The finite cylinder model was used to generate the two curves shown	63
Figure 4.27	Sr-85 releases from cement/sulfate waste forms during static experiments at 50° and 60°C. The solid line is the result of the finite cylinder model for the first 6 days of leaching at 60°C	64
Figure 4.28	Cs-137 and Sr-85 leaching from static experiments that are CO ₂ -free or exposed to air	65
Figure 4.29	Calcium cumulative fraction leached at 20° and 50°C in static leach tests open to air and CO ₂ -free. Specimens are portland cement containing 5 wt% sodium sulfate	66
Figure 4.30	Alkalinity in leachate at 20° and 50°C in static tests open to air and CO ₂ -free	67
Figure 5.1	Cumulative fraction leached of Cs-137 plotted against the square root of time. If diffusion is the leaching mechanism then the plot should be linear to about 0.20 cumulative fraction release. After that, it should slowly curve down	70
Figure 5.2	Leaching of Cs-137 from cement/ash waste forms. The solid lines are calculated from the finite cylinder model	71
Figure 5.3	Comparison of Cs-137 releases from cement waste forms containing incinerator ash with specimens containing sodium sulfate. The curve is the modeled data for the cement/sulfate specimens	72

LIST OF FIGURES - continued

		Page
Figure 5.4	Long-term comparison of Cs-137 releases from cement waste forms containing incinerator ash with specimens containing sodium sulfate	72
Figure 5.5	Cumulative fraction leached of Sr-85 is plotted against the square root of time for triplicate specimens of portland cement containing incinerator ash . .	73
Figure 5.6	The finite cylinder model does not adequately model the Sr-85 data from cement/ash waste forms	74
Figure 5.7	Cs-137 cumulative fraction leached vs time from portland I cement containing 15 wt% incinerator ash at 20°, 40°, 50°, and 60°C in deionized water	76
Figure 5.8	Averaged Cs-137 cumulative fraction releases from cement/ash specimens shown for the first nine sampling intervals. While the order of release from the 20°, 40°, and 50°C specimens remain unchanged, the releases from the 60°C specimen were anomalous for the last two points	77
Figure 5.9	An Arrhenius plot of the diffusion coefficient for cement/ash specimens leached at 20°, 40°, 50°, and 60°C. There is no statistically significant difference in D_e caused by temperature under these test conditions	77
Figure 5.10	Sr-85 cumulative fraction leached vs time from portland I cement containing 15 wt% incinerator ash at 20°, 40°, and 50°C in deionized water	78
Figure 5.11	An Arrhenius plot of the diffusion coefficient D_e showing that Sr-85 leaching at 60°C is lower than expected	79
Figure 5.12	Size effect on releases of Cs-137 for cement/ash waste forms. Size is expressed as the ratio of waste form volume to surface area (V/S), with the smaller waste form having the lower ratio	80
Figure 5.13	Releases of Cs-137 from portland cement containing 15 wt% incinerator ash. Static and semidynamic leach tests were run at 60°C. The finite cylinder model diverges from the data after 12 days	83
Figure 5.14	Although leaching from a static test at 50° or 60°C is faster than at 20°C, the CFL values taken for tests at 50° and 60°C are almost identical	84
Figure 5.15	The combined effect of small size, elevated temperature, increased volume of leachant, and increased frequency of replacement gave results that were not greater than just small size and elevated temperature. Specimens were portland cement containing 15 wt% incinerator ash	84

LIST OF FIGURES - continued

		Page
Figure 5.16	Arrhenius plot for Cs-137 releases from cement/ash specimens at 20°, 40°, 50°, and 60°C. Changes in the volume of leachant made no difference to leaching at 60°C, but at 50°C smaller volumes (or no leachant replacements) could reduce leaching	85
Figure 5.17	Releases of Cs-137 from triplicate specimens of portland cement containing incinerator ash are shown for the optimized accelerated test and for the baseline. The acceleration factor is approximately 6	86
Figure 5.18	Releases of Cs-137 from accelerated tests are plotted against releases from the baseline test. The results produce a linear plot in two segments. The break is caused by the change in sampling interval during the baseline test	86
Figure 5.19	Sr-85 releases from cement/ash specimens during static tests run at 50° and 60°C	88
Figure 5.20	Releases of Sr-85 during static and semidynamic tests at 60°C. The finite cylinder model fits the data during the daily leachant replacement intervals, but overestimates it for longer intervals	89
Figure 5.21	Arrhenius plot of Sr-85 diffusion coefficients for cement/ash specimens showing that increasing the leachant volume to 6.5 liters increased releases at 60°C	90
Figure 5.22	Data from the accelerated test and from the baseline test are plotted together. The acceleration factor is approximately 17	91
Figure 5.23	Triplicate data sets from the optimized accelerated test and the baseline test. One specimen is modeled with the finite cylinder model but none fit the model very well	91
Figure 5.24	Plotting the CFL data from the baseline experiment against the CFL data from the accelerated test, a linear plot should result if the leaching mechanism has not changed. The break in slope is caused by a change in sampling intervals during the baseline test, but each segment is linear	92
Figure 5.25	Sr-85 releases from cement/ash waste forms were no different for specimens exposed to atmospheric carbon dioxide than they were for specimens from which carbon dioxide was excluded	93
Figure 5.26	Dissolved strontium released from cement/ash waste forms in static leach tests shows no effect of carbonation at 20° or 50°C	94

LIST OF FIGURES - continued

		Page
Figure 5.27	Dissolved calcium released from cement/ash waste forms in static leach tests shows no effect of carbonation, although the 20°C CO ₂ -free experiment had slightly higher calcium concentrations	94
Figure 6.1	Cs-137 cumulative fraction leached vs time from bitumen containing 40 wt% sodium tetraborate at 20°, 40°, and 50°C leached in deionized water	98
Figure 6.2	Leaching of cobalt is enhanced in a leachant containing 100 ppm EDTA. The cesium releases are slightly suppressed by the presence of additional sodium	99
Figure 6.3	Average values of Cs-137 cumulative fraction leached from experiments with daily replacements of leachant and with less frequent replacements . . .	100
Figure 6.4	Release of Cs-137 from bitumen is related to the amount of salt loading . .	101
Figure 6.5	Releases of Cs-137 from specimens with various waste loadings during the early portion of the leaching experiment	102
Figure 6.6	While leaching of Sr-85 from specimens containing 40 wt% salt was comparable to Cs-137, releases from the 20 wt% and 30 wt% specimens was lower	104
Figure 6.7	Releases of cobalt are much lower than for Cs-137 and Sr-85, but are systematic with loading up to 400 days	104
Figure 6.8	Values of pH of leachates are typically around 9 at 20°C. Data is for bitumen containing 30 wt% sodium tetraborate	105
Figure 6.9	Schematic showing the mechanism of leaching of a soluble salt incorporated in bitumen	107
Figure 6.10	An unleached surface of a bitumen specimen containing 40 wt% sodium tetraborate. Outlines of salt grains can be seen	108
Figure 6.11	After leaching, the surface of a 40 wt% loaded bitumen specimen is characterized by swelling and burst blisters where the saturated salt solution broke through the bitumen	109
Figure 6.12	At a magnification of 1000 times, a single blister with numerous holes illustrates how saturated salt solution is leached	109

LIST OF FIGURES - continued

		Page
Figure 6.13	An interior sample from the same leached specimen (Figure 6.10) shows that the same process operates inside the form. It is not just a surficial phenomenon	110
Figure 6.14	Bitumen forms containing 40 wt% sodium tetraborate. The one at left is as fabricated. The one at right was leached for 320 days in deionized water at 20°C. Samples were 4.8 cm diameter by 6.5 cm high right cylinders	110
Figure 6.15	Schematic model of expected leaching behavior of bitumen waste forms incorporating soluble waste and/or waste which swells upon hydration. The dashed vertical line separates Region A, in which no swelling has occurred, and Region B, in which there has been enough water uptake to cause swelling. The leach rate increases markedly with swelling	111
Figure 6.16	Layer thickness between salt particles is shown as a function of waste loading and particle size. Specimens with loadings of 30 wt% and 40 wt% begin the rapid leaching phase within 4 to 6 days of the start of an experiment indicating that a layer thickness of 30µm is critical to waste form performance in the short term	113
Figure 6.17	CFL versus time for Cs-137 leached from neat bitumen in deionized water at 20°C. The solid line represents the finite cylinder calculation for a D_e of 1.6×10^{-14} cm ² /s	114
Figure 7.1	Releases of Cs-137 from VES are related to the loading of a sodium sulfate salt, with significant scatter in leaching data for higher loadings	118
Figure 7.2	Releases from VES containing 20 wt% salt can be modeled by a single diffusion coefficient and the finite cylinder model	119
Figure 7.3	Releases from VES containing 40 wt% sodium sulfate can be modeled by the finite cylinder model and a single diffusion coefficient for the first 20 days of the experiment only. After that, the increased leachant replacement interval appears to inhibit releases	119
Figure 7.4	Cs-137 releases from specimens that are 10 cm in diameter and 13 cm in height, showing that the finite cylinder model and two diffusion coefficients can accurately model the data	120

LIST OF FIGURES - continued

		Page
Figure 7.5	Cs-137 releases from VES containing 40 wt% salt during an experiment with daily replacements of the leachant. The finite cylinder model fits the data accurately	120
Figure 7.6	Average releases of Cs-137 at 20°, 40° and 50°C during the first 11 days of leaching for VES waste forms containing 40 wt% sodium sulfate	121
Figure 7.7	Arrhenius plot of diffusion coefficients for VES leached at 20°, 40° and 50°C. These specimens contained 40 wt% sodium sulfate	122
Figure 7.8	Average releases of Cs-137 from three different sized specimens of VES containing 40 wt% sodium sulfate	123
Figure 7.9	Releases of Cs-137 from VES/sodium sulfate at 60°C from static and semi-dynamic tests are indistinguishable from each other	127
Figure 7.10	Leaching of Cs-137 in semidynamic tests using 6.5 liters of water at each interval showed relatively uniform behavior and a definite temperature effect	128
Figure 7.11	The finite cylinder model fits data from experiments run at 60° and 20°C, during the daily replacements of leachant. When the intervals of replacement are longer, the model overestimates releases	129

LIST OF TABLES

	Page
Table 2.1 Summary of Types of Waste Forms	4
Table 2.2 Composition (weight %) for Each of the Waste Form Types Containing Simulated Waste	5
Table 3.1 Graphical presentations of Leaching Data as a Function of Time	12
Table 3.2 Activation Energies Calculated from Leaching Data	30
Table 3.3 Applicability of Mathematical Models to Leaching Results for Various Waste Forms Leached in Deionized Water at 20°C	33
Table 4.1 Diffusion Coefficients D_e for Cs-137 from Portland Cement + Sodium Sulfate Waste Forms	51
Table 4.2 Diffusion Coefficients D_e for Sr-85 from Portland Cement + Sodium Sulfate Waste Forms	61
Table 5.1 Adsorption of Radionuclides by Incinerator Ash and Cement/Ash Waste Forms	75
Table 5.2 Diffusion Coefficients for Cs-137 from Portland Cement/15 wt% Incinerator Ash Waste Forms	81
Table 5.3 Effect of Waste Loading on the Diffusion Coefficients for Cs-137 from Portland Cement/15 wt% Incinerator Ash Waste Forms	82
Table 5.4 Diffusion Coefficients for Sr-85 from Portland Cement/15 wt% Incinerator Ash Waste Forms	87
Table 5.5 Effect of Loading on the Diffusion Coefficient for Sr-85 from Portland Cement plus Ash	88
Table 6.1 Effect of Salt Loading on Leaching of Cs-137 from Bitumen Waste Forms	103
Table 7.1 Diffusion Coefficients for Cs-137 for Vinyl Ester-Styrene + 40 wt% Sodium Sulfate	124
Table 7.2 Diffusion Coefficients for Sr-85 for Vinyl Ester-Styrene + 40 wt% Sodium Sulfate	125
Table 7.3 Diffusion Coefficients for Co-57 for Vinyl Ester-Styrene + 40 wt% Sodium Sulfate	126

EXECUTIVE SUMMARY

The prediction of long-term leachability of low-level radioactive waste forms is an essential element of disposal-site performance assessment. This report describes experiments and modeling techniques used to develop an accelerated leach test that meets this need.

The acceleration in leaching rates caused by the combinations of two or more factors were experimentally determined. These factors were identified earlier as being able to individually accelerate leaching. They are: elevated temperature, the size of the waste form, the ratio of the volume of leachant to the surface area of the waste form, and the frequency of replacement of the leachant.

The solidification agents employed were ones that are currently used to treat low-level radioactive wastes, namely portland type I cement, bitumen, and vinyl ester-styrene. The simulated wastes, sodium sulfate, sodium tetraborate, and incinerator ash, are simplified representatives of typical low-level waste streams. Experiments determined the leaching behavior of the radionuclides of cesium (Cs-137), strontium (Sr-85), and cobalt (Co-60 or Co-57) from several different formulations of solidification agents and waste types. Leaching results were based upon radiochemical and elemental analyses of aliquots of the leachate, and on its total alkalinity and pH at various times during the experiment (up to 120 days). Solid phase analyses were carried out by Scanning/Electron Microscopy and Energy Dispersive Spectroscopy on the waste forms before and after some leaching experiments.

Temperatures up to 50°C accelerated leaching from portland cement containing 5 wt% sodium sulfate, but above this temperature the releases of some elements declined due to changes in the structure of the cement. At 50°C, the leaching of Cs-137 was accelerated by about a factor of 18. Accelerated leaching of Sr-85 required larger volumes of leachate and gave an acceleration factor of 17. The release of Sr-85 can be modeled if leaching is not influenced by secondary reactions such as carbonation, and larger volumes of water are required to prevent these reactions.

The accelerated leaching conditions were optimized for portland cement containing 15 wt% of incinerator ash. The greatest accelerating factor for Cs-137 occurred at 50°C in a semidynamic test with 1.3 liters of water, giving an acceleration factor of 6. The finite cylinder model does not adequately describe long-term leaching of Cs-137 from this type of waste form. Temperatures up to 50°C accelerated the release of Sr-85 with an optimum acceleration factor of 17; at 60°C, the rate decreased, although an increased volume of leachant brought the rate up slightly. At 50°C the presence of atmospheric carbon dioxide had no effect on the leaching of radionuclides. The leaching of Sr-85 can only be modeled for the first five days of the experiment with the finite cylinder model. Thereafter, releases are overestimated. As with Cs-137, a model is needed with an adsorption term that is a function of time.

The leaching of bitumen wastes cannot be accelerated uniformly. Electron microscopy confirmed the hypothesis in the literature on the physical mechanism of leaching. The complex relationships of leaching from bitumen waste forms are discussed.

Leaching from vinyl ester-styrene containing sodium sulfate was accelerated by temperature of 60°C and by using 6.5 liters of water at each replacement interval. This combination of factors increased the leaching rate by a factor of 17. Leaching of this waste form can be modeled by diffusion.

A variety of mathematical models were reviewed, including models for diffusion from a semi-infinite medium, and from a finite medium. The results of our experiments were modeled using diffusion from a finite cylinder to see whether the mechanism of leaching was consistent throughout the leaching cycle and could be compared with results of a standard (baseline) semidynamic leach test.

Accelerated leaching can be performed for cement and vinyl ester-styrene waste forms in a way that does not change the mechanisms of leaching and gives results that can be modeled. A significant reduction in the time required to show consistent leaching properties for a major fraction leached was demonstrated.

This work will lead to the development of an accelerated leach test that can be used for cement-based waste forms, and for thermosetting polymers.

1. INTRODUCTION

This topical report presents the results from experimental and modeling efforts to provide a basis for the development of an accelerated leach test to predict long-term leachabilities of low-level waste forms. The results of an experimental investigation of combined factors that accelerated leaching are discussed. The investigation is based on work, detailed in a previous topical report [1], that discussed changes of leach rates caused by individual factors such as temperature, the size of the waste form, and the chemical composition and volume of the leachant.

The approach taken to study combined leach-rate acceleration factors requires a series of experiments using two or more of the factors that previously were identified as having a positive effect on leach rates. The results of these experiments are then modeled to determine if the leaching mechanism is the same as that observed in earlier "baseline" experiments. In turn, the models can be used to determine if leaching is being suppressed by some experimental artifact. The "baselines" are results from a standard leach test (ANS 16.1) [2] used as a reference for the accelerated tests.

The solidification agents used are ones that are currently used to treat low-level waste either in the United States or abroad, namely portland type I cement, bitumen and vinyl ester-styrene. The simulated wastes that are solidified (sodium sulfate, sodium tetraborate and incinerator ash) represent typical low-level waste streams.

This two-tiered approach, using experimental results for modeling and then optimizing conditions for new experiments based on the modeling results was applied to waste forms based on portland cement and on vinyl ester-styrene. There is no model for bitumen waste forms. However, experimental investigations of this material clarified the mechanisms of release and are also presented in this report.

Leaching of radionuclides from disposed low-level radioactive waste is the first event in a sequence that must be understood to produce reasonable risk assessments. For wastes treated

with a solidification agent, chemical reactions between the solidification agent and components of the waste render some radionuclides insoluble and, therefore, immobile. Other elements are nonreactive and may be highly mobile. To adequately perform radiological assessments, the reliable prediction of the long-term leaching behavior of waste forms depends highly on the integrity of the waste form in its disposal environments. Leaching studies are a key element in understanding these processes (and others) that lead to releases. This knowledge, in turn, is important to developing means of preventing releases. Moreover, leaching may be an important degradation process for many of the structural materials considered for engineered disposal units. Studies of mechanisms that transport water through these barrier materials (and transport radionuclides out) are closely related to studies of leaching mechanisms.

Determining the mechanisms of leaching is the first step in defining what mathematical models (if any) can describe leaching in a way that can be projected beyond the available data. A variety of leaching mechanisms have been proposed for different types of waste forms, but very few have been incorporated into computer programs. Fortunately, the mathematics of diffusion have been so reduced that computer programs can be written relatively easily. Diffusion through a porous medium is the most common mechanism for low-level waste forms. Where other mechanisms have been identified, or where other processes affect diffusion, different computer programs are required. The scope of the accelerated leach test project was not to develop computer programs to model leaching. A thorough understanding of leaching mechanisms will lead to more sophisticated modeling and a better ability to provide long-term predictions for risk assessments.

2. MATERIALS AND METHODS

This section summarizes the materials used for fabricating the waste form, the leach test methods, and the analytical methods. The solidification agents, portland type I cement, bitumen, and vinyl ester-styrene copolymer were primarily selected to represent a cross-section of material properties. The waste streams chosen are sodium sulfate wastes generated at Boiling Water Reactors (BWRs), boric acid waste generated at Pressurized Water Reactors (PWRs) and incinerator ash, which is becoming a major waste stream as advanced volume-reduction processes become common.

The choice of solidification agents was based on two criteria: (i) that they were either in use or being considered for use in low-level waste management, and (ii) that they cover a range of materials properties. By providing a detailed knowledge of the leaching behavior of several types of materials, e.g., hydraulic cement, thermoplastic binders, and thermosetting polymers, it is anticipated that the results would apply in general to solidification agents that may be developed in the future.

The following test specimens were investigated:

- Solidification agents.
- Solidification agent with radioactive tracers.
- Solidification agents containing simulated waste.
- Solidification agents containing simulated waste with radioactive tracers.

The samples containing radioactive tracers were used to investigate the leaching behavior of radionuclides of cesium, strontium and cobalt from the matrices. The other samples were used to study the leaching of the components of the solidification agent and nonradioactive elements from the waste.

Table 2.1 summarizes the types of waste forms containing simulated wastes that were selected for study. Table 2.2 lists their compositions, corresponding to the abbreviated summary in Table 2.1.

Table 2.1

Summary of Types of Waste Forms

Portland I Cement

5 wt% Sodium Sulfate

Portland I Cement

15 wt% Incinerator Ash

Bitumen

20 wt% Sodium Tetraborate

30 wt% Sodium Tetraborate

40 wt% Sodium Tetraborate

Vinyl Ester-Styrene

20 wt% Sodium Sulfate

30 wt% Sodium Sulfate

40 wt% Sodium Sulfate

Table 2.2

Composition (weight %) for Each of the Waste Form Types
Containing Simulated Waste

Portland Type I Cement/Sodium Sulfate

Vinyl Ester-Styrene/Sodium Sulfate

<u>Component</u>	<u>Weight %</u>	<u>Activity (μCi)</u>	<u>Component</u>	<u>Weight %</u>	<u>Activity (μCi)</u>
Cement Powder	65	-	Vinyl Ester- Styrene Monomer	54.7	-
Sodium Sulfate (anhydrous)	5	-	Sodium Sulfate (anhydrous)	39.3	-
Water	30	-	Water	1.8	-
Co-57	-	6.3	Catalyst	1.5	-
Cs-137	-	6.3	Promoter	0.06	-
Sr-85	-	12.5	Co-57	-	100
			Cs-137	-	100
			Sr-85	-	200

Portland I Cement/Incinerator Ash

Vinyl Ester-Styrene/Sodium Sulfate

<u>Component</u>	<u>Weight %</u>	<u>Activity (μCi)</u>	<u>Component</u>	<u>Weight %</u>	<u>Activity (μCi)</u>
Cement Powder	60	-	Vinyl Ester- Styrene Monomer	67.6	-
Incinerator Ash	15	-	Sodium Sulfate (anhydrous)	30.0	-
Water	25	-	Water	0.6	-
Co-57	-	100	Catalyst	1.7	-
Cs-137	-	100	Promoter	0.07	-
Sr-85	-	200	Co-57	-	16.5
			Cs-137	-	16.5
			Sr-85	-	25.5

Vinyl Ester-Styrene/Sodium Sulfate

Bitumen/Sodium Tetraborate

<u>Component</u>	<u>Weight %</u>	<u>Activity (μCi)</u>	<u>Component</u>	<u>Weight %</u>	<u>Activity (μCi)</u>
Vinyl Ester- Styrene Monomer	77.3	-	Bitumen	60.0	-
Sodium Sulfate (anhydrous)	20.0	-	Sodium Tetraborate (anhydrous)	40.0	-
Water	0.6	-	Co-57	-	91
Catalyst	2.0	-	Cs-137	-	91
Promoter	.08	-	Sr-85	-	182
Co-57	-	16.5			
Cs-137	-	16.5			
Sr-85	-	25.5			

Table 2.2 (continued)

Composition (weight %) for Each of the Waste Form Types
Containing Simulated Waste

Bitumen/Sodium Tetraborate

<u>Component</u>	<u>Weight %</u>	<u>Activity (μCi)</u>
Bitumen	70.0	-
Sodium	30.0	-
Tetraborate (anhydrous)		
Co-57	-	39
Cs-137	-	39
Sr-85	-	78

Bitumen/Sodium Tetraborate

<u>Component</u>	<u>Weight %</u>	<u>Activity (μCi)</u>
Bitumen	80.0	-
Sodium	20.0	-
Tetraborate (anhydrous)		
Co-57	-	100
Cs-137	-	100
Sr-85	-	200

2.1 Waste Form Types

Studies were made to select the composites of solidification agent/waste material that are chemically compatible. Formulations of the waste form were optimized to maintain physical integrity when immersed in water during the leaching experiments.

2.1.1 Portland I Cement Containing Sodium Sulfate as Simulated Waste. Sodium sulfate waste is a product of ion exchange resin regeneration at BWR power stations. It is usually concentrated by evaporation to approximately 22 wt% solids content. Further, evaporation of this concentrate to dryness results in sodium sulfate decahydrate (Glauber's salt). Glauber's salt dehydrates to anhydrous sodium sulfate at 32°C.

Up to approximately 45 wt% sodium sulfate can be solidified with cement. However, waste forms containing more than approximately 8 wt% sodium sulfate were unstable when immersed in deionized water, disintegrating before completion of a 90-day immersion test. A formulation of 5 wt% sodium sulfate, 30 wt% water, and 65 wt% cement was selected for testing, corresponding to a waste-to-binder ratio, i.e., evaporator concentrate to cement, of 0.54.

2.1.2 Portland I Cement Containing Incinerator Ash as Simulated Waste. Up to 50 wt% incinerator ash can be solidified by portland I cement without free-standing water being present. However, on curing specimens swell developing large voids. A formulation of 15 wt% ash, 25 wt% water and 60 wt% cement was selected for leach testing because this composition produced waste forms with few voids.

Incinerator ash was obtained from the waste incinerator of the Tennessee Valley Authority. The major components of incinerator ash are typically uncombusted carbon, aluminum oxide (Al_2O_3), ferric oxide (Fe_2O_3), and silicon dioxide (SiO_2). The ash was passed through a 2.38mm sieve size to produce a uniform powder, free of large clinkers and metal objects.

2.1.3 Vinyl Ester-Styrene Containing Sodium Sulfate as Simulated Waste. Mixtures of up to 60 wt% dry sodium sulfate with vinyl ester-styrene monomer polymerized satisfactorily to produce waste forms with hard surfaces. The leaching of sodium sulfate from solidified waste forms was used to select a composition which maximized the amount of incorporated waste while minimizing leaching. The amount of sodium that was leached increased rapidly at waste loadings above 40 wt%; therefore, this was the maximum loading used.

2.1.4 Bitumen Containing Sodium Tetraborate as Simulated Waste. Boric acid waste generated at a typical PWR Plant contains approximately 12 wt% boric acid in aqueous solution. Solidification of the waste with bitumen requires that the water is evaporated off. Because boric acid dehydrates at 160°C, the loss of water causes foaming of the bitumen mixture. A satisfactory pretreatment is to neutralize the boric acid waste stream with sodium hydroxide to pH 9.3: sodium tetraborate is the predominant product [3]. Evaporation of the solution to dryness results in the hydrated crystalline salt, sodium tetraborate decahydrate (borax). The borax must be further dried at 200°C to produce the anhydrous tetraborate.

A solid waste form can be produced by mixing the anhydrous sodium tetraborate with molten bitumen. We used waste loadings of 20 wt%, 30 wt% and 40 wt% of sodium tetraborate in bitumen.

2.2 Preparation of Samples

Cylindrical samples were prepared for leaching experiments with approximate dimensions of 4.8 cm diameter and 6.4 cm length ($V/S=0.84$). Based on past experience, this size is convenient for laboratory studies. Additional samples were prepared for size-scale studies, including smaller cylinders, approximately 2.5 cm diameter by 2.5 cm height ($V/S=0.42$), and larger cylinders approximately 10 cm diameter by 13 cm height ($V/S=1.85$).

Radioactive samples prepared for leach testing had the radioactive tracers Co-57, Cs-137, and Sr-85 incorporated into the waste. The low energy gamma ray emitted by Co-57

($T_{1/2}=270$ days) is better suited to the automated NaI counting system than is Co-60, and also works well with the intrinsic Ge counting system.

2.3 Leaching Tests

The ANS 16.1 Leach Test is a semi-dynamic leaching test in which the leachate is replaced periodically after intervals of static leaching [2]. Specimens are placed into the leachant solution in such a way that all the external surface area is directly exposed to the solution. Specimens are leached in individual containers containing a ratio of 10 cm between the volume of the leachant and the external geometric surface area of the specimen unless otherwise specified. Specimens are usually tested in triplicate to determine the variation in leaching. The results are expressed as incremental fraction release, as cumulative fraction release, or as a release rate, to facilitate alternative methods of treating the data.

The leachant is typically distilled water with a conductance of less than $5\mu\text{mhos/cm}$. The sampling interval was modified to give more frequent intervals than specified in the ANS 16.1 Method and, in some cases, to extend the duration of the test beyond the 90-day standard.

Our study differed from the ANS 16.1 test procedure by changes in the leachant replacement intervals. Extremes ranged from daily replacements to static tests with no replacements. Other variations included experiments run at elevated temperatures in an environmental chamber (Forma Scientific) with strict temperature controls.

2.4 Analytical Methods

Leachates are analyzed for a variety of materials, depending on the composition of the solidification agent and the simulated waste. Cement leachates are subjected to the most analysis since reactions within the matrix cause significant differences in leaching among different elements. Specific analytical methods are given below.

2.4.1 Radiochemical Analysis. The radiochemical component of the leachate, such as Cs-137, Sr-85 and Co-60 (or Co-57) is analyzed by gamma-ray spectroscopy using an intrinsic germanium detector or a sodium iodide detector in accordance with the methods described in ASTM D3648-78 [4] and ASTM D3649-78 [5].

2.4.2 Elemental Leachate Analysis. Analysis of leachates for non-radioactive elements is conducted with standard methods such as ASTM E663 [6] and those in Analytical Methods for Atomic Absorption Spectrophotometry, revised January 1982, Perkin-Elmer Corporation, Norwalk, CT, [7].

2.4.3 Alkalinity Measurements. The total alkalinity of leachates is measured by titration to the phenolphthalein end point according to Method Number 403 from Standard Methods for the Examination of Water and Waste Water, 15th edition, 1980 [8].

2.4.4 pH Measurements. The pH of leachates is measured using ASTM D1293 [9] with a combination probe.

2.4.5 SEM/EDS. Waste forms are analyzed before and after leaching by Scanning/Electron Microscopy (SEM) to observe any changes in morphology, and by Energy Dispersive Spectroscopy (EDS) to determine the elemental ratios in profile and on the surfaces of the waste form. The methods used are discussed by Goldstein and Yakowitz in Practical Scanning Electron Microscopy, Electron and Ion Microprobe Analysis, (1975) [10].

3. LEACHING MECHANISMS AND MODELS

3.1 Introduction

Standard leach tests provide no assurance that the optimal conditions for leaching are used. Moreover, while many tests assume that diffusion is the operative mechanism of leaching, typically no effort is made to determine the actual mechanism. The goal of an accelerated test is to measure the maximum leach rates for a waste form material in the shortest time, by conducting the test under the most favorable conditions. The effect of many leach test conditions were measured and reported earlier [1]. Determination of the optimum conditions for the development of an accelerated test now requires the application of specific models to predict radionuclide releases from specific waste form materials under the leaching conditions which were used. Some modeling concepts were reviewed earlier by Dougherty and Colombo [11]. In this section, the application and implications of mathematical modeling will be examined to find the most favorable leaching conditions for an accelerated leach test.

3.2 Methods of Presenting Leaching Data as a Function of Time

It should be noted that proper consideration of radioactive decay has been assumed for all of the following discussion.

3.2.1 Tabular and Graphical Methods. Several ways of graphically presenting experimental data on the leaching of radionuclides from waste form solids have been used by many laboratories worldwide. The International Atomic Energy Agency (IAEA) and the American Nuclear Society (ANS) proposed specific leach tests and methods of expressing the results. Table 3.1 lists ways to present leaching results as a function of time.

Table 3.1

Graphical presentations of leaching data as a function of time.

Type	Amount Leached	Time Function
A	CFL(V/S)	t
B	CFL	t ^{1/2}
C	CFL	t
D	log CFL	log t
E	IFL	Δ(t ^{1/2})

- a_n = amount leached in leaching interval n
 A_0 = initial amount of material being leached
CFL = $\Sigma a_n/A_0$ cumulative fraction leached
CFL(V/S) = cumulative fraction leached normalized to specimen size
IFL = a_n/A_0 incremental fraction leached
t = total leaching time
V = sample volume, cm³
S = sample geometric surface area, cm²

The IAEA recommends presenting the results as a plot or in tabular form as shown in Table 3.1, Types (A and B). Both of these forms of presentation imply the use of a specific mathematical modeling mechanism for leaching (discussed later). The sample size "normalizing factor" V/S is operative only if the implied leaching mechanism is bulk diffusion from a semi-infinite medium and all its limitations apply. Also, the implication that CFL is a linear function of t^{1/2} only works if diffusion is the operative mechanism.

Presentations of the leaching data according to Types C and D in Table 3.1 were used in this report to avoid the inference of a specific leaching mechanism until it is demonstrated as

being operative. The plots of log CFL vs log t are especially convenient forms of presenting data that span several orders of magnitude.

Finally, presentation Type E of Table 3.1 was recommended as a means of determining the diffusion coefficient, since the data points are not coupled [12].

Correlation diagrams in which CFL from one experiment is plotted against the CFL of a reference experiment at identical points in elapsed time have proven useful in demonstrating that changes in the leaching mechanism were not induced by changes in the leaching conditions [1]. If the data from an experiment lie on a straight line, then the two sets of data linearly correlate. Presumably, data taken at different temperatures will be linearly correlated as long as the mechanism of leaching is unchanged. The slope of the line, for linearly correlated data, provides a relative measure of the leachability compared to that of the reference experiment.

3.2.2 Empirical Equations. Empirical and semi-empirical equations for fitting data were used extensively to reduce large amounts of experimental data to a few parameters. These methods are quite accurate within the bounds of the experimental data but useless for extrapolation beyond the measured limits. Nevertheless, these equations are convenient means of data reduction, where mathematical solutions to the appropriate transport equations are not readily available.

Simple exponential equations were used by Godbee and Joy for their data on the leaching of asphalt-sludge leaching [13]. Recently, Côté et al. [14] used a semi-empirical equation to evaluate the leaching of heavy metals (As, Cd, Cr, and Pb) from cement-based waste forms. The calculated parameters were used to determine the relative merit of the waste forms, not to predict the effects of long-term leaching.

3.2.3 Mathematical Solutions to Mass Transport Equations. Models based on mass transport theory that have been validated with experimental data are an excellent means of estimating the amounts of material released by solidified waste. The mathematical theory of transport by diffusion from solids is based on Fick's hypothesis that the diffusion rate is

proportional to the concentration gradient [15,16]. The fundamental partial differential equation for diffusion is:

$$\frac{\partial C}{\partial t} = D_e \nabla^2 C \quad (1)$$

where,

∇^2 = Laplacian Operator

$\partial^2/\partial x^2$ in one dimension,

C = concentration of species,

t = time,

D_e = effective diffusion coefficient in a porous medium.

Mathematical solutions to the transport equation (1) have been applied to the leaching of radionuclides for waste solids [17].

3.2.3.1 Analytical Solutions for Diffusion. General solutions to the diffusion equation (1) can be obtained, provided that the diffusion coefficient is constant. The constant coefficient assumes that there are no significant changes with time in the physical or chemical structure of the waste form during the leaching process and no dependence on the concentration of the diffusing species. In most systems the diffusion coefficient depends on the concentration of the diffusing substance in the solid. However for dilute solutions, the dependence on the concentration of the diffusing species is slight and the diffusion coefficient can be assumed to be constant.

The Semi-Infinite Medium Model. The exact form of the solution to the mass transport equation of diffusion depends on the initial and boundary conditions of the problem. A simple case is that of a semi-infinite solid with a constant diffusion coefficient where the cumulative fraction leached is predicted as:

$$\frac{\Sigma a_n}{A_0} = 2 \frac{S}{\bar{V}} \left[\frac{D_e t}{\pi} \right]^{1/2} \quad (2)$$

where,

Σa_n = the total amount of radioactive material released in all leaching periods up to time, t,

A_0 = the initial amount of radioactive material,

V = the volume of the waste form,

S = the surface area of the waste form,

D_e = the effective diffusion coefficient in a porous medium.

The semi-infinite medium solution has been used extensively to demonstrate that the operating mechanism for leaching is diffusion where graphical presentation of CFL vs $t^{1/2}$ is linear when CFL is less than about 0.20. Diffusion coefficients then can be calculated from the slope of the line. In practice, it is necessary to add an intercept to equation (2) since extrapolation to $t=0$ does not pass through zero.

Finite Medium Model. Finite samples that release radioactive materials by a diffusion mechanism to aqueous solutions are linear with $t^{1/2}$ up to a CFL of about 0.20. Exact solutions for finite shapes were described by Crank [15]. Since waste forms and samples for leaching are generally cylindrical, Nestor [18] applied this solution to the leaching of radioactive waste. The solution of the mass transport equation for a cylinder that is uniform and homogenous has a zero surface concentration during the leaching process and with a constant diffusion coefficient is given as:

$$\frac{\Sigma a_n}{A_0} = 1 - \frac{32}{\pi^2 r^2} \sum_{n=1}^{\infty} \sum_{m=1}^{\infty} \frac{e^{-t D_e [\beta_m^2 + (2n-1)^2 \pi^2 / 4l^2]}}{(2n-1)^2 (\beta_m)^2} \quad (3)$$

where,

r = the cylinder radius, cm,

l = the cylinder half-height, cm, and

β_m = the positive roots of the zero-order Bessel function, $J_0(r\beta_m) = 0$, cm^{-1} .

The convergence of equation (3) is slow but computer programs were developed to determine the cumulative fraction leached. The ANS 16.1 leach test standard provides a tabular method of calculating D_e from leaching data for cylindrical waste forms [2]:

$$D_e = Gd^2/t \quad (4)$$

where,

G = dimensionless time factor [2]

d = cylinder diameter

and is listed for l/d ratios of 0.3 to 5.0 and for a CFL of 0.20 to 0.99. The dimension l is the half-height of the cylinder.

The most useful application of the finite cylinder equation (3) would be to predict leaching at longer times using optimal values of D_e , especially with a graphical presentation of the data and the computed leach curve. Deviation of the predicted curve (using a constant diffusion coefficient) from the data would most likely be due to physical or chemical changes in the waste form or changes in the leaching conditions.

3.2.3.2 Concentration Dependent Diffusion. In most leaching environments the diffusion coefficient depends on the concentration of the diffusing species and the ionic strength of solution. The diffusion coefficient can be written in the form:

$$D_e(C) = D_e^0 \{1-f(C)\} \quad (5)$$

where,

- $D_e(C)$ = the diffusion coefficient at concentration, C,
- D_e^0 = the diffusion coefficient at infinite dilution or $t=0$,
- C = the concentration of the species,
- $f(C)$ = function of C.

However, in dilute solutions, the dependence is slight or negligible. To develop an accelerated leach test, the accelerating factors of leachant volume to sample surface area, and the frequency of leachant replacement will be chosen to avoid such concentration effects on the diffusion coefficient.

The effect of changes in concentration is of interest in predicting how waste forms leach in the disposal environment. Some insight can be gained by static test results, where the concentration buildup of all the leached species is continuous.

3.2.3.3 Skin Effects of the Sample's Surface. Many solids have a surface skin that can be observed visually and which exhibits properties that differ from those of the bulk material. Evidence of a surface layer was reported for cement based-waste forms by Fuhrmann and Colombo [19]. The effects are expected to be secondary to bulk diffusion, but of appreciable significance as an explanation for observed changes in the diffusion coefficients for Sr-85 and Cs-137. In a private communication between H. Godbee and R. Pietrzak, a model was used that incorporated the concept of rapid sorption followed by desorption at the surface skin to effectively model leaching data from cement waste forms.

3.2.3.4 Diffusion + Reaction (K_d). Mass transport of the diffusing radionuclides from solidified waste can be limited by local instantaneous equilibrium. The simplest case is where the adsorbed species (S) is proportional to the mobile species (C):

$$S = K_d C \quad (6)$$

The solutions for the semi-infinite media and the finite cylinder are identical to equations (2) and (3) respectively, where:

$$D_e = D_f(\delta/r^2)[1/(1 + \rho_a K_d/\epsilon)] \quad (7)$$

where,

- δ = constrictivity,
- r^2 = tortuosity,
- ρ_a = apparent density,
- ϵ = porosity,
- D_f = diffusion coefficient in free liquid,
- K_d = sorption coefficient, mL/g.

Models for diffusion and kinetically controlled reactions, interface resistance, irreversible reactions, dissolution, desorption, and moving boundaries were reported for numerous practical applications. Several such models were reviewed in an earlier report [11].

3.2.3.5 Anomalous Transport. The diffusion of radionuclides from several types of solidified waste forms (such as with bitumen containing soluble waste) cannot be described adequately by diffusion transport equations with a constant boundary. Penetration of water into the waste form eventually causes swelling and the characteristic leach curve shows time- and waste loading-dependent stages. Empirical methods such as polynomial curve fits can quantify the radionuclide leach characteristics for relative comparison but not for long-term predictions.

Qualitative differences in the shapes of the leach curve for CFL versus time have been observed frequently. This difference is illustrated in Figure 3.1, adapted from Crank [15]. The curve labeled "Fickian" represents a monotonically increasing curve expected for pure diffusion. The "Sigmoid" and "Two Stage" curves in Figure 3.1 are typical of leach curves for solids exhibiting a time lag in the diffusion curve, due to the effects of slow penetration by water into the waste form. Two or more parameters are necessary to describe the interacting diffusion and relaxation effects inherent in the advancing boundary and solubilization of the waste. No

single model can account for every aspect of anomalous diffusion, especially in polymers, although many have been advanced with varying degrees of success.

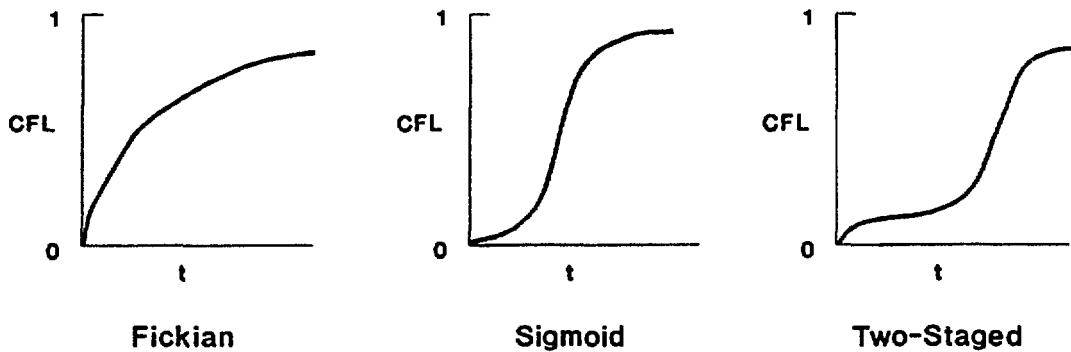


Figure 3.1 A comparison of characteristic leach curves: Fickian, Sigmoid, Two-staged. After Crank [15].

3.2.4 Numerical Solutions to the Transport Equations. Most mathematical solutions for transport of radionuclides are in the form of infinite series. Evaluation of these equations is not simple. In addition, mathematical solutions are not available for many specific experimental situations. Because of the availability of high speed computers, numerical techniques to evaluate partial differential equations of transport can be readily done without finding the mathematical solution first. The modeling of leaching where the diffusion coefficients are concentration dependent, or anomalous diffusion is operating, may be most efficiently handled by numerical techniques.

A general discussion of numerical modeling is given by Crank [15]. Kienzler et al. used a numerical model for leaching using a concentration-dependent diffusion coefficient [20].

Recently, Nimmual reported the numerical modeling of Sr-85 from cement where the partial differential equation for transport by diffusion included a desorption term [21]:

$$\frac{\partial C}{\partial t} = D_e \nabla^2 C + KP \quad (8)$$

where,

- K = a constant,
- P = the desorption rate for Sr-85.

3.2.5 Temperature Effects and the Arrhenius Equation. The leaching of radionuclides from waste forms generally can be increased by elevated temperatures, with some notable exceptions. For diffusion-controlled leaching the diffusion coefficients exhibit Arrhenius type behavior. More specifically:

$$D_e = A e^{-E_a/RT} \quad (9)$$

where,

- A = pre-exponential factor,
- E_a = activation energy,
- R = gas constant (1.99 cal/mole-K),
- T = temperature, K.

Diffusion processes are expected to have activation energies of about 5-6 kcal/mole as reported for cement [11,22,23]. The plot of Log D_e versus $1/T$ should be linear with the slope of the line equal to $-2.303E_a/R$. Parallel lines should be observed for each type of material and isotope.

Although many materials exhibit favorable Arrhenius behavior for leaching, some materials such as bitumen soften and are self-sealing, and produce a negative effect. In these cases, elevated temperature does not act as an accelerating factor.

3.3 Application of Modeling Techniques

This section deals with the applicability of specific models to particular waste form materials and leaching conditions to describe and extrapolate leaching data to long-terms. There are more detailed discussions in the chapters, dealing specifically with each type of waste form, that consider the effects of leaching condition factors and the optimization of combined leaching factors.

3.3.1 Modeling Releases from Cement. Dougherty et al. reported experimental results from an extensive series of tests to investigate the effects of leach-test condition factors [1]. Efforts to quantify some significant observations led to the use of the semi-infinite media and the finite cylinder diffusion models for leaching for cement and cement-solidified wastes.

3.3.1.1 Diffusion Coefficient (D_e) Calculated from the Semi-Infinite Model. Materials for which plots of CFL versus $t^{1/2}$ are linear can be used to calculate D_e for a particular leaching experiment by the application of equation (2). The linear least-squares regression slope of the data for CFL less than 0.20 will be directly proportional to the diffusion coefficient, D_e . The diffusion coefficients for cement, cement containing sodium sulfate, and cement containing incinerator ash were determined for each material under all the leaching conditions used during this program. An example is shown in Figure 3.2, where CFL for Cs-137 is plotted against $t^{1/2}$. A linear least-squares regression line is shown for the observed data. A slope of 8.663×10^{-2} days^{1/2} and an intercept of 4.767×10^{-3} was found, with a correlation factor for the least squares line of 0.996. From the slope of the line, a diffusion coefficient of 4.9×10^{-8} cm²/s was calculated. A "data base" of the diffusion coefficients for all experiments made on cement-based waste forms conducted during this program was established in this manner. This " D_e data base" for cement-based waste forms then was used to determine quantitatively the effects of the leaching condition factors.

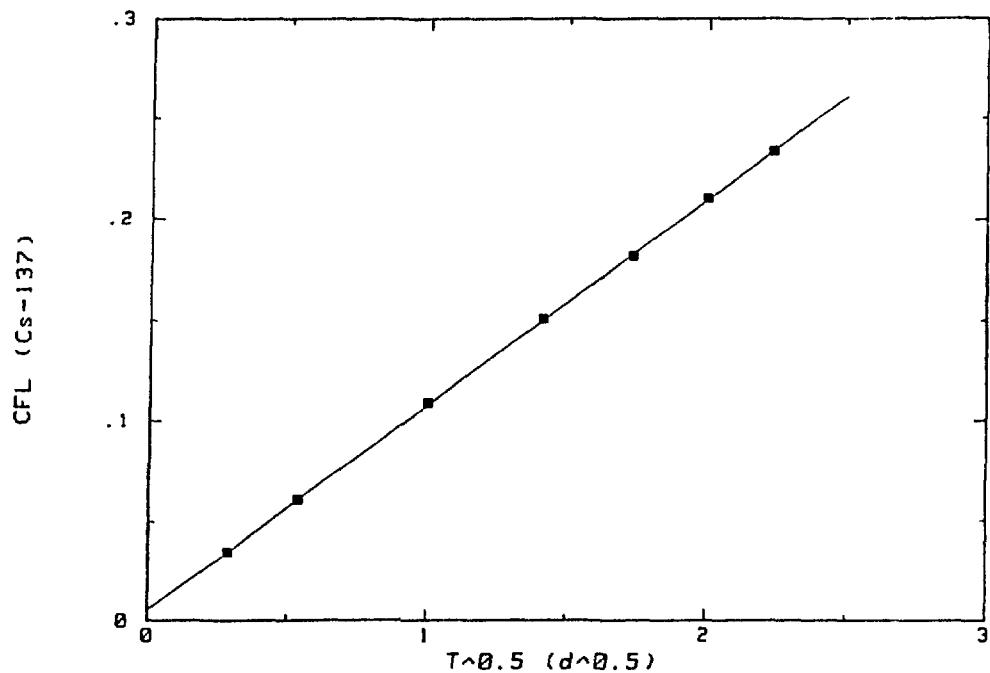


Figure 3.2 Cs-137 CFL versus $t^{1/2}$ (in days $^{1/2}$) from cement containing sodium sulfate leached in deionized water at 20°C.

3.3.1.2 The Finite Cylinder Model. When laboratory samples are leached beyond 0.2 CFL, the effects of depletion must be considered. Consequently, models must be applied that account for depletion of the leached species. The leaching of Sr-85 and Cs-137 from cement containing 5 wt% sodium sulfate, in deionized water at 20°C is shown in Figure 3.3. The solid line is the result for CFL from the finite cylinder model using diffusion coefficients of $6.4 \times 10^{-10} \text{ cm}^2/\text{s}$ for Sr-85, and $4.2 \times 10^{-8} \text{ cm}^2/\text{s}$ for Cs-137. Bulk diffusion accounts for the entire leaching curve in both cases. Particular note should be made that the leaching conditions remained constant (the leachant was changed at daily intervals) and there were no obvious changes in the waste forms.

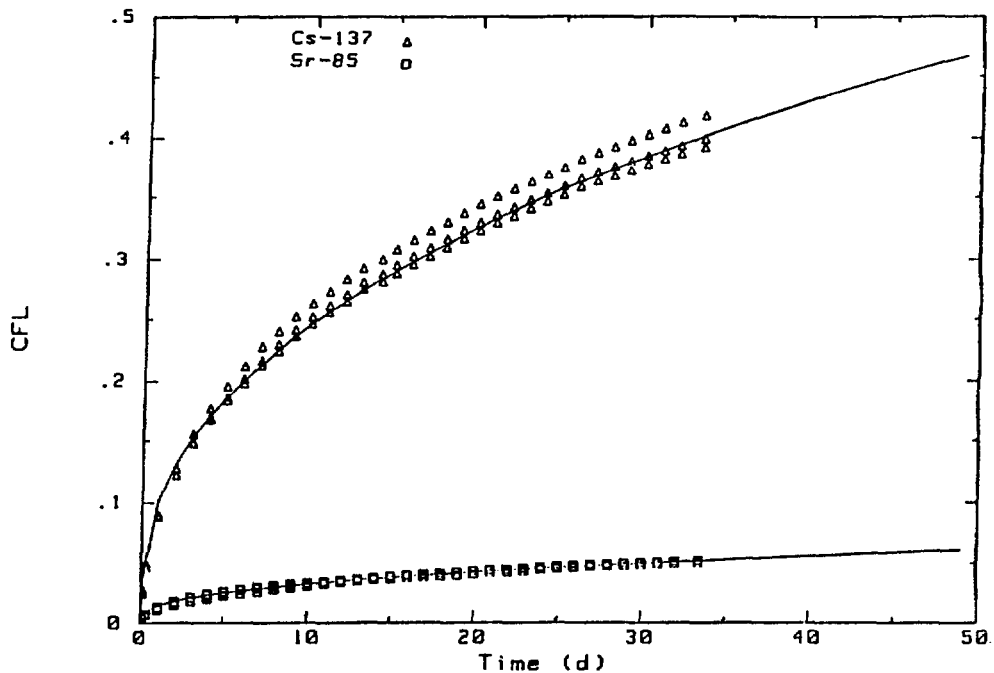


Figure 3.3 CFL of Sr-85 and Cs-137 versus time leached from cement containing 5 wt% sodium sulfate in deionized water at 20°C. The leachant was changed daily. Releases were modeled using the finite cylinder model.

3.3.1.3 Effects of Leaching Conditions. Although standard leach tests such as ANS 16.1 and especially the IAEA test [24] take precautions to provide ideal conditions for leaching which do not affect the magnitude of the diffusion coefficient, this is by no means guaranteed. Any modification of the test procedure, especially those which accelerate leaching, may have an adverse effect. Ideally, the leaching conditions for each temperature should produce the maximum observable effective diffusion coefficient.

The Leachant Replacement Interval. Three basic types of leach tests have been employed extensively: the static test, the semidynamic test and the flow test (Figure 3.4). During the static test, the leachant is never changed and leachable constituents continue to build up throughout the experiment. Static tests adversely affect the test results by slowing the leach rate and consequently making the diffusion coefficient appear to continually decrease. The advantage of the static test is its simplicity. The flow leach test appears to offer the best conditions for leaching provided that the flow rate is sufficient to maintain a very dilute solution

in contact with the waste form. However, the flow test is complex to perform and especially difficult at temperatures above 20°C.

Test Methods

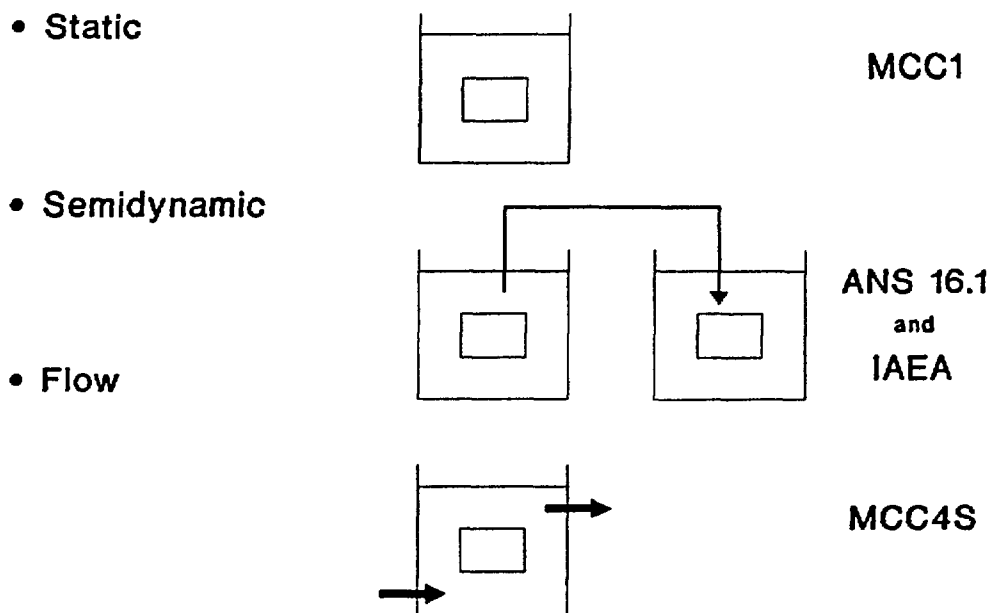


Figure 3.4 A comparison of some basic leaching techniques: Static, Semidynamic, and Flow tests

The best compromise appears to be the semi-dynamic test as exemplified by the IAEA or the ANS 16.1 test. These tests are convenient to perform and attempt to maintain dilute solutions of leachant in contact with the specimen. Because the incremental amounts of leached substances generally decreases with time, these methods successively increase the intervals between changes of leachant. Even though the leached radionuclide concentrations are very low, the buildup of other substances brought into solution by the leachant may adversely affect the leaching process. This effect can be seen in Figure 3.5 which compares the leaching results for Sr-85 from two sets of cement samples containing 5 wt% sodium sulfate when the replacement intervals were different. When the leachant was changed daily over a period of 35 days, the results could be fully accounted for by a $D_e = 4.0 \times 10^{-10} \text{ cm}^2/\text{s}$.

However, changing the sampling schedule from daily to weekly after the first week of leaching (ANS 16.1) resulted in a sharp break in the leaching curve which could only be accounted for by lowering D_e from 2.5×10^{-10} to 5.0×10^{-11} cm²/s, and continuing to calculate the CFL versus time curve by the use of the finite cylinder model. The small initial difference between the two sample sets reflects the inherent problems of comparing samples prepared on two different occasions.

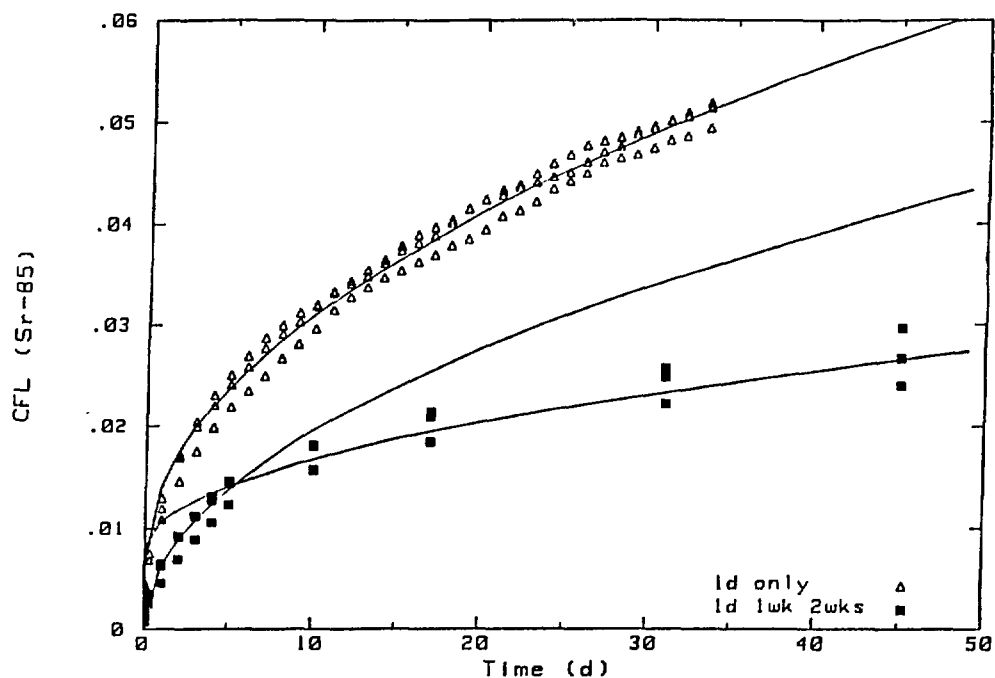


Figure 3.5 CFL of Sr-85 leached from cement containing 5 wt% sodium sulfate in deionized water at 20°C. A comparison of the effect of change in the leachant replacement schedule is shown. The triangles represent data from an experiment with daily leachant replacement. The squares represent data from the ANS 16.1 test.

Cs-137 leached from cement containing 15 wt% incinerator ash showed a similar change in the leach rate when the replacement interval for deionized water at 20°C was changed from daily to two weeks, as shown in Figure 3.6.

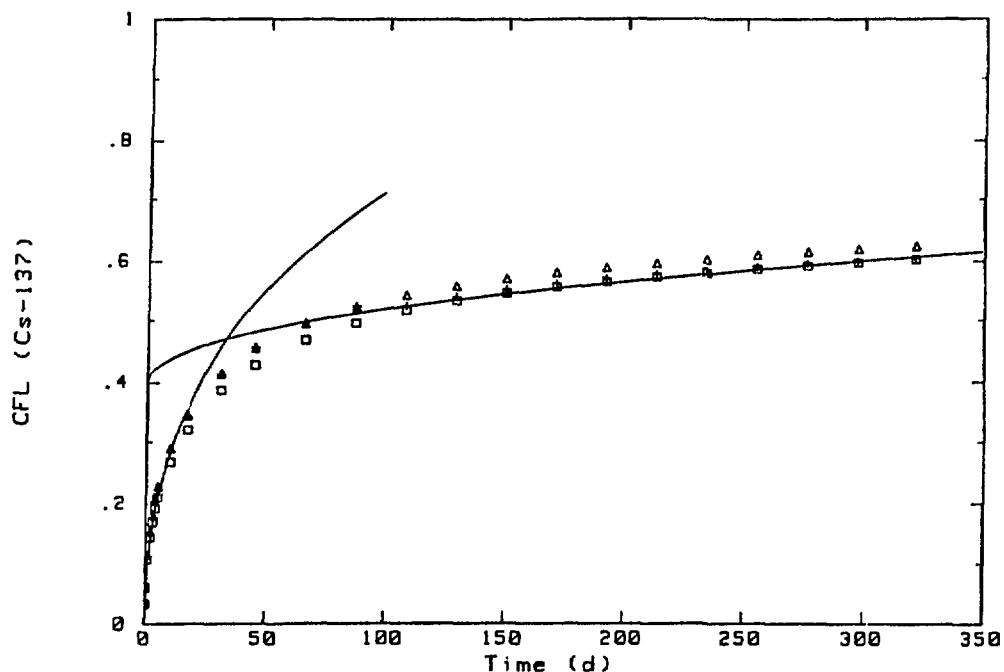


Figure 3.6 Cs-137 CFL versus time for cement containing 15 wt% incinerator ash at 20°C. The solid lines represent the finite cylinder model prediction with $D_e=6.0 \times 10^{-8} \text{ cm}^2/\text{s}$ for the early results of 0 to 20 days and $D_e=1.0 \times 10^{-9}$ for the long-term results.

The IAEA procedure recommends that the leachant be renewed once per day until its pH drops below eight for cement [24]. The ANS 16.1 test does not consider this factor. Different waste forms and isotopes are expected to have varying sensitivity to the changes in the leachant replacement interval. Consequently, all estimates of the effective diffusion coefficients for this program were made from the data for the daily changes by using the semi-infinite model where the CFL versus $t^{1/2}$ is linear.

The Volume of the Leachant and Surface Area of the Sample. Since the frequency of leachant replacement affects the diffusion of radionuclides from waste forms, we investigated the effect of the ratio of the volume of the leachant volume to the sample's surface area. Increasing the relative volume would decrease the absolute concentrations of leached materials in equal sampling intervals for a semidynamic test. The ANS 16.1 standard leach test

recommends a volume to surface area ratio of 10/1 cm. The effect of increased ratios of 30/1 and 50/1 are compared to the results for daily sampling in Figure 3.7. The increased ratio of volumes to surface area enhanced the leaching of Sr-85, although not as much as by simply changing the leachant on a daily basis.

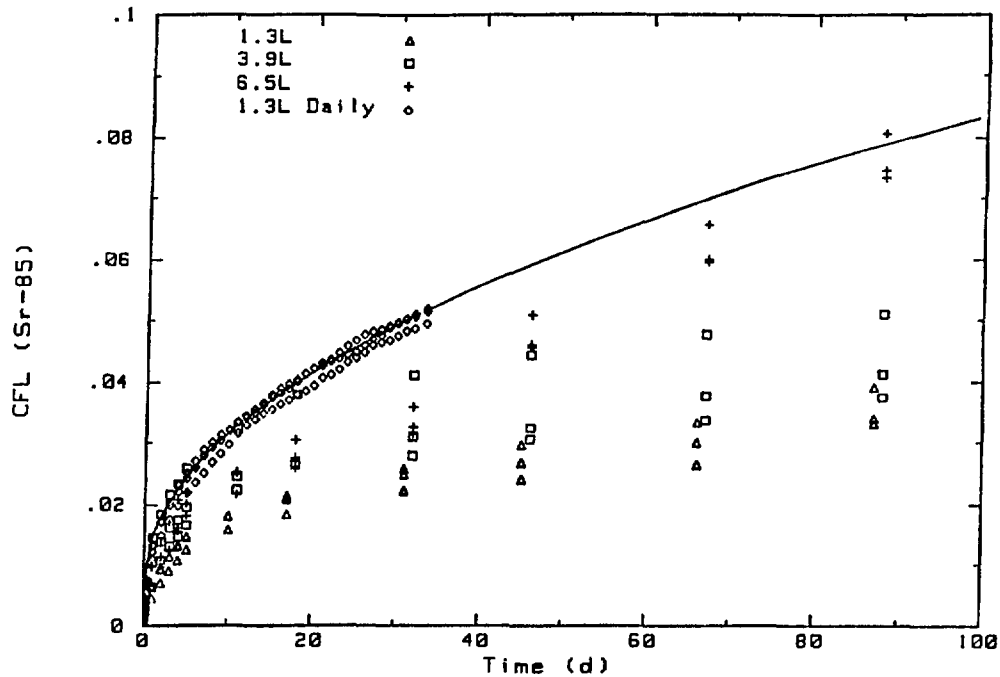


Figure 3.7 CFL of Sr-85 versus time from cement containing 5 wt% sodium sulfate leached in deionized water at 20°C. A comparison of results was made between results for leachant volume to sample surface area ratios of 10/1, 30/1 and 50/1.

Effect of Sample Size. The ability to correct for size is critical to the development of a leach test that can be extrapolated to full-scale waste forms. Several studies of sample size and radioactive leaching have been reported for cement waste forms [25,26,27]. The semi-infinite model equation (2) indicates that the effective diffusion coefficients, D_e , should be independent of sample size or, specifically, the ratio of the sample's volume to its surface area (V/S). In each case reported, D_e was relatively independent of the sample's scale, as is illustrated for Cs-137 leached from cement containing ion exchange resin [26]. Figure 3.8 shows the normalized

cumulative fraction leached ($CFL \times V/S$) plotted against time on a log-log scale for samples sizes ranging from a V/S ratio of 0.8 to 9.1. Six different sized specimens show a band with a width of about a factor of 2. This spread in the data is probably caused by the inherent variability among batches of waste forms. Similar variability was observed for scaling experiments as reported earlier in this program [1].

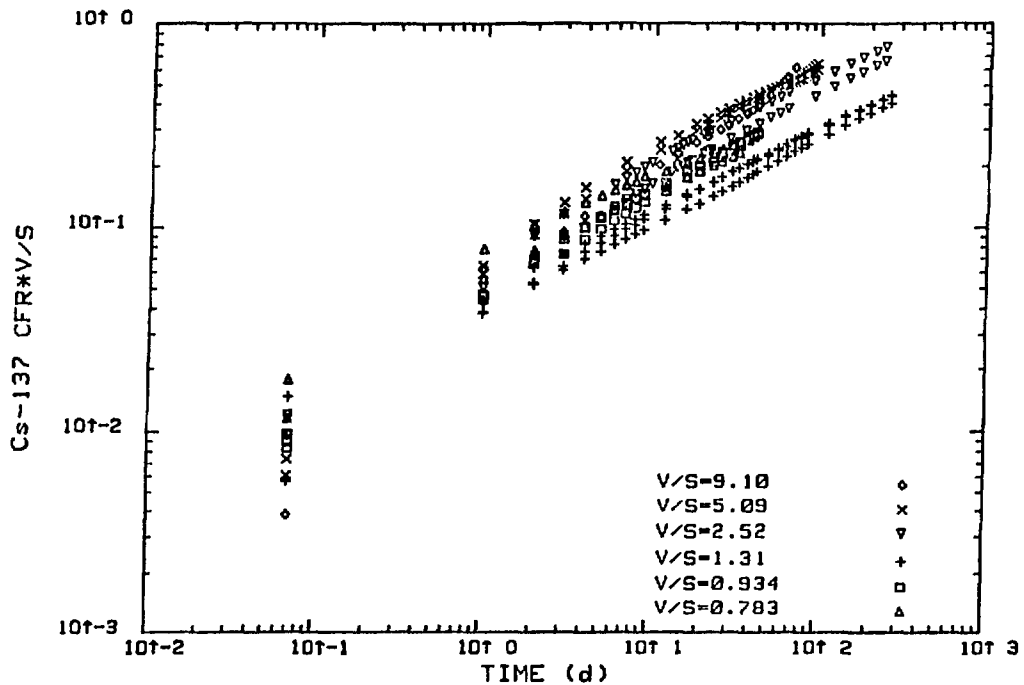


Figure 3.8 Log ($CFL \times V/S$) versus log t for Cs-137 from cement containing ion exchange resin. Six sizes of cylindrical waste forms are compared after correction with V/S .

Temperature. In leaching experiments with cement specimens, as the temperature increases so do the concentrations of dissolved specimens in the leachate for any given interval of time. Experiments at elevated temperatures therefore may require increased volumes of leachant or frequent replacement. To optimize the effect of increased temperatures on leaching, the leachate must remain as dilute as possible, yet still contain easily measurable

amounts of the radionuclides being studied. Calculations of activation energies from equation (9) must assume that the leaching conditions have been optimized at each temperature. The Arrhenius isotherms (as exemplified by Figure 3.9 for Cs-137 and Sr-85 from neat cement) are expected to be parallel lines for each waste form material and isotope, since the activation energies for diffusion are expected to be relatively constant (4 to 6 kcal/mole). Table 3.2 gives the calculated activation energies obtained for Cs-137 and Sr-85 from cement waste forms. Activation energies for Sr-85 are higher than expected for diffusion, indicating that an additional process is retaining the Sr-85. More energy is required to leach a given quantity of Sr-85, giving a higher activation energy.

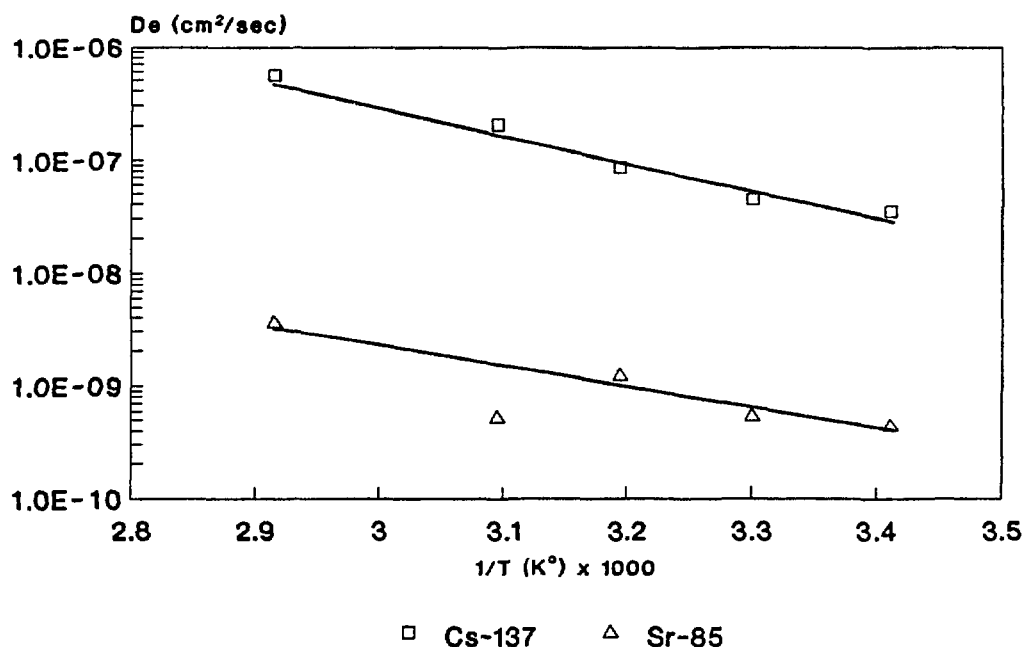


Figure 3.9 Arrhenius plot of Log D_e versus 1/T for Cs-137 and Sr-85 leached from neat cement in deionized water.

Table 3.2
Activation Energies Calculated from Leaching Data

Waste Form	E_a (kcal/mole °K)	
	Sr	Cs
Cement	-	5.2 ± 1.7
Cement + 5 wt% Na_2SO_4	14.3 ± 4.5	5.4 ± 0.9
Cement + 15 wt% Ash	16.7 ± 7.7	4.9 ± 1.5
Simple ions in water	4 - 6	4 - 6

3.3.2 Vinyl Ester-Styrene + Sodium Sulfate. The leaching of radionuclides from vinyl ester-styrene containing 20, 30, and 40 wt% sodium sulfate follows a diffusion mechanism. As discussed in Section 7, the data can be well described by the finite cylinder model (Figure 3.10).

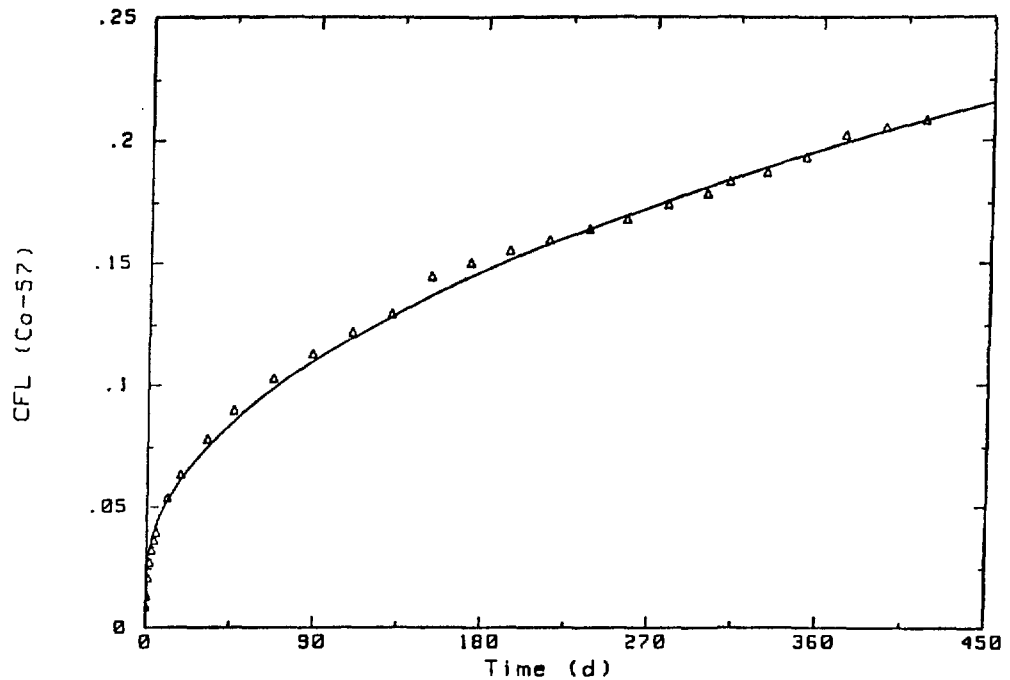


Figure 3.10 CFL versus time for Co-57 from vinyl ester-styrene containing 20 wt% sodium sulfate leached in deionized water at 20°C. The solid line represents the finite cylinder calculation.

3.3.3 **Bitumen.** The long-term leaching of Cs-137 from neat bitumen in deionized water at 20°C can be well described as simple diffusion. However, the leaching data for bitumen containing the soluble salt sodium tetraborate is quite different. Figure 3.11 shows the average CFL of Cs-137 from bitumen containing various amounts of sodium tetraborate leached in distilled water at 20°C. The leaching curves are highly dependent on the waste loading and show a distinct initiation time and sigmoid shape. The leaching curves for Cs-137 from bitumen with sodium tetraborate appear to belong to the case of anomalous non-Fickian leaching behavior. The observed swelling of these waste forms strongly influences the leaching process, as specimens that are the most highly loaded are the first to swell and exhibit the most rapid leaching behavior.

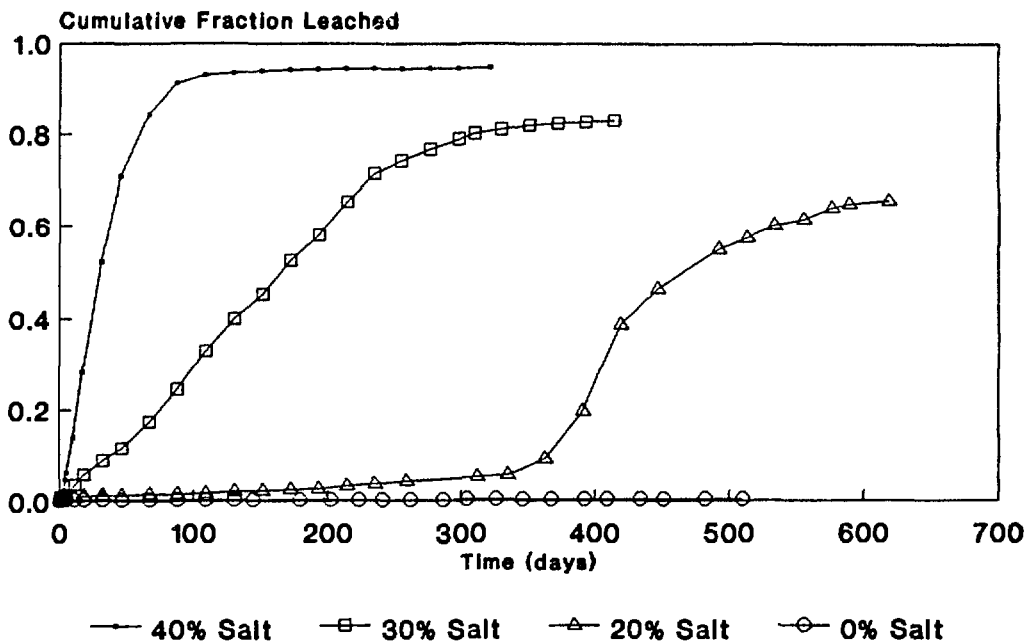


Figure 3.11 CFL versus time for Cs-137 leached from bitumen containing 0, 20, 30 and 40 wt% sodium tetraborate in deionized water at 20°C.

3.4 Summary

Several modeling techniques were tried to reduce the leaching data obtained in this program to characteristic parameters. The most successful was the application of bulk diffusion

equations (2) and (3) to obtain diffusion coefficients. The general applicability of these equations to waste form types is shown in Table 3.3. Cement-based waste forms in general, vinyl ester-styrene containing 20 or 30 wt% sodium sulfate, and neat bitumen leaching could be modeled if the effects of changes in the replacement interval of the leachant were taken into account. Diffusion coefficients were calculated for all the experiments that could be successfully modeled by a simple diffusion mechanism. These coefficients will be used in the following sections to evaluate the effects of the test acceleration factors.

Efforts are continuing to obtain values of the diffusion coefficients that are optimized for the best fit of the leaching data through the use of the finite cylinder model equation (3). The magnitude of additional effects such as chemical reactions on diffusion, and the effects of the surface skin are also being further investigated since they may be significant under accelerated test conditions.

For materials which could not be modeled, graphical methods will be employed to evaluate the leach test conditions. The principles which generally apply to a diffusion mechanism for leaching are expected to be operative but complicated by additional mechanisms, such as adsorption. Further efforts to model materials which show anomalous leaching characteristics are being made.

Table 3.3

Applicability of Mathematical Models to Leaching Results for
Various Waste Forms Leached in Deionized Water at 20°C.

Binder	Waste	Co-57	Sr-85	Cs-137
Cement		NO	D	D
Cement	Sodium Sulfate	NO	D	D
Cement	15 wt% Ash	NO	D	D
Cement	25 wt% Ash	NO	D	D
Cement	35 wt% Ash	NO	D	D
VES	20 wt% Na ₂ SO ₄	D	D	D
VES	30 wt% Na ₂ SO ₄	D	D	D
VES	40 wt% Na ₂ SO ₄	D	D	D
Bitumen		D	NO	D
Bitumen	20 wt% Na ₂ B ₄ O ₇	A	A	A
Bitumen	30 wt% Na ₂ B ₄ O ₇	A	A	A
Bitumen	40 wt% Na ₂ B ₄ O ₇	A	A	A

NO = not observed

D = Diffusion only, equations (2) and (3) are applicable.

A = Anomalous, no satisfactory mathematical model available.

4. PORTLAND CEMENT CONTAINING SODIUM SULFATE AS SIMULATED WASTE

4.1 Introduction

Portland cement is the solidification agent most commonly used for low-level radioactive waste. It is used either without modification or with any of a variety of additives and admixtures intended to improve properties of the waste form. Portland cement solidifies by a series of hydration reactions primarily involving dicalcium silicate and tricalcium silicate, but also involving smaller quantities of tricalcium aluminate and tetracalcium aluminoferrite [28,29]. Other compounds such as gypsum ($\text{CaSO}_4 \cdot 2\text{H}_2\text{O}$) and portlandite ($\text{Ca}(\text{OH})_2$, a product of the hydration reactions) are involved in the setting and hardening of cement [28]. Portland cement solidifies into a porous structure; its porosity is proportional to the amount of water mixed with the cement powder and strongly influences the properties of the hardened cement, including its leachability.

The various components of cement react with water, with each other, and also with some components of waste streams to form new compounds. This process can be beneficial, as in the case of incinerator ash, where some components of the waste join in the cement-forming reactions. In other cases, such as sodium sulfate, the process can be detrimental because the waste inhibits the setting process or forms new high-volume compounds that disrupt the structure of the cement.

Chemical reactions between cement and waste components can influence the leaching process for different radionuclides. In addition, the physical structure of cement waste forms change over time as the cement ages, as it leaches, and as it reacts with the waste and with the environment. Since leaching from a porous medium is partly controlled by the porosity/tortuosity/constrictivity of the material, changes in structure will affect leaching.

While the leaching behavior of cement waste forms is more complex than for other solidification agents, it is a particularly important topic because cement is so commonly used as a solidification agent.

4.2 Modeling and Mechanisms of Leaching

To determine if diffusion is the dominant leaching mechanism for Cs-137 from cement/sodium sulfate waste forms, the cumulative fraction leached was plotted against the square root of time for three types of experiments: ANS 16.1, daily leachant replacement, and flowing leachant (Figure 4.1). This plot will yield a straight line if diffusion is the leaching mechanism and if none of the experimental conditions are limiting releases. This statement is true up to about CFL=0.2 (20% release), then depletion begins to slow down the leach rate. The plot of Cs-137 releases during the ANS 16.1 test is linear until the replacement interval of the leachant becomes greater than one day, when the data falls below the projected line. This change occurs at about 20% release, indicating that: 1) depletion is becoming important, 2) diffusion is being inhibited, or 3) some process, such as adsorption or precipitation, is removing the tracer from solution.

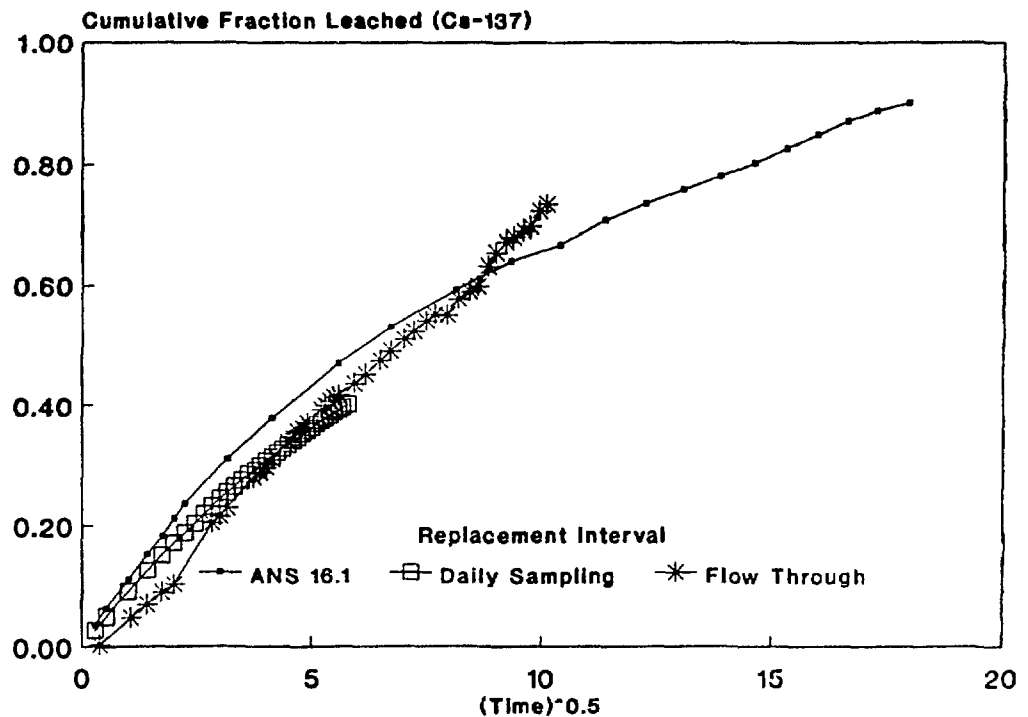


Figure 4.1 Averages of triplicate data for three types of leach tests: ANS 16.1, semi-dynamic with daily leachant replacements and flow-through tests. These data are plotted against the square root of time which produces a linear plot up to CFL=0.2 if diffusion is the leaching mechanism.

If leaching is suppressed by longer intervals of replacement, suppression would be the result of increases in concentration of dissolved ions in the leachate. This can be shown by comparing the data from a leach test with daily or flowing leachant replacement (Figure 4.1) with data from a test with less frequent replacement. The curves showing Cs-137 releases from experiments using flowing leachant or daily replacements are very similar to those using the ANS 16.1 replacement schedule. Curves for all three both experiments are linear below 25% release, with the data from the two semidynamic-type tests tending to curve downward after that point.

To obtain better information, a more sophisticated approach is necessary. Therefore, a model was used that is based on Nestor's approximation for diffusion from a finite cylinder [18]. This model takes depletion into account, so comparisons can be made to greater CFL values. However, our computer program for the finite cylinder model has a limited number of iterations. Consequently, it is useful for CFL values less than about 0.95 (95% release) (see Section 3).

This model can be used to describe Cs-137 releases during the early part of the semi-dynamic experiments. However, as shown in Figure 4.2 (curve #1), the model results are significantly greater than the data after 50 days. Since depletion is included in the calculation, this finding implies that some outside factor is inhibiting leaching. By using a second diffusion coefficient and starting the calculations at time=0 and CFL=0.2, a good fit can be obtained for times greater than 100 days. The lowering of the leach rate with time does not appear to be caused by an ongoing change in the material because a single diffusion coefficient is effective in modeling the data from 100 to 500 days. If the material were progressively changing, it could not be modeled by one diffusion coefficient for this long period. Therefore, the reduced frequency of leachant replacement may cause the drop in release rate. To test this hypothesis, the finite cylinder model was applied to data from a flow experiment, which provided a greater total volume of leachant than did the semidynamic ANS 16.1 leach test. The model fit the flow data very well from the start of the experiment (Figure 4.2, curve #2) to about 75 days. After 75 days, some small cracks in the material caused a change in the leach rate that can be seen on the figure. The good modeling fit leads to the conclusion that for Cs-137 (at 20°C in 1300

ml of distilled water), diffusion is the primary leaching mechanism. Minor suppression of leach rate occurs during longer intervals of the ANS test which can be overcome by using more frequent leachant replacements or flowing leachant.

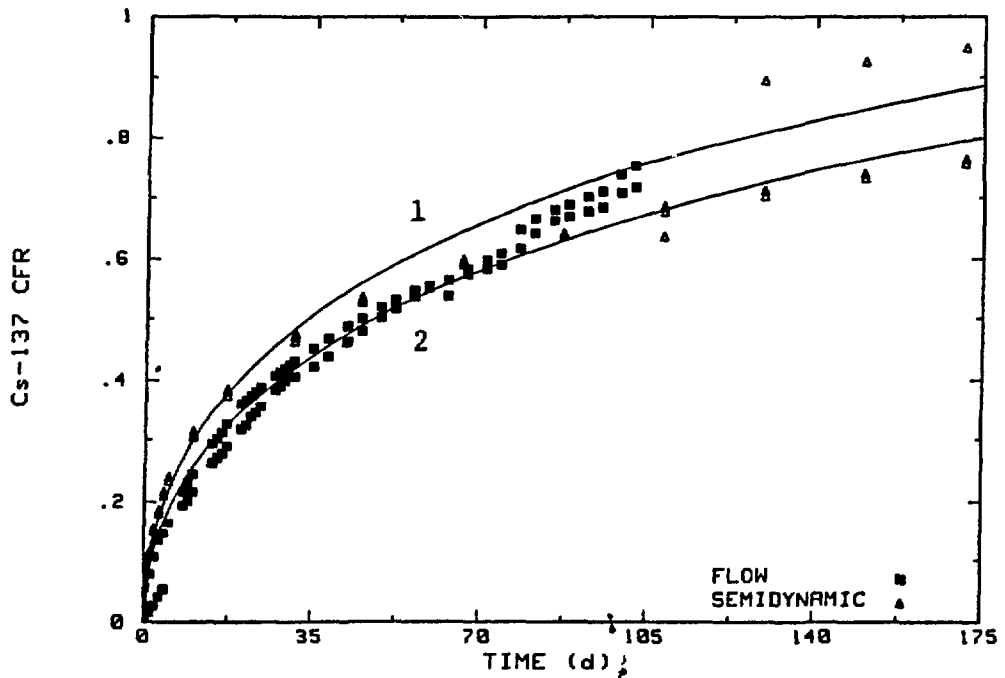


Figure 4.2 The finite cylinder model fails to follow the Cs-137 release data for the semidynamic ANS 16.1 test (1), but does accurately model the data from the flow test (2).

A comparison was also made of the data from the ANS 16.1 test with data from a test with daily leachant replacement (Figure 4.3). Unfortunately, the daily replacement test did not run long enough to show any difference between the two. The model fits both quite well for the time covered.

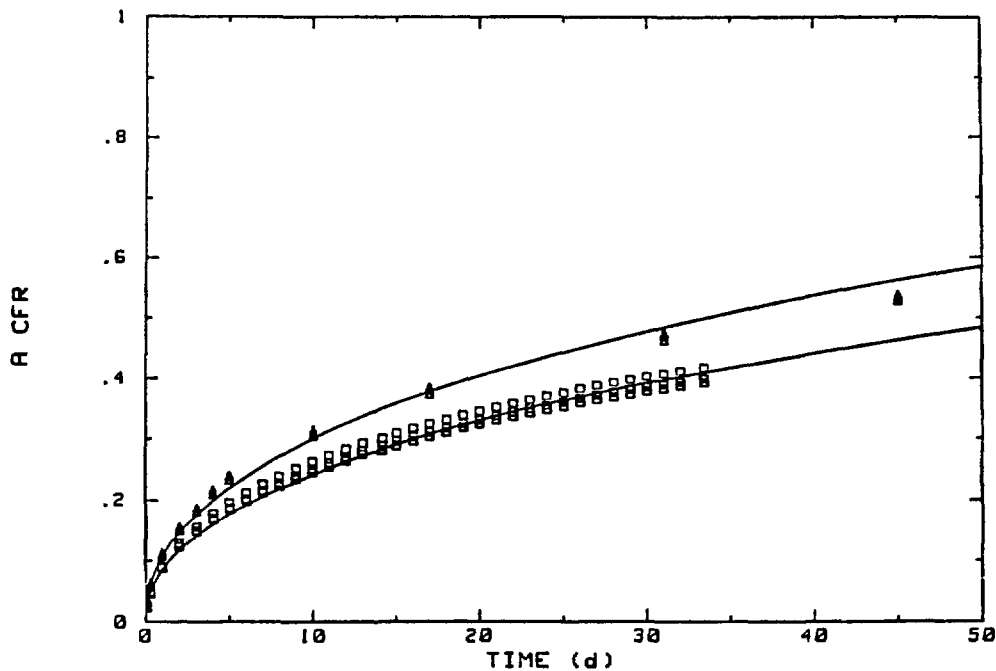


Figure 4.3 Experimental data and model results for Cs-137 from experiments with daily leachant replacements and with the ANS 16.1 schedule of leachant replacement.

The same approach was taken for Sr-85. CFL was plotted against the square root of time for three specimens leached with the ANS 16.1 test (Figure 4.4). A definite reduction in leach rate occurs when the replacement frequency becomes longer than one day. In this case, the cause is less ambiguous than with the Cs-137 data (see Figure 4.1) because the Sr-85 releases are far below the 20% depletion limit. Consequently, it is not depletion causing this drop in leach rate but inhibition of diffusion caused by increased concentration of strontium in the leachate, or retention of strontium on a new solid phase.

The finite cylinder model was also used on Sr-85 leaching data. The ANS 16.1 replacement schedule required treatment similar to that used for Cs-137. The data could only be modeled using two separate diffusion coefficients, one for the short term (5 days) and another for the longer term (Figure 4.5). Modeling data from the experiment with daily replacement was simpler and a good fit could be obtained with a single diffusion coefficient. In the case of frequent leachant changes, the leaching mechanism for Sr-85 can be seen to be diffusion.

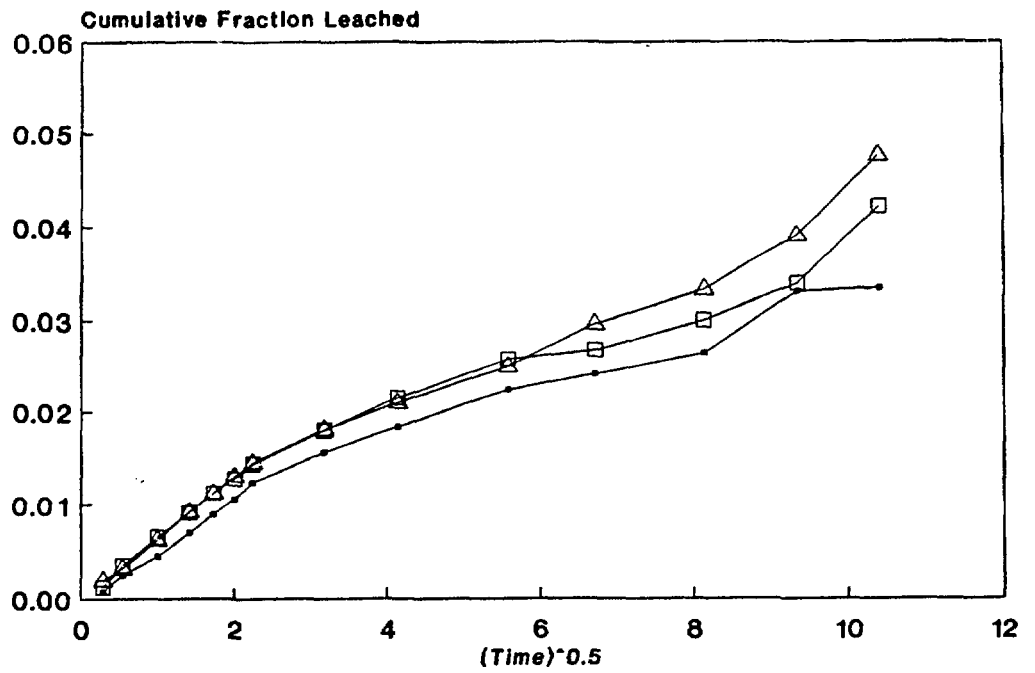


Figure 4.4 Triplicate baseline data for Sr-85 are the plotted against the square root of time. There is a change in leach rate after the first week of an ANS 16.1 test.

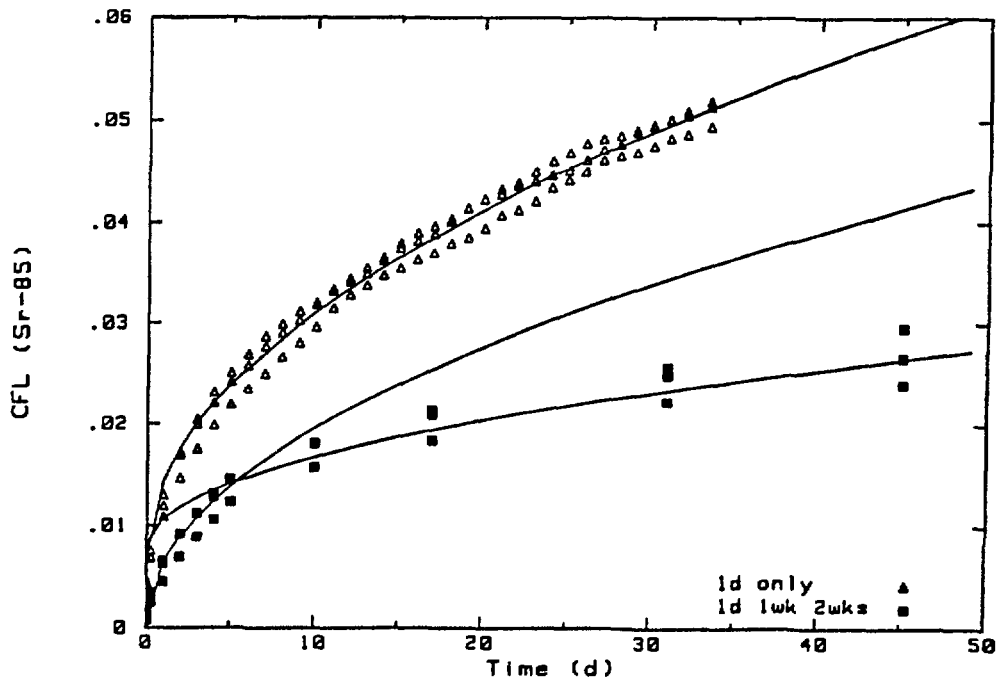


Figure 4.5 Modeling Sr-85 releases required two diffusion coefficients, one for the early portion of the experiment and one for long-term leaching. For the experiment with daily leachant replacements, the model fits with one diffusion coefficient.

Releases of Sr-85 are plotted against the square root of time in Figure 4.6 from three types of experiments: a semi-dynamic test with daily leachant replacement, a flow-through test, and an ANS 16.1 test with lengthening intervals of leachant replacement. The daily test data is linear throughout its duration, indicating that diffusion is the leaching mechanism. Results from one specimen in the flow-through test are similar to those from the daily experiment and are shown on the plot, but the other specimen is significantly different. This finding is believed to be due to mixing problems in the sample cell during the flow-through test. In Figure 4.6, the plots for the ANS 16.1 test and the flow-through test curve upward after about 0.05 CFL; this change was caused by samples cracking.

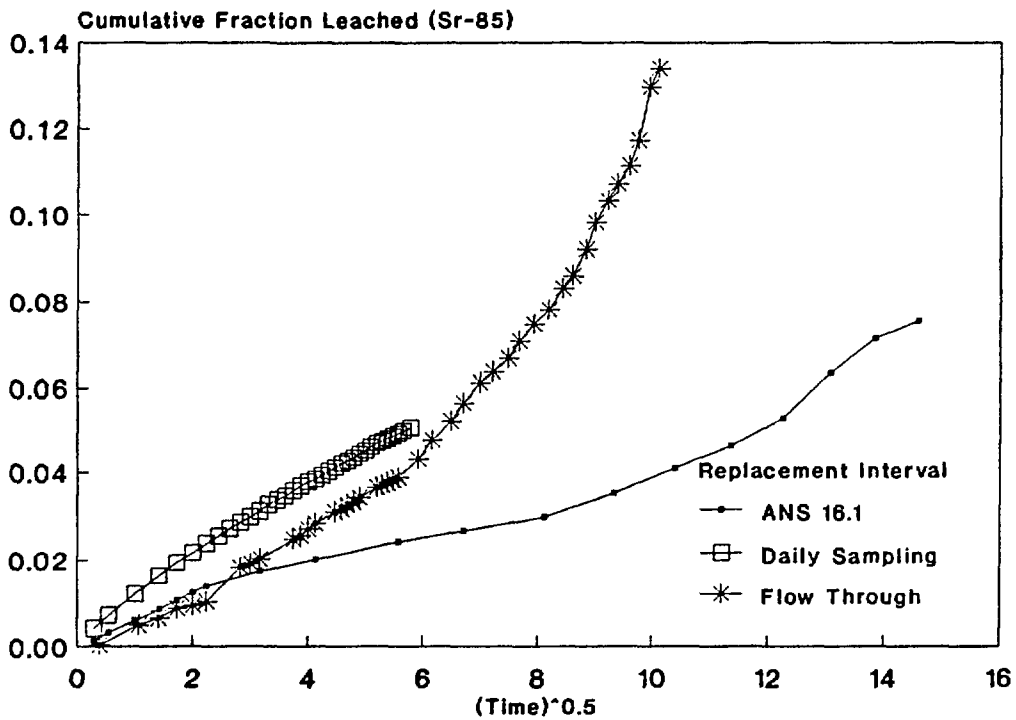


Figure 4.6 Data from three types of leach tests: ANS 16.1, semidynamic with daily leachant replacements and flow-through tests. These data are plotted against the square root of time which produces a linear plot if diffusion is the leaching mechanism.

While it is apparent that diffusion is the short-term leaching mechanism for Cs-137 and Sr-85 from cement/sodium sulfate waste forms, it is not necessarily correct for long times. Portland cement is a reactive material that changes with time. Alterations in porosity, in surface chemistry, and structure and in bulk composition influence leaching significantly. For example, absorption of Cs-137 and Sr-85 on carbonate minerals growing on the surface of cement wastes that are exposed to air has been observed [19]. This type of process is not necessarily important during leach tests at 20°C where efforts are made to minimize concentrations of dissolved species in the leachate. However, with high leachate concentrations, in static leach tests, or in tests at elevated temperatures, back-reactions could become significant. Consequently, when changing test conditions, care must be taken that no secondary reactions are introduced that cause an apparent reduction in leach rate.

4.3 Single Factors that Accelerate Leaching

Three single factors were identified earlier that could increase leach rates in a way that do not alter the leaching mechanisms of cement/sodium sulfate waste forms [1]. These are:

- 1) increased temperature
- 2) decreased size
- 3) increased replacement frequency of leachant/leachant volume

While no actual mass transport modeling was included in the report, some mechanistic interpretations were made, based on activation energies and linear correlation plots. Since then the finite cylinder model was applied to some of this data. This work, as well as the earlier findings, are discussed below as background to new results presented later.

4.3.1 Temperature. Temperature is expected to be an accelerating factor when diffusion is the dominant leaching mechanism, and should follow the Arrhenius function unless other experimental factors limit releases.

4.3.1.1 Portland Cement Paste. Elevated temperatures accelerate leaching of Cs-137 from hardened portland cement paste by as much as a factor of 30 at 70°C [30]. At 50°C, leaching is accelerated by a factor of 11 (Figure 4.7) as measured by the time required to reach a fraction release of 18% [30]. An Arrhenius plot of the diffusion coefficients calculated from this data (Figure 4.8), shows that even at 70°C, the leaching of Cs-137 fits the Arrhenius function. This is indicated by the 70°C data being on a line with the data from experiments run at other temperatures. Consequently, leaching of Cs-137 from portland cement paste containing radioactive tracers can be accelerated at 70°C and still maintains the leaching mechanism. The average activation energy calculated for Cs-137 is 5.4 kcal/mol, a value which is consistent with that for diffusion of simple ions in water.

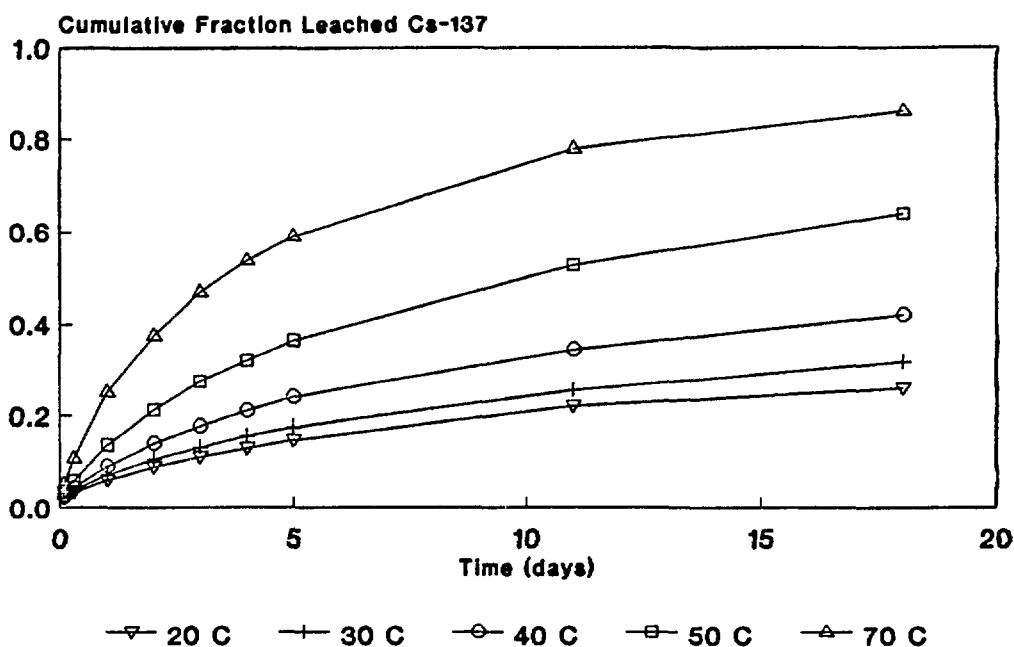


Figure 4.7 Cumulative fractions leached (CFL) of Cs-137 from portland type I cement paste specimens leached at 20°, 30°, 40°, 50° and 70°C.

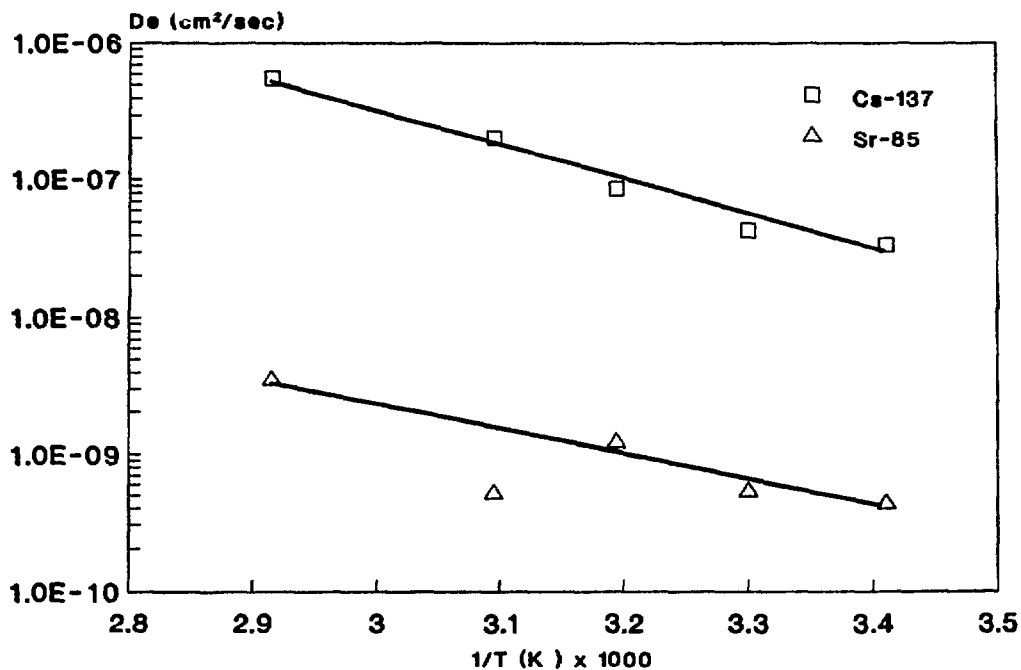


Figure 4.8 Arrhenius plot of the diffusion coefficients from portland cement paste containing Cs-137 and Sr-85, leached at 20°, 30°, 40°, 50°, and 70°C.

Releases of Sr-85 from specimens of cement paste are about two orders of magnitude lower than those of Cs-137, and the effect of increasing temperature is inconsistent (Figure 4.9). These releases are significantly altered by secondary reactions, making interpretation difficult. In later experiments, precautions were taken to keep some of these reactions (such as carbonation) from occurring. Diffusion coefficients calculated from the early part of these data were used to generate the Arrhenius plot for Sr-85 (Figure 4.8). With the exception of the data taken at 50°C, the diffusion coefficients fall where expected. Also, the Cs-137 and Sr-85 plots have similar slopes, which suggests that diffusion is the primary release mechanism in both cases. No Co-60 was observed in any leachate from these specimens. At the pH of cement waste forms (about 12), cobalt forms an insoluble hydroxide that cannot be leached.

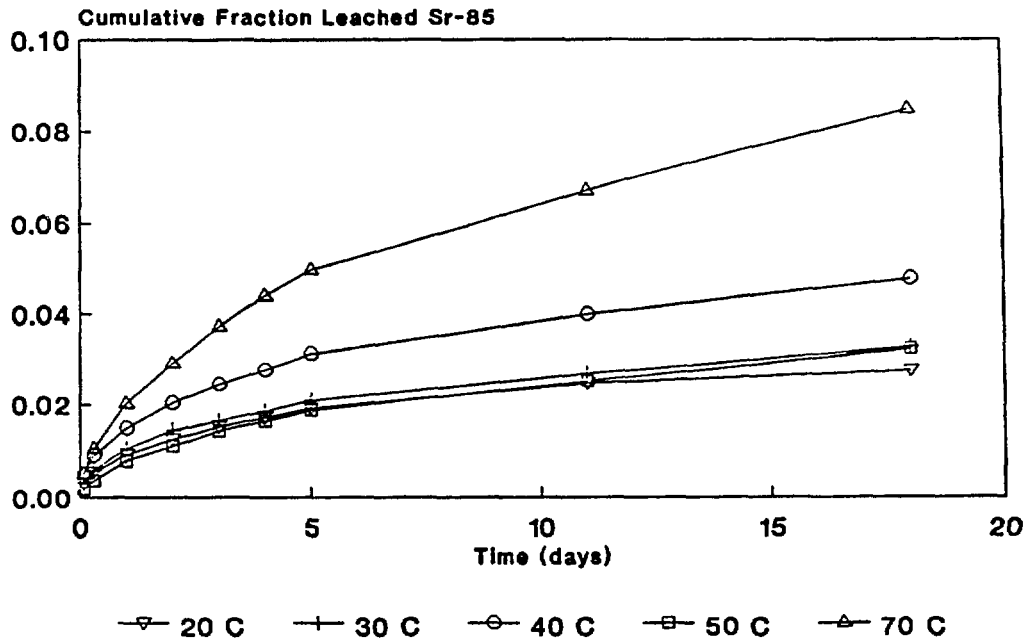


Figure 4.9 Cumulative fraction leached for Sr-85 from portland cement paste containing radioactive tracers at temperatures ranging from 20°C to 70°C.

4.3.1.2 Portland Cement Plus 5 wt% Sodium Sulfate. Leaching of portland cement containing sodium sulfate as a simulated waste can be accelerated by temperature but the results show a significant amount of variability between specimens (Figure 4.10). The scatter in the data is not related to the material itself since at 20°C there is little variability. Therefore, it must be related to experimental conditions, such as temperature or volume of the leachant. Increases in leach rate of cement/sulfate specimens are not as great, at any given temperature, as they are for cement paste specimens. This difference could be caused by increases in concentrations of dissolved species which would slow diffusion. Alternately, this reduction could be caused by changes in the structure of the material, particularly at its surface. What is believed to be the mineral ettringite (calcium aluminate trisulfate-32 hydrate) formed on the surface of specimens leached at 50°C, extensively altering the pore structure of the cement [1].

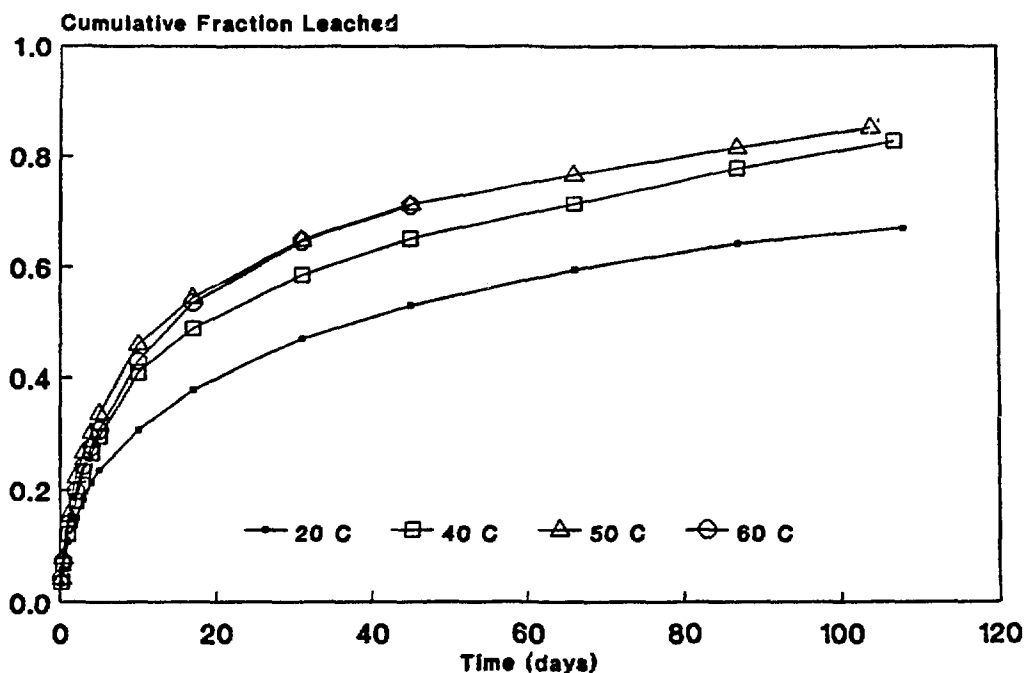


Figure 4.10 Cumulative fraction leached for Cs-137 vs time from portland I cement containing 5 wt% sodium sulfate at 20°, 40°, 50°, and 60°C.

The Arrhenius plot of Cs-137 leached at 20°, 40°, 50°, and 60°C (Figure 4.11) shows that at elevated temperature the Cs-137 diffusion coefficients are higher than at 20°C and the data at 20°, 40° and 50°C are linearly correlated. The 60°C data fall below the trend of the other temperatures, suggesting that leaching at 60°C is inhibited in some way (e.g., plugging of pores, precipitation, saturation effects of leachant). Depletion does not appear to cause this change, so it could indicate a change in mechanism at 60°C. It is more likely that the reduction in leach rate is caused by a change in structural (e.g., porosity) control on leach rate since the data for 50°C and 60°C follow the same curve shape. Activation energies were calculated at each interval using temperatures of 20°, 40°, and 50°C with an average activation energy of 5.6 kcal/mole for the first week of leaching (similar to activation energies calculated for leaching from cement paste).

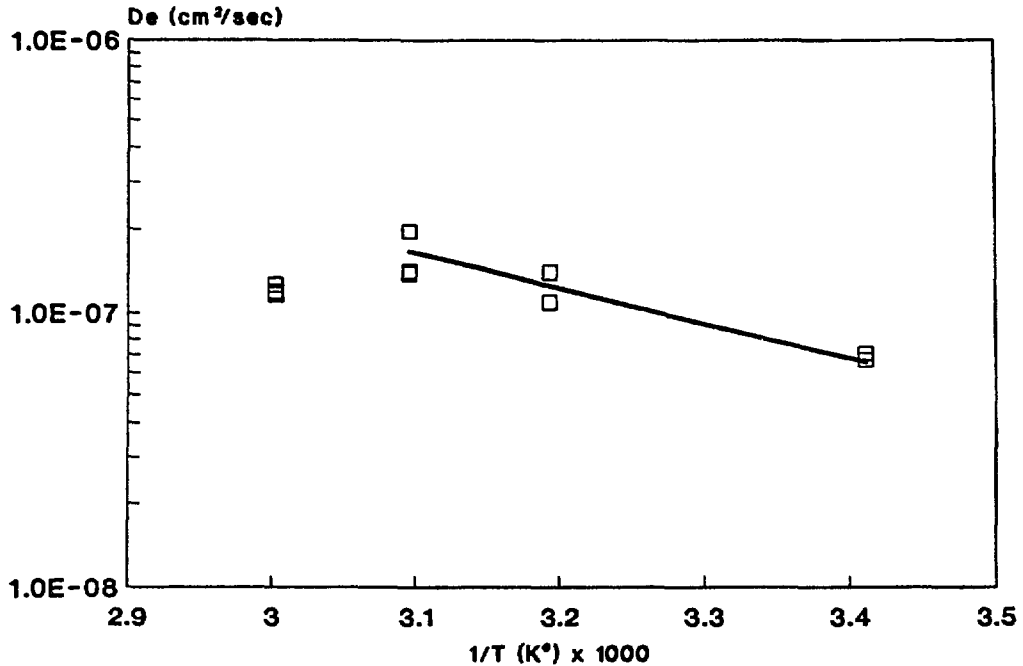


Figure 4.11 Arrhenius plot of Cs-137 leached from cement containing 5 wt% sodium sulfate showing diffusion coefficients as a function of the reciprocal temperature in Kelvins. Experiments were conducted at 20°, 40°, 50° and 60°C.

Leaching of Sr-85 from cement/sodium sulfate waste forms is also accelerated by increasing the temperature (Figure 4.12). This figure also shows that after the first week of the experiment (when the frequency of leachant replacement is changed to intervals longer than one day), the leach rate decreases dramatically. Depletion is not the cause, since the total release is less than 20%. Also, there is much less scatter in the data during daily leachant replacement intervals. The Arrhenius plot of Sr-85 (Figure 4.13) shows that leaching of Sr-85 increases consistently with increasing temperature up to 50°C, but at 60°C, leaching is much lower than expected. This data is calculated from the first week of leaching and, therefore, reflects releases during daily replacements. The diffusion coefficients for Sr-85 are about two orders of magnitude lower than those for Cs-137. This difference would cause less build up of Sr-85 in the leachate and may account for its more orderly behavior. Of particular importance is the observation that for both Cs-137 and Sr-85, releases at 60°C are lower than anticipated, indicating a change in leaching mechanism or change in the physical structure of the waste form between 50°C and 60°C.

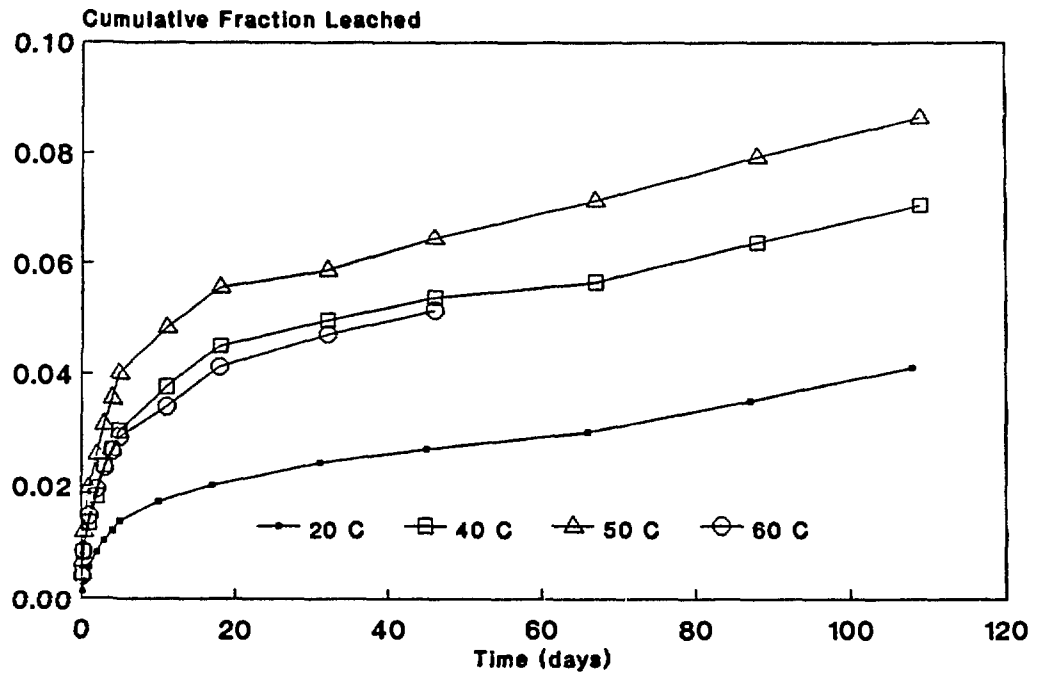


Figure 4.12 Sr-85 cumulative fraction leached vs time from portland I cement containing 5 wt% sodium sulfate at 20°, 40°, 50°C, and 60°C leached in deionized water.

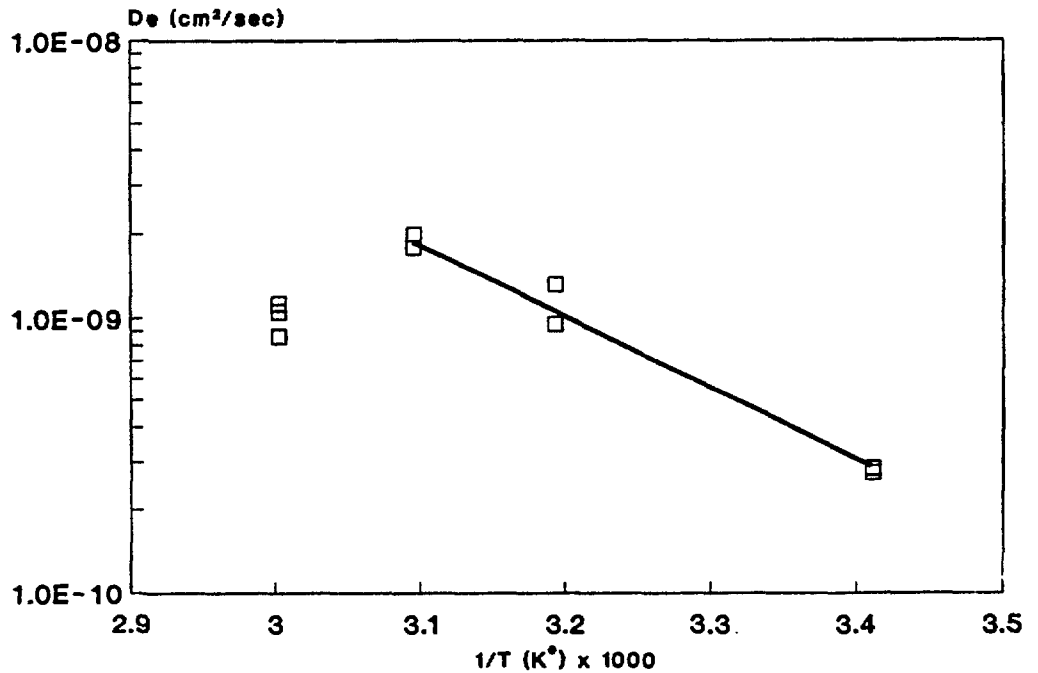


Figure 4.13 Arrhenius plot of Sr-85 showing diffusion coefficients as a function of the reciprocal temperature in Kelvins.

4.3.2 Specimen Size. The size of the specimen is also an acceleration factor for cement/sodium sulfate waste forms. This finding is expected if diffusion is the leaching mechanism since the diffusion coefficient is independent of sample size. A change in the volume to surface area (V/S) ratio from 0.84 (4.8 x 6 cm cylinders) to 0.42 (2.5 x 2.5 cm cylinders) resulted in a three-fold increase in the cumulative fraction releases (Figure 4.14). Also, this figure indicates that for these waste forms the intersample variation of leaching data is similar for small specimens and larger ones.

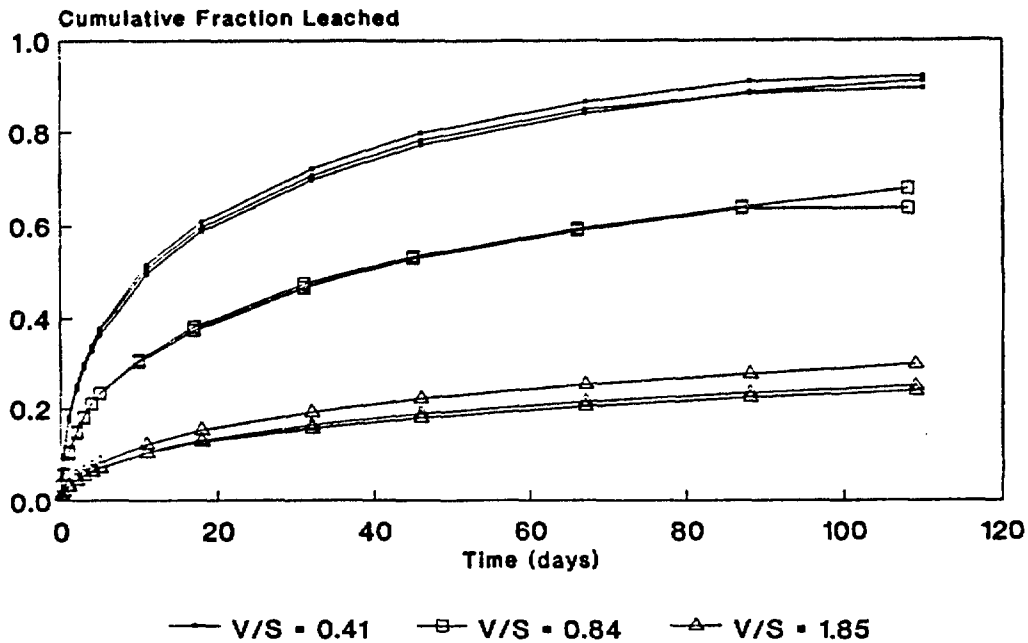


Figure 4.14 Cs-137 cumulative fraction leached vs time from portland I cement containing 5 wt% sodium sulfate at waste form volume to surface area (V/S) ratios of 0.41, 0.84 and 1.85. Samples were leached in deionized water at 20°C.

4.3.3 Volume of the Leachant. Increased volume or replacement frequency of the leachant can be an effective acceleration factor, but it is highly dependent on other experimental conditions and on the properties of the waste form itself. The effect of replacement

frequency was discussed in the section on modeling cement/sodium sulfate waste forms and will not be expanded on here. Volume of the leachant is an important factor that is explored in the subsequent section on combined acceleration factors.

4.4 Combined Acceleration Factors for Portland Cement Containing Sodium Sulfate

The work on single acceleration factors that was summarized in the previous section was used as the starting point for a continued investigation. The results reported in this section are from experiments in which combinations of acceleration factors were used to maximize leaching without altering its mechanism.

4.4.1 Cs-137 Results. Table 4.1 summarizes the experimental procedures and results for Cs-137 leaching as expressed by D_e , the effective diffusion coefficient. D_e was calculated from the slope of the line on a plot of cumulative fraction leached versus the square root of time.

Selected diffusion coefficients from Table 4.1, plotted in Figure 4.15, show the range of leaching obtained under different accelerated leach test conditions. Results from one of the baseline specimens are also plotted. Two points are important. One, these modeled curves are only useful up to about 95% release because they are based on the finite cylinder with a limited number of iterations. Second, increased intervals between the replenishment of the leachate appears to have caused the leach rate from the baseline experiment to drop off when the interval is three weeks. Consequently, the modeled curve (#3 in Figure 4.15) accurately predicts leaching from the baseline experiment in the early part of the data, but not after about 40 days. The modeled curves in the figure must be thought of as predicting results of accelerated experiments with frequent replacement of leachant. Consequently, experimental parameters need to be optimized, so that the experimental results match the modeling results.

TABLE 4.1

Diffusion Coefficients D_e for Cs-137
from Portland Cement + Sodium Sulfate Waste Forms

Leach Test	Volume (liters)	Temperature (°C)	Size D x H ¹ (cm)	Average D_e , Cs-137 (cm ² /s)
Semidynamic	6.5	50	5 x 7	2.5×10^{-7}
Static	6.5	50	5 x 7	2.3×10^{-7}
Semidynamic (daily)	3.0	50	2.5 x 2.5	1.6×10^{-7}
Static	1.3	50	5 x 7	1.3×10^{-7}
Semidynamic	6.5	60	5 x 7	1.3×10^{-7}
Semidynamic	0.3	50	2.5 x 2.5	1.2×10^{-7}
Semidynamic	1.3	60	5 x 7	1.2×10^{-7}
Static	6.5	60	5 x 7	1.2×10^{-7}
Semidynamic	0.3	50	2.5 x 2.5	1.1×10^{-7}
Static	6.5	50	5 x 7	8.5×10^{-8}
Static (CO ₂ -free)	6.5	50	5 x 7	7.8×10^{-8}
Static	1.3	20	5 x 7	4.8×10^{-8}
Static	6.5	20	5 x 7	4.8×10^{-8}
Semidynamic	1.3	20	5 x 7	4.4×10^{-8}

1 = Right cylinder
D = diameter
H = height

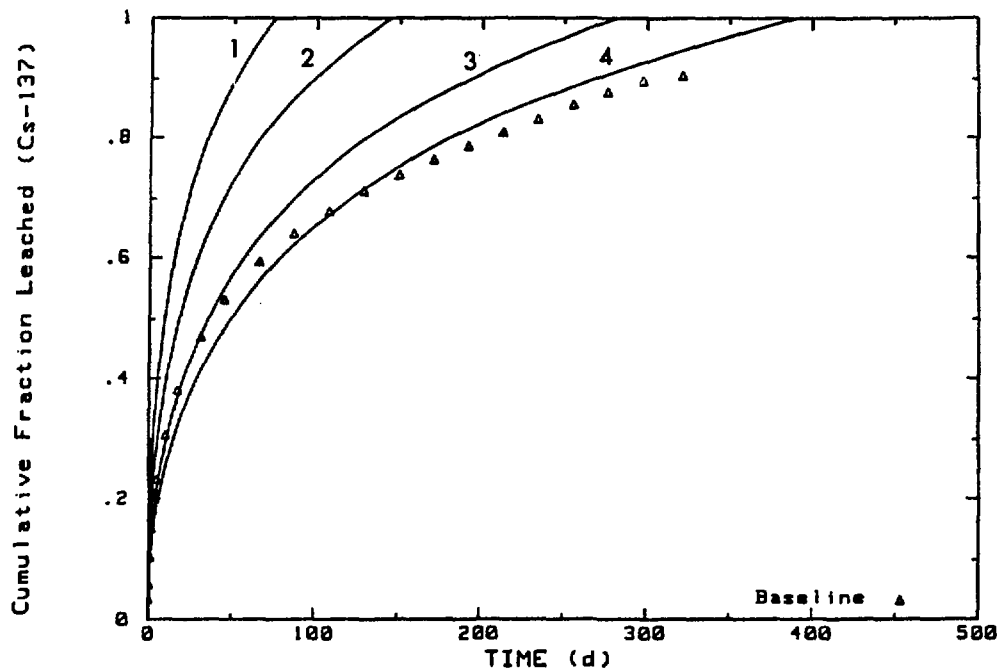


Figure 4.15 Curves are calculated from the finite cylinder model, using selected diffusion coefficients from Table 4.1 to show ranges of leaching obtained under different test conditions. Also shown are data points (the triangles) for the baseline leaching experiment run at 20°C in 1.3 liters of water.

The modeled curves give the range of releases expected from extrapolations of experimental data obtained in this program. Curve #1 is for a semidynamic leach test run at 50°C with 6.5 liters of distilled water used at each replacement. This combination gave the most acceleration of Cs-137 leaching. Curve #4 is for the lowest diffusion coefficient observed, which was from a static leach test at 20°C in 1.3 liters of distilled water. Curve #3 uses the diffusion coefficient for the first week of data from the baseline experiment, which was a semidynamic ANS 16.1 test at 20°C in 1.3 liters of water. While the early data is well represented by the modeled curve, the later portion of the modeled curve overestimates releases during the baseline experiment by about 12%. This overestimation is attributed to suppression caused by elevated concentrations of ions in solution during the prolonged replacement intervals.

The average results from the two experiments giving the greatest acceleration are shown in Figure 4.16. For comparison, data from the baseline experiment are also shown. The two

accelerated experiments gave similar results for Cs-137 with considerable overlap among the points, particularly before day 10. These experiments indicate that for Cs-137 a static test at 50°C can be used in place of a semidynamic test as long as the test runs no more than about 10 days and the volume of the leachant is 6.5 liters or more for 4.8 cm diameter x 6.4 cm height specimens. These conditions would give approximately a 5-fold acceleration. However, scatter among the triplicate points at the increased temperature is twice the scatter observed at 20°C. Using the average diffusion coefficients from the triplicate specimens in the semidynamic test (50°C, 6.5 liters water) to model the data to CFL=0.8, gives an acceleration factor of 8 compared to the baseline data (Figure 4.15).

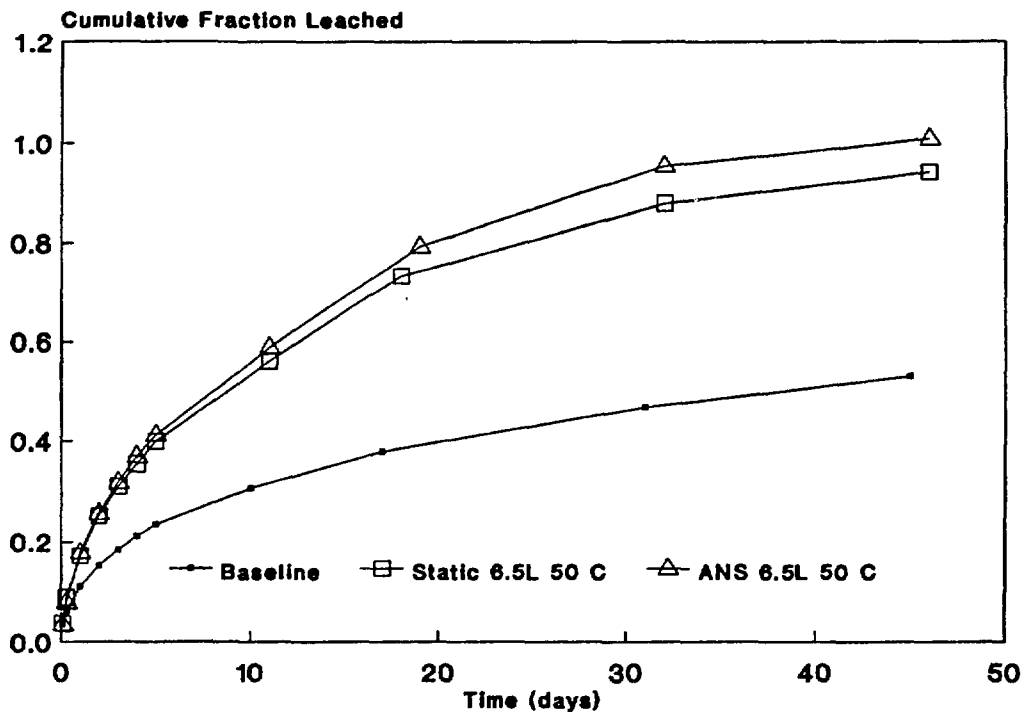


Figure 4.16 Data from the two experiments that gave the greatest amount of acceleration for Cs-137 are compared to the baseline (ANS, 1.3 liters, 20°C) data. Each point represents the average value of triplicate specimens.

Performing similar semidynamic experiments at 60°C gave diffusion coefficients that were lower than those obtained at 50°C (see Table 4.1) by a factor of two (Figure 4.17). This was

also the case for static leach tests, which used 6.5 liters of water (Figure 4.18). These observations, that Cs-137 releases are lower at 60° than at 50°C, were confirmed in separate semi-dynamic experiments by Na and K leached from the cement matrix itself (Figures 4.19 and 4.20). There are two possible explanations for this anomalous behavior which was not observed for plain cement containing radioactive tracers: 1) secondary reactions are taking place that incorporate these elements in the reaction products, and 2) changes are developing in the physical structure, such as porosity of the matrix.

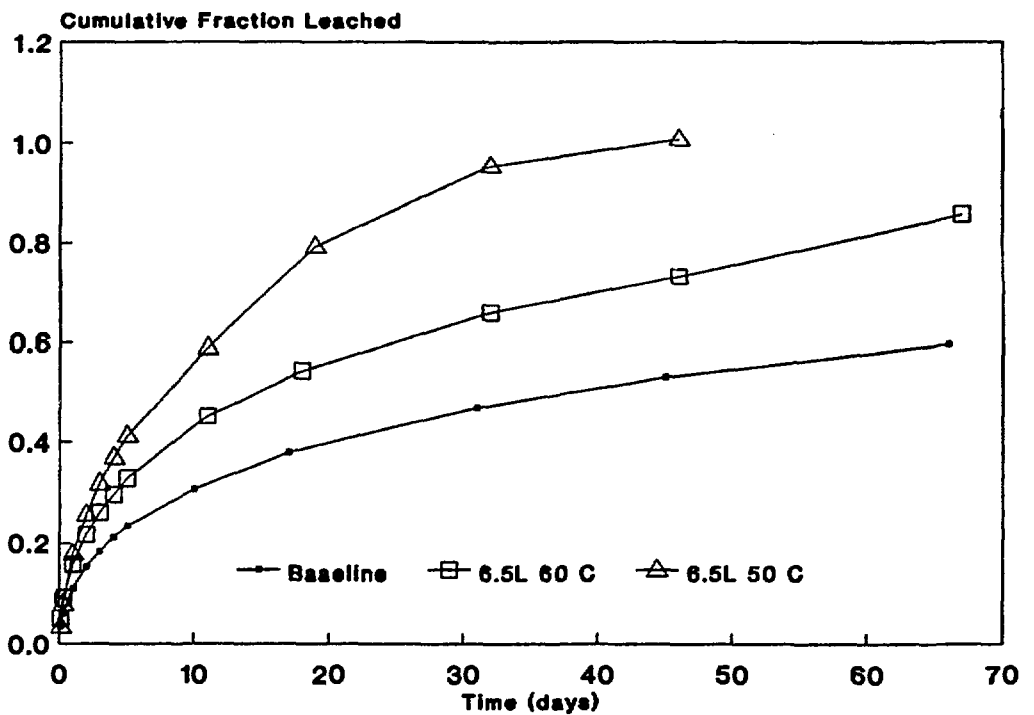


Figure 4.17 Average cumulative fraction release curves for Cs-137 show that leaching at 60°C is substantially lower than at 50°C during a semidynamic leach test.

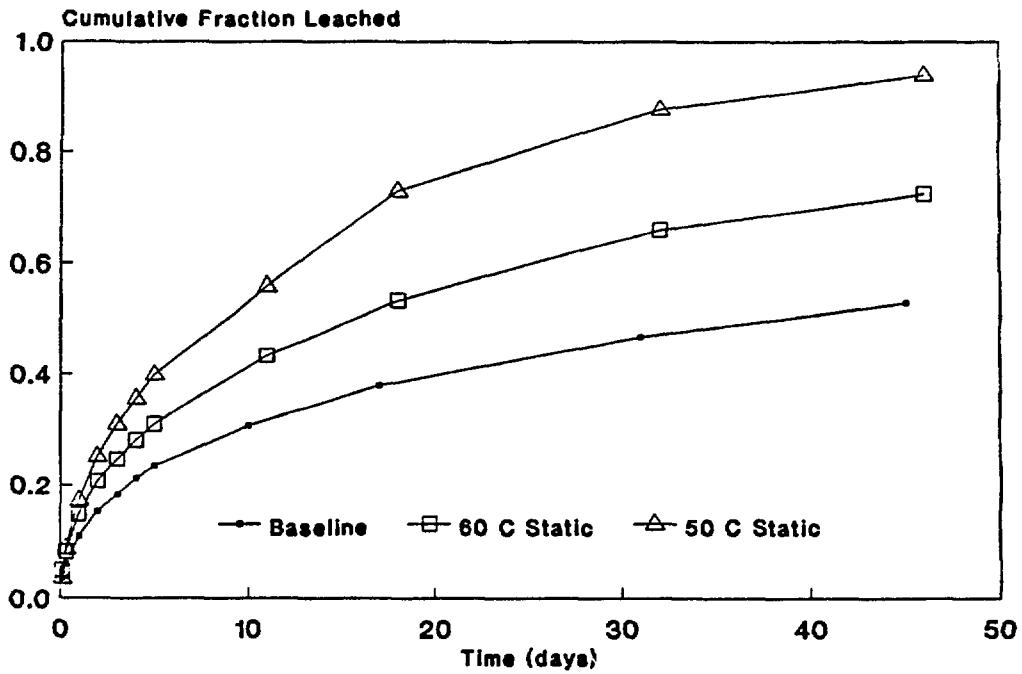


Figure 4.18 Leaching of Cs-137 is lower at 60°C than it is at 50°C in static leach tests of cement/sulfate waste forms.

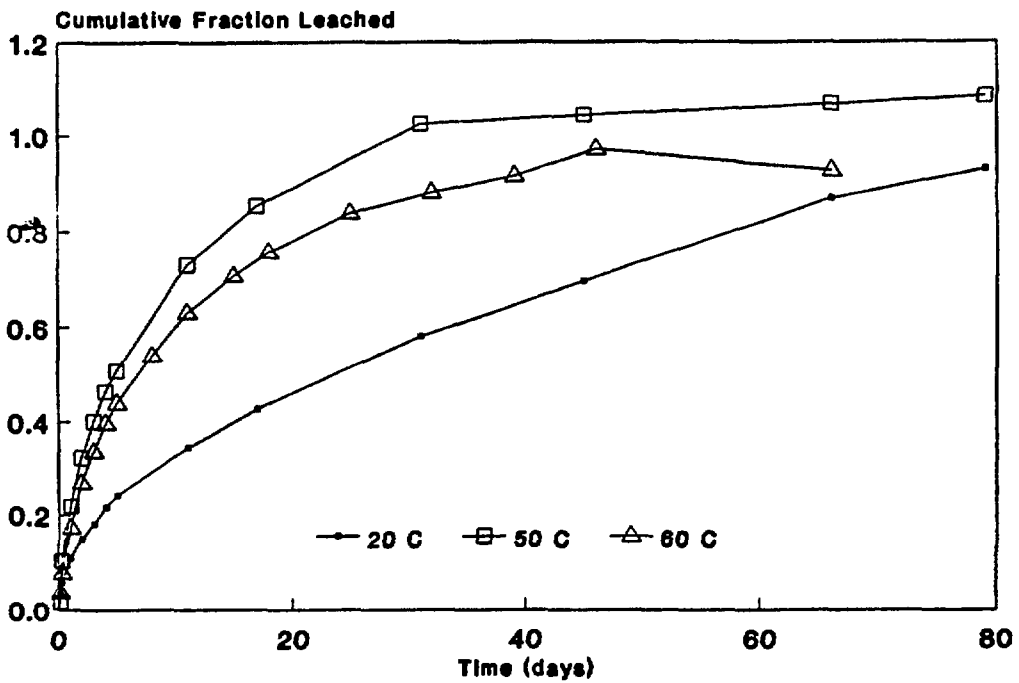


Figure 4.19 Leaching of sodium from cement/sulfate specimens is lower at 60°C than it is at 50°C in static leach tests.

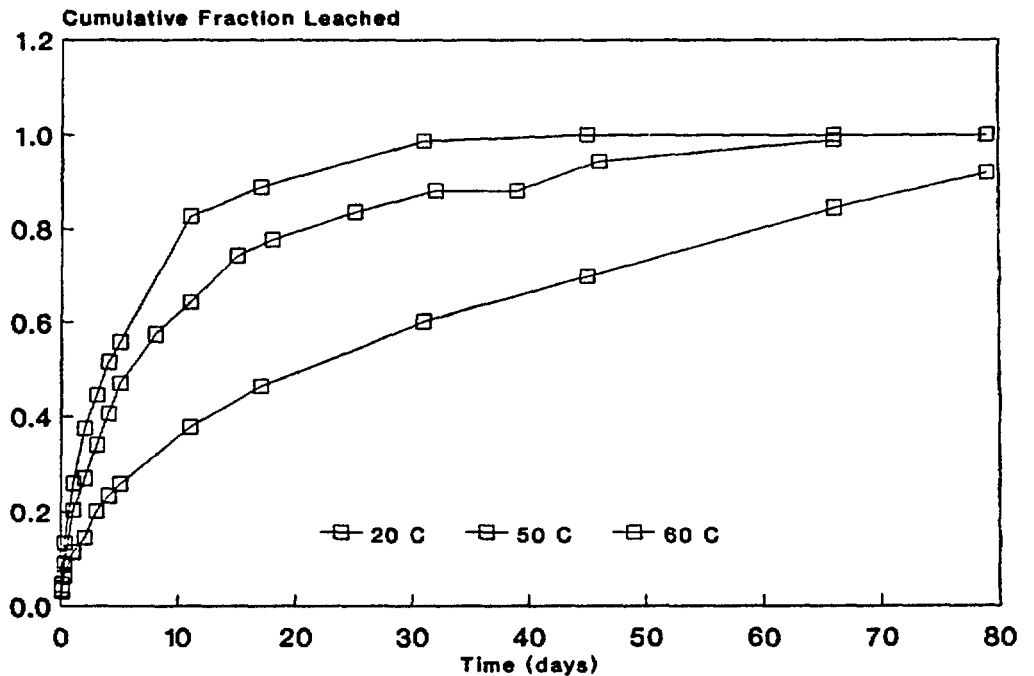


Figure 4.20 Leaching of potassium is lower at 60°C than it is at 50°C in static leach tests.

To further analyze the Cs-137 data, the results of static and semidynamic leach tests were plotted (Figure 4.21) and curves for the finite cylinder model were fit through the data. The curves are based on averages of the effective diffusion coefficients. The data from the two experiments run at 60°C have little scatter and the model fits them very closely. These data still represent the diffusion of Cs-137, although it is severely inhibited, perhaps by a change in pore structure. Results obtained at 50°C also show that leaching is by diffusion during the first 11 days of the experiment. Thereafter, the scatter becomes larger and the data tend to rise above the modeled curve. Cracking may have affected some of the specimens, leading to this variability. Nevertheless, the model fits the data from the early part of the experiment when the leachant was replenished daily.

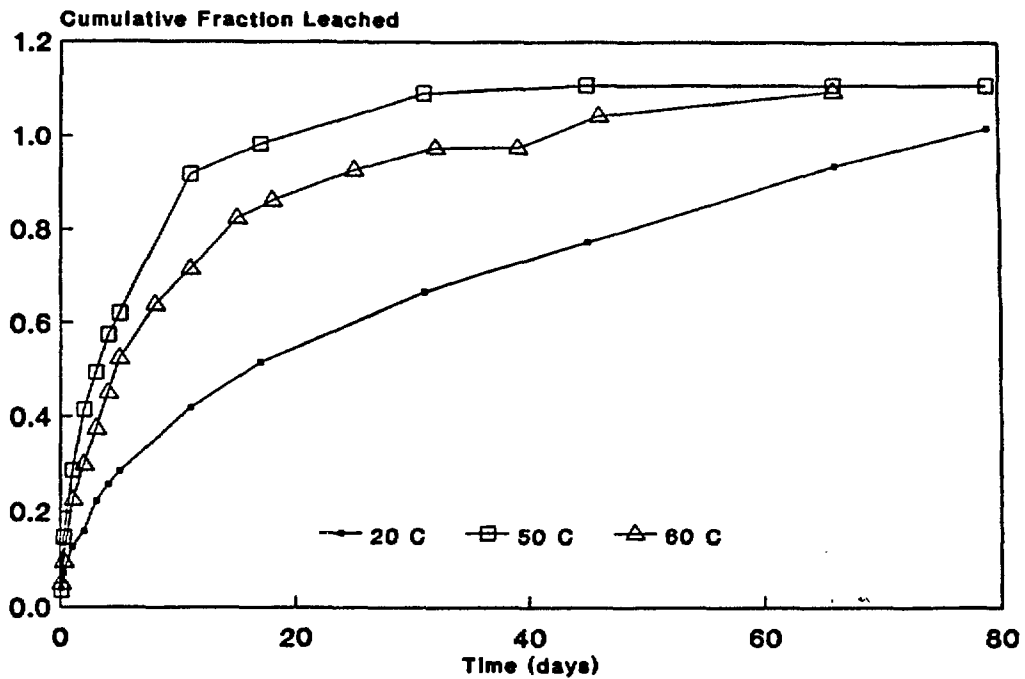


Figure 4.21 Data for Cs-137 from cement/sulfate specimens during static and semidynamic leach tests at 50° and 60°C. The solid lines are calculated from the finite cylinder model.

Results of experiments using smaller specimens (2.5 x 2.5 cm) are shown in Figure 4.22 for Cs-137. The average D_e values are given in Table 4.1, one of which represents the optimized accelerated leach test, run at 50°C in 3 liters of distilled water (the ratio of leachant volume to waste form surface area was larger than for any other experiment). This experiment demonstrated that additional leachant volumes were unnecessary for Cs-137, since releases were the same in 3 liters with daily replacements as they were in 0.3 liters at 50°C with less frequent replacements.

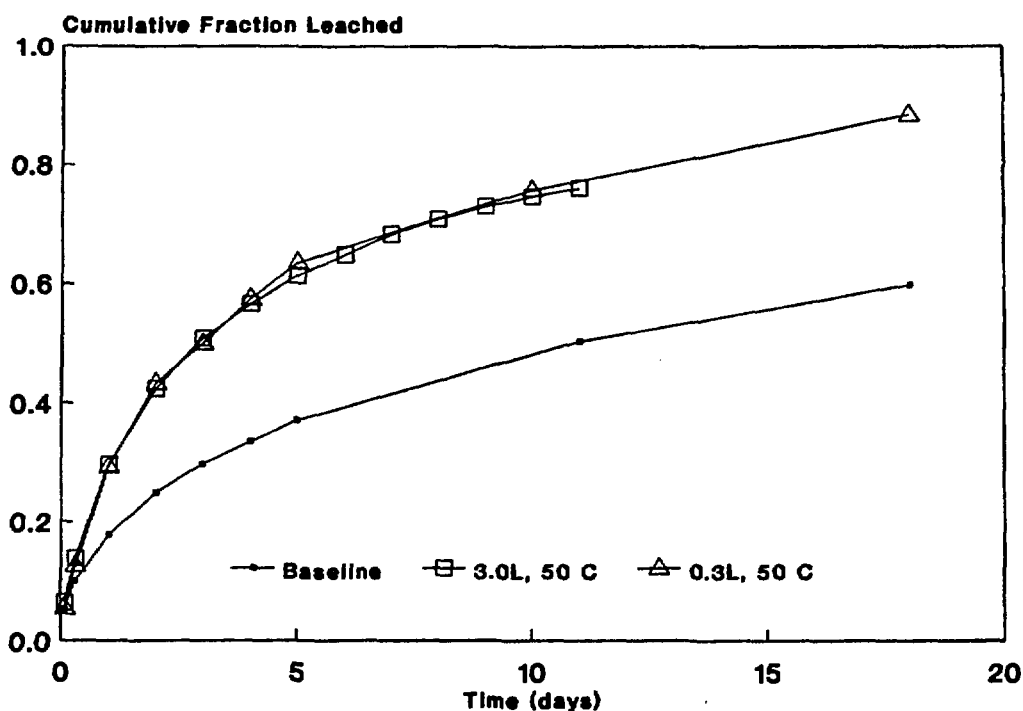


Figure 4.22 Comparison of Cs-137 releases from small cement/sulfate specimens (2.5 x 2.5 cm) leached at 20°C and at 50°C in different leachant volumes. Cs-137 releases are relatively insensitive to leachant volumes.

In the "modeling" part of this section, it was shown that the finite cylinder approach effectively models Cs-137 releases from experiments run at 20°C with daily replacements of leachant. The data from the optimized leach test, described previously (50°C, 2.5 x 2.5 cm specimens and 3 liters of water replaced daily) were compared to the finite cylinder model (Figure 4.23). The model fits the data closely until about CFL=0.65 (65% release), then the model slowly overestimates leaching. While the model remains within the intersample variability at 75% release, the trend of the model is moving away from the data. This trend may be the result of the particular finite cylinder model used which tends to overestimate at high CFL's. A more sophisticated finite cylinder model may fit the data better. Comparing the data from this experiment with the baseline data (20°C, 5 x 7 cm specimens in 1.3 liters of water) shows the degree of acceleration achieved. Releases obtained in 11 days from the accelerated test required about 200 days from the baseline, an acceleration factor of approximately 18.

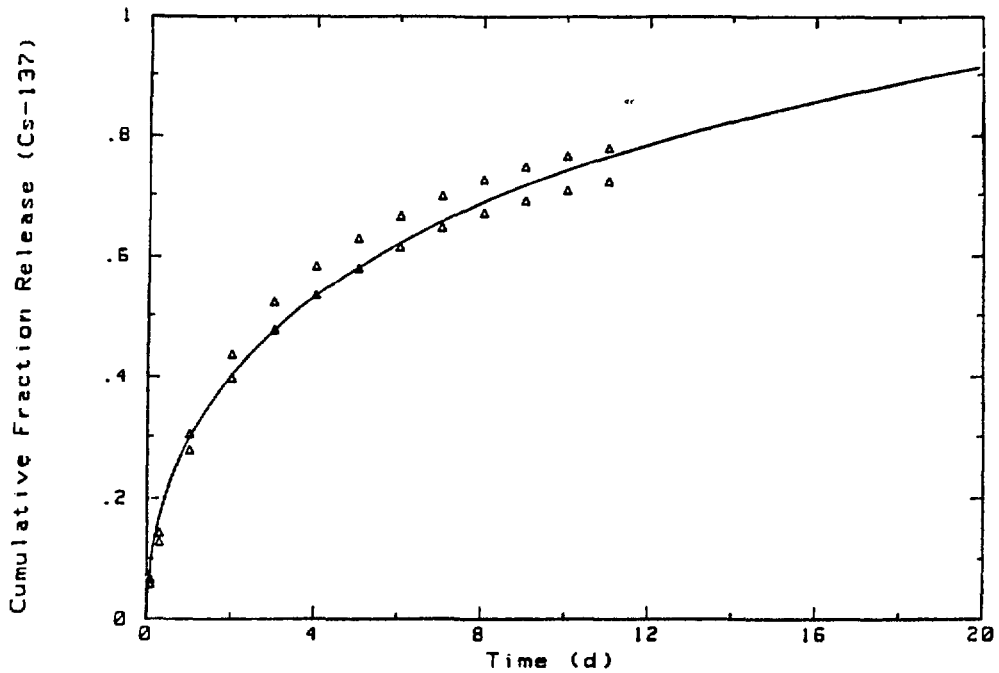


Figure 4.23 Data from a leach test using 2.5 x 2.5 cm cement/sulfate specimens at 50°C in 3 liters of water with daily leachant replacement. The finite cylinder model may be overestimating releases after CFL=0.65.

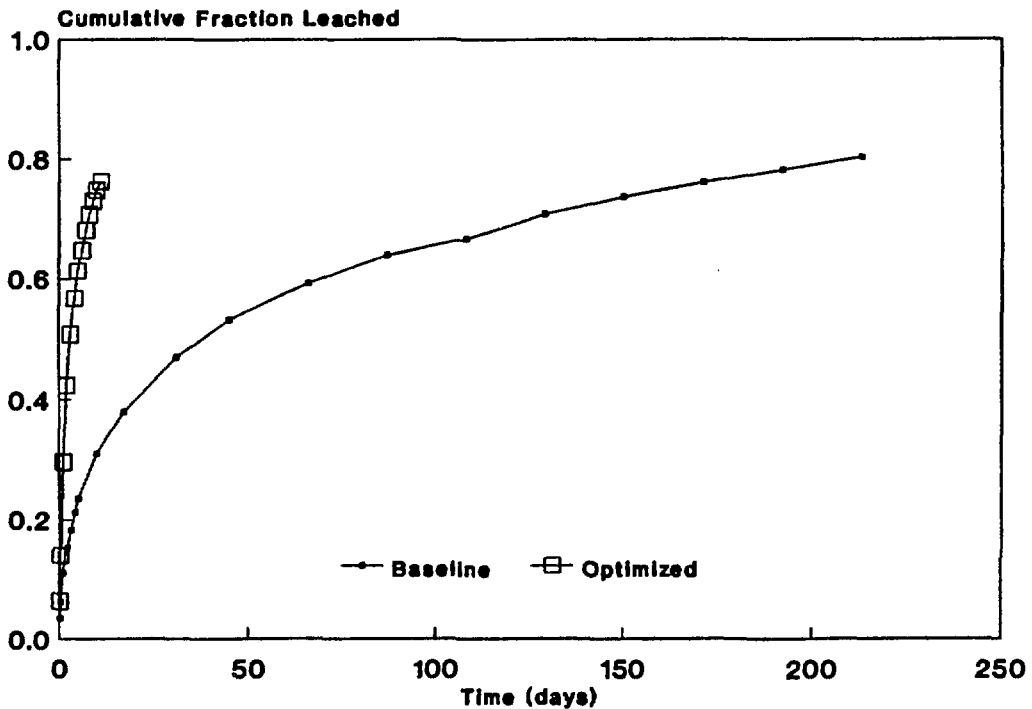


Figure 4.24 Cs-137 results from the optimized accelerated leach test for cement/sulfate specimens are compared to results from the baseline test. The acceleration factor is approximately 18.

Secondary reactions (such as those that may be affecting leaching at 60°C) are those that influence the concentrations of species in leachate after leaching from the waste form has taken place. These reactions could be 1) plate-out onto container walls, 2) precipitation, or 3) reactions involving the surface of the waste form, causing changes in its porosity or mineralogy. In systems containing cement, the latter two changes often occur due to formation of CaCO_3 from reactions with the CO_2 in the air. The possibilities of plate-out or precipitation were eliminated when the final volume of the leachant was acidified in the leaching container after the waste forms were removed at the end of the experiments. While sizable amounts of CaCO_3 were present, no significant quantities of Cs-137 were added to solution when the CaCO_3 was dissolved. This leaves open the possibility of reactions occurring on the surface of the waste form that keep Cs-137 from entering or remaining in solution.

Physical change in the structure of the matrix itself can alter leach rates. For example, cracking increases leach rates while a reduction in porosity slows leaching. Growth of new mineral phases in the waste form arising from reactions between SO_4^{-2} anions and cement components fills in large pores in waste forms [1,30]. This reaction may be enhanced at 60°C as compared to 50°C since earlier work indicated that a change in leaching mechanism takes place around 60°C [30]. No change was observed for cement paste specimens leached at 60°C (see Figure 4.11). The presence of Na_2SO_4 may have some effect on the chemistry of the leaching process, and direct observation of changes in pore structure due to new phases in specimens that contain SO_4 supports this idea [1,30]. While the evidence is not conclusive, it is reasonable to attribute the lowering of leach rates at temperatures of 60°C (as compared to 50°C) to changes in physical structure of the waste forms as a result of reactions with Na_2SO_4 .

4.4.2 Sr-85 Results. Results of Sr-85 leaching from experiments using combined acceleration factors are summarized in Table 4.2 as average diffusion coefficients. They are ranked in order of the fastest leach rate (largest D_e). Two tests with the largest diffusion coefficients were both semidynamic and were run at 60°C.

Table 4.2

Diffusion Coefficients D_e for Sr-85 from
Portland Cement + Sodium Sulfate Waste Forms

Leach Test	Volume (liters)	Temperature (°C)	Size D x H ¹ (cm)	Average D_e , Sr-85 (cm ² /s)
Semidynamic	6.5	60	5 x 7	2.2×10^{-9}
Semidynamic (daily)	3.0	50	2.5 x 2.5	1.1×10^{-9}
Semidynamic	1.3	60	5 x 7	1.0×10^{-9}
Static	6.5	60	5 x 7	8.4×10^{-10}
Semidynamic	0.3	50	2.5 x 2.5	6.8×10^{-10}
Static	6.5	50	5 x 7	3.1×10^{-10}
Semidynamic	1.3	20	5 x 7	2.6×10^{-10}
Static (CO ₂ -free)	6.5	50	5 x 7	1.4×10^{-10}

1 = Right cylinder
D = diameter
H = height

As shown in Figure 4.6 of the "Modeling" part of this section, leaching of Sr-85 from cement/sodium sulfate waste forms is controlled by diffusion and is optimized at 20°C by daily replacements of leachant. With longer replacement intervals, diffusion is still the leaching mechanism but the rate is reduced significantly. This effect is much more pronounced for Sr-85 than for Cs-137.

Accelerated leaching of Sr-85 from cement containing sodium sulfate requires larger volumes of leachant than for Cs-137 (discussed below). The temperature constraint of 50°C required by Cs-137 does not seem to be necessary for Sr-85, but this is being investigated further. Optimized leaching conditions for a specimen containing both radionuclides are a 2.5 x 2.5 cm specimen in 3 liters of distilled water (changed daily) at 50°C. These conditions give an average diffusion coefficient of $1.06 \times 10^{-9} \text{ cm}^2/\text{s}$ for Sr-85. Figure 4.25 shows results from an optimized accelerated leach test compared to results from a baseline test. The acceleration factor is approximately 17, similar to that of Cs-137. The accelerated leach test results for Sr-85 can be modeled by the finite cylinder model. The leaching results of one specimen in the accelerated test indicates that some cracking began to take place at $\text{CFL} \approx 0.05$. One of the baseline specimens cracked at $\text{CFL} \approx 0.04$, giving the anomalous jump in the data at 130 days.

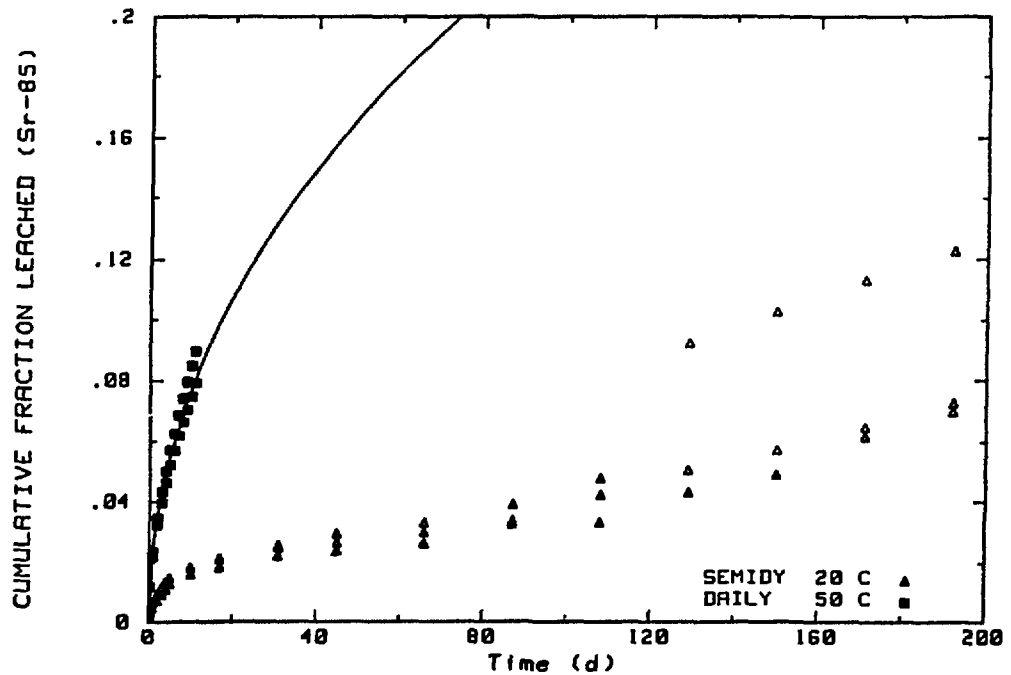


Figure 4.25 Data from two sets of portland cement specimens containing 5 wt% sodium sulfate. The optimized accelerated test is indicated by the filled squares and has an acceleration factor of about 17 compared to the baseline data. The finite cylinder model result is shown as the line through the optimized test data.

Comparing the data from two experiments (Figure 4.26) shows the effect of different volumes of leachant at 60°C. At CFL=0.05 (5% release), there is a factor of 4 to 5 increase in leaching with a volume of 6.5 liters per interval compared to 1.3 liters; the difference in volume has a significant effect, even during daily replacements. The solid curves are calculated with the finite cylinder model and accurately follow the data during the daily replacement intervals. The model then projects cumulative fraction release values as if the daily replacements had continued. During the first 6 days there were 7 intervals, so the experiment with the 6.5 liter volume used 45.5 liters of water while the experiment with 1.3 liters used 9.1 liters. This made a substantial difference of more than a factor of 2 in diffusion coefficient.

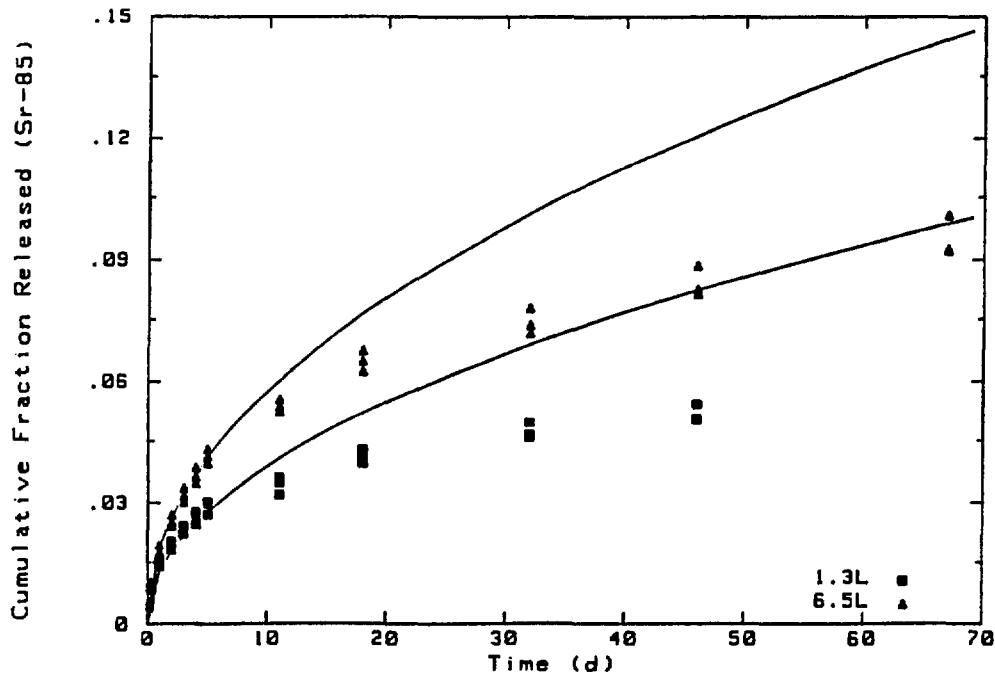


Figure 4.26 Releases of Sr-85 from cement/sulfate waste forms during two semidynamic experiments run at 60°C but having different leachant volumes. The finite cylinder model was used to generate the two curves shown.

Leaching of Cs-137 using static tests as well as other types of tests showed that releases are greater at 50°C than at 60°C. This finding was confirmed by data for potassium and sodium. The data for Sr-85 from static experiments run at 50° and 60°C with 6.5 liters of water

(Figure 4.27) show a different type of behavior. Sr-85 leached steadily at 60°C during the first week of the experiment in a manner that is diffusion-controlled. The modeled curve is for a diffusion coefficient that is identical to the lower curve on Figure 4.26 for the 1.3 liter semidynamic experiment. Both experiments had similar total volumes of water for the first week (7.2 liters compared to 6.5 liters) which resulted in similar diffusion coefficients. However, later in the 60°C experiment, Sr-85 releases leveled off or decreased slightly. The 50°C data behaved in the same way but earlier in the experiment, with Sr-85 activities in the leachate clearly declining for one specimen. This behavior can only be explained by a secondary reaction that removes Sr-85 from solution. Presumably, it is precipitated with CaCO_3 .

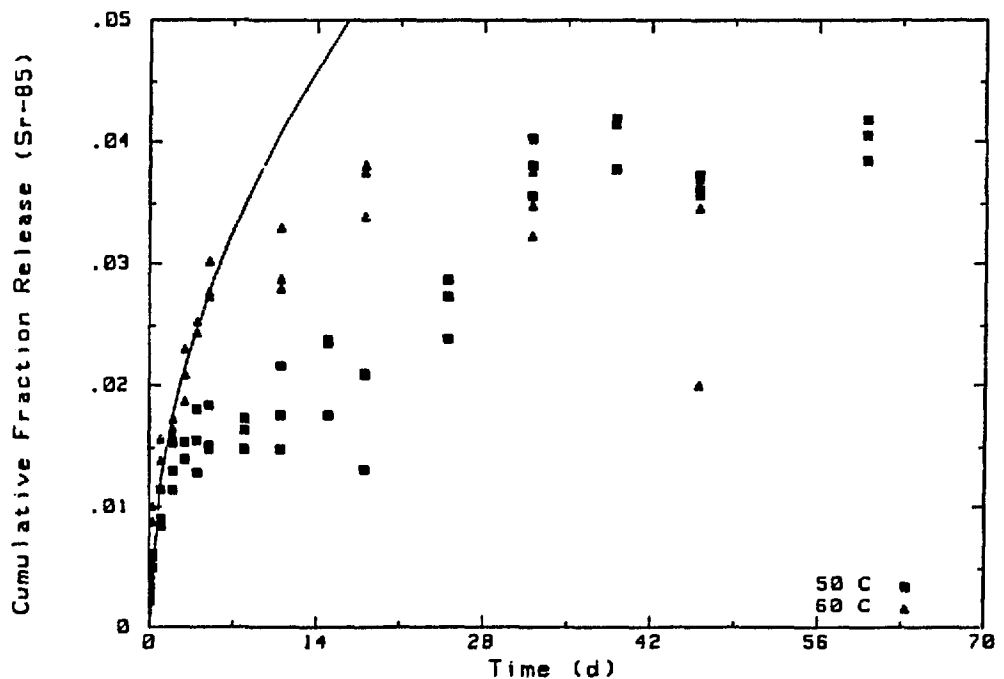


Figure 4.27 Sr-85 releases from cement/sulfate waste forms during static experiments at 50° and 60°C. The solid line is the result of the finite cylinder model for the first 6 days of leaching at 60°C.

Because the leachate rapidly becomes basic when cement is leached, it becomes a sink for CO_2 and readily absorbs the gas from air. This process leads to the formation of carbonic acid, bicarbonate and, when Ca is available, to CaCO_3 . Carbonate formation was observed to occur on cement paste specimens leached in distilled water and to have some effect on potassium and, by analogy, on Cs-137 profiles in the waste form [19]. Moreover, in seawater, rapid inhibition of Sr-85 releases were observed after heavy carbonation of waste form surfaces occurred [31]. To explore this problem, a set of static experiments were run at 50°C under conditions that were designed to minimize CO_2 intrusion from the air.

Results of these experiments (Figure 4.28) show no difference in radionuclide releases between the regular static experiments and those that were CO_2 -free. When calcium is analyzed for a replicate set of experiments conducted at 20°C and 50°C (Figure 4.29), there is no change in dissolved calcium concentration at 20°C under CO_2 -free conditions. However, at 50°C , there is a 50% increase in dissolved calcium in the CO_2 -free experiments as compared to the 50°C experiment that is open to air.

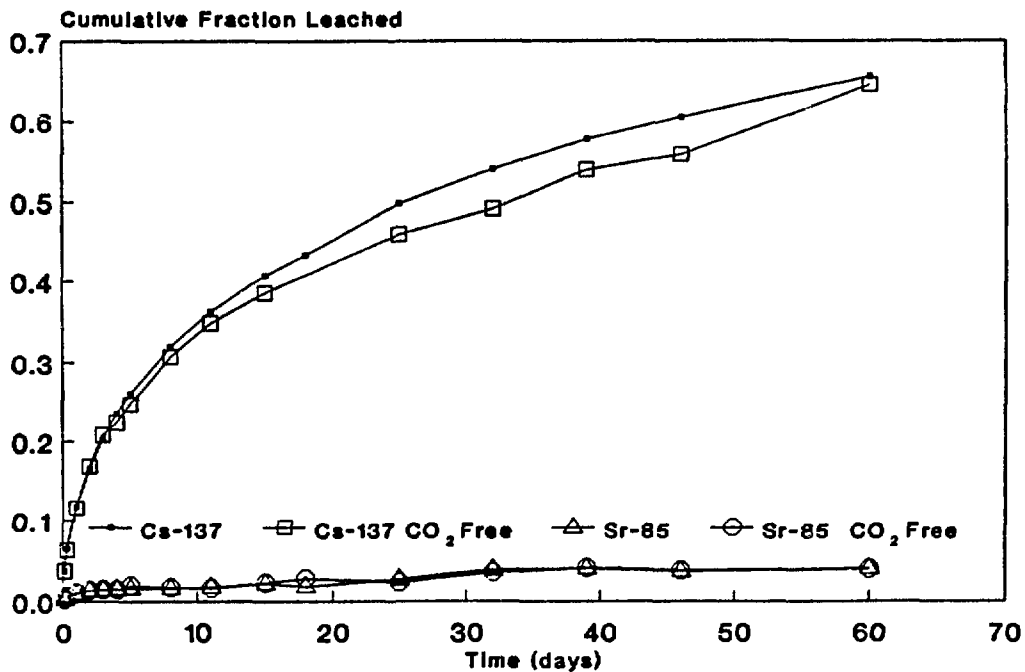


Figure 4.28 Cs-137 and Sr-85 leaching from static experiments that are CO_2 -free or exposed to air.

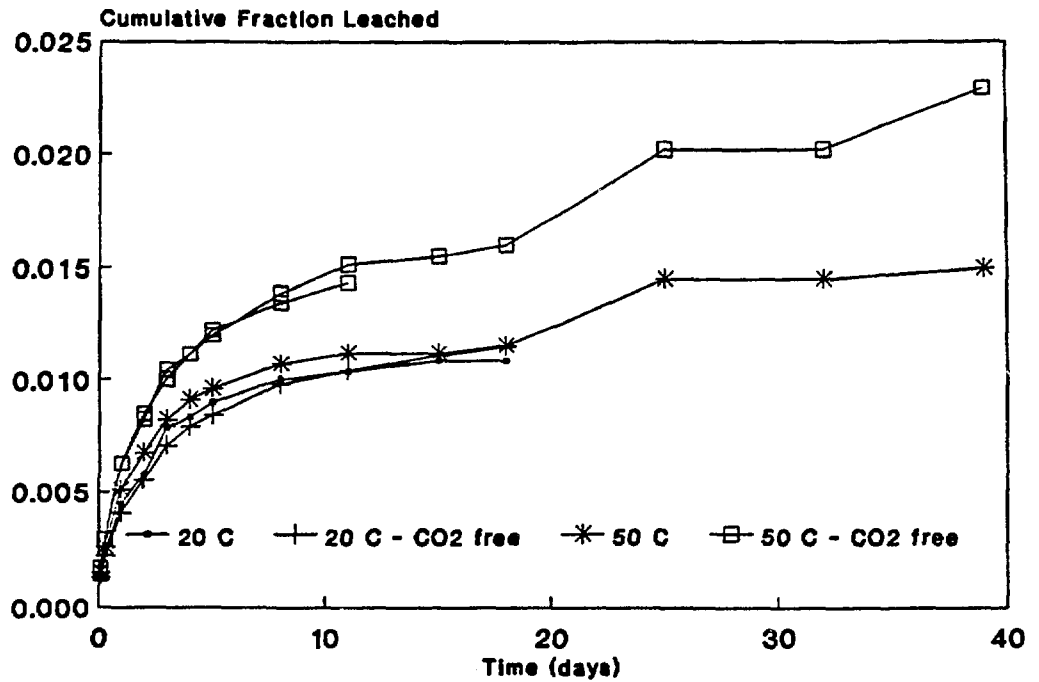


Figure 4.29 Calcium cumulative fraction leached at 20° and 50°C in static leach tests open to air and CO₂-free. Specimens are portland cement containing 5 wt% sodium sulfate.

Since leachate alkalinity can be a measure of dissolved carbonates, it is also related to formation of CaCO₃. Alkalinity, however, was only slightly altered by CO₂-free conditions (Figure 4.30). There was no effect at 20°C.

At 50°C the alkalinity from the CO₂-free experiment was slightly higher than the alkalinity in the experiment exposed to air. This is reasonable considering that precipitation of CaCO₃ will use up carbonate in solution and will also use OH⁻ ions, which are a major source of alkalinity that leaches from cement.

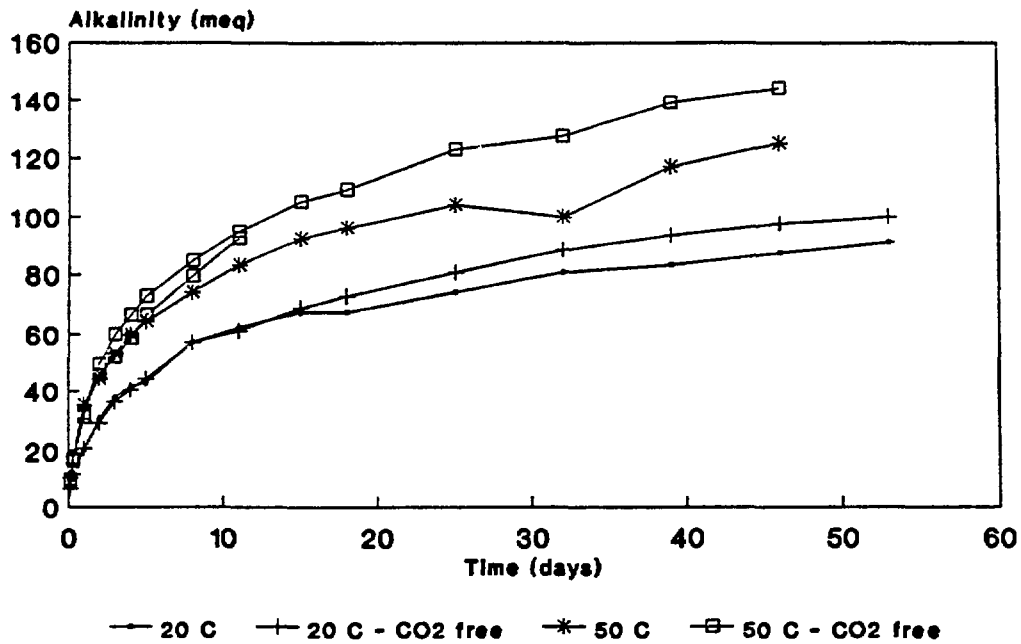


Figure 4.30 Alkalinity in leachate at 20° and 50°C in static tests open to air and CO₂-free.

While there is an effect on calcium concentrations in the leachate due to the presence of available CO₂, formation of CaCO₃ in this case does not have any influence on Cs-137 and Sr-85 activity in solution in the leachate.

4.5 Conclusions

The leaching results for Cs-137 and Sr-85 from cement incorporating sodium sulfate were modeled by using the mathematical equation for bulk diffusion. Diffusion coefficients for each experiment were computed. Agreement of results for samples of varying size were within a factor of two. Linear Arrhenius behavior for the diffusion coefficients was observed at temperatures of 20° to 50°C.

Leaching of Cs-137 from cement containing sodium sulfate as a simulated waste can be accelerated by temperatures up to 50°C, giving an acceleration factor of 18. Above that temperature, a change in mechanism takes place that causes a decrease in leach rate.

Additional volume is advisable at elevated temperatures, but Cs-137 is not very sensitive to this parameter. Releases of Cs-137 can be modeled using the finite cylinder model and long-term projections can be made.

Releases of Sr-85 can also be accelerated possibly to higher temperatures than can Cs-137. Up to 50°C, there is no apparent change in mechanism. Above that, the evidence is conflicting. Leaching of Sr-85 from cement/sodium sulfate waste forms requires larger volumes of water than does Cs-137. For 5 x 7 cm waste forms at 50° or 60°C a minimum of 6.5 liters of leachant (replaced daily) is required. Releases of strontium can be modeled when leaching is not influenced by any secondary reactions. This requires a large volume of water to keep concentrations below levels that would promote reactions. Optimized leaching conditions of 50°C, 3 liters of water (replaced daily) and a specimen size of 2.5 x 2.5 cm give an acceleration factor of approximately 17.

5. PORTLAND CEMENT CONTAINING INCINERATOR ASH

5.1 Introduction

As discussed in Section 4, portland cement is a highly reactive material. In the case of sodium sulfate salts, chemical reactions occur with cement that form new minerals and alter the structure of the surface and/or the bulk material. These reactions appear to change the leaching behavior of cement waste forms, particularly at 60°C or above. Another type of waste that could become common in the near future is incinerator ash. Ash contaminated with radionuclides must be solidified for disposal to reduce dispersion, and portland cement is one of the most commonly used solidification agents. Consequently, one of the waste forms being studied is portland type I cement containing incinerator ash.

Although relatively high loadings of incinerator ash can be achieved with portland cement, for this study 15 wt% ash was mixed with portland type I cement. This mixture was considered a sufficiently high loading to provide useful results without risking problems of heterogeneous specimens, potentially a major problem with waste forms containing ash simply by the variable nature of the ash itself.

5.2 Modeling and Mechanisms of Leaching

Cement waste forms containing 15 wt% incinerator ash are physically stable and have not been observed to fail immersion tests. Leaching of Cs-137 from cement/ash waste forms is diffusion-controlled during the first week of leaching when the interval for the replacement of leachant is one day. This is shown by plotting cumulative fraction leached against the square root of time (Figure 5.1). The early part of the data is linear, consistent with what is expected if diffusion is the leaching mechanism. After the first week (CFL=0.25), the CFL falls below the projected line. As with cement containing sodium sulfate this could be caused by Cs-137 depletion.

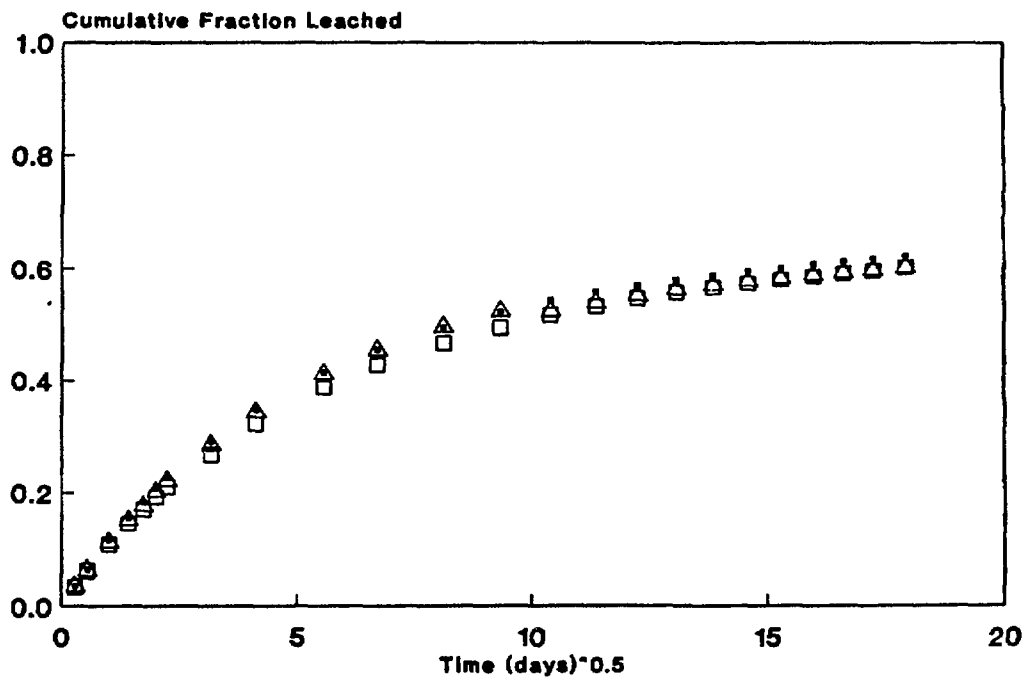


Figure 5.1 Cumulative fraction leached of Cs-137 plotted against the square root of time for triplicate specimens. If diffusion is the leaching mechanism then the plot should be linear to about 0.20 cumulative fraction release. After that it should slowly curve down.

The finite cylinder model overestimates (Figure 5.2) the cumulative fraction leached of Cs-137 once longer replacement intervals are used, indicating that more than diffusion and depletion are operating. By moving the intercept to CFL=0.4, a second diffusion coefficient can be used to model the later part of the leaching curve although there appears to be some difference in curve shape between the data and the model.

Lacking a long-term experiment with daily intervals for the replacement of the leachant, an alternative is to compare the cement/ash data with data from cement/sodium sulfate (Figure 5.3). The latter was shown to be diffusion-controlled although leaching is inhibited by concentration effects during the longer intervals of replacement. During daily replacements of the leachant, there is little difference between the two sets of data. However, by 18 days the cement/ash wastes are leaching significantly slower than the cement/sulfate. Diffusion from the sulfate waste forms are inhibited by depletion and by concentration effects that are greater than those observed for cement/ash waste forms. By using the finite cylinder to model the

cement/ash releases, it becomes apparent that Cs-137 leaching from cement/ash waste forms is reduced by more than simple depletion or concentration effects. By comparing the long-term data from these two materials, this reduction becomes even more apparent (Figure 5.4).

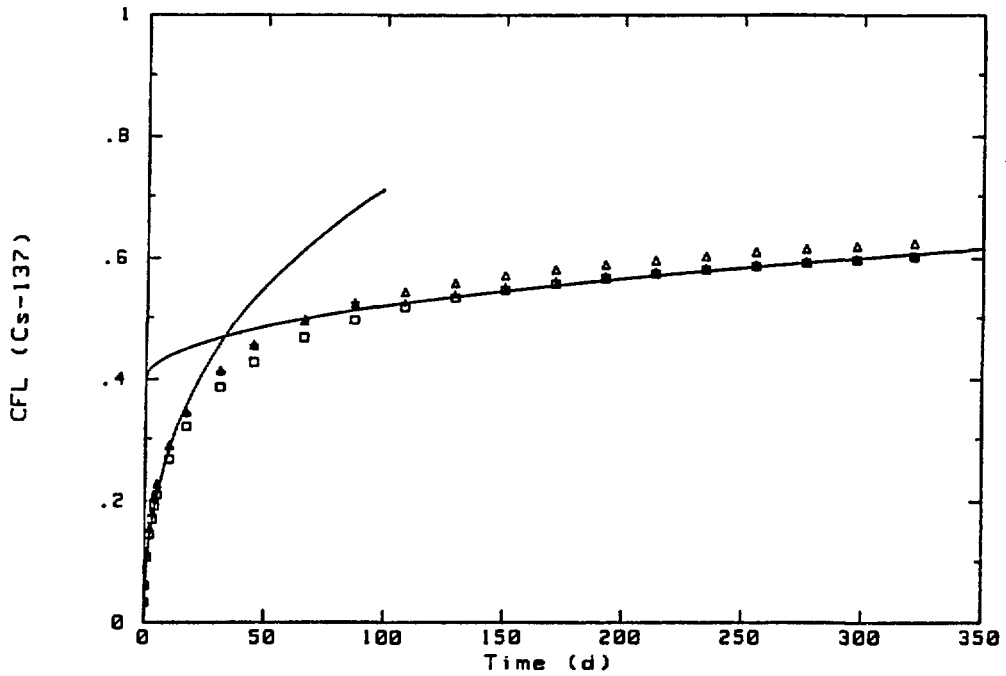


Figure 5.2 Leaching of Cs-137 from cement/ash waste forms. The solid lines are calculated from the finite cylinder model.

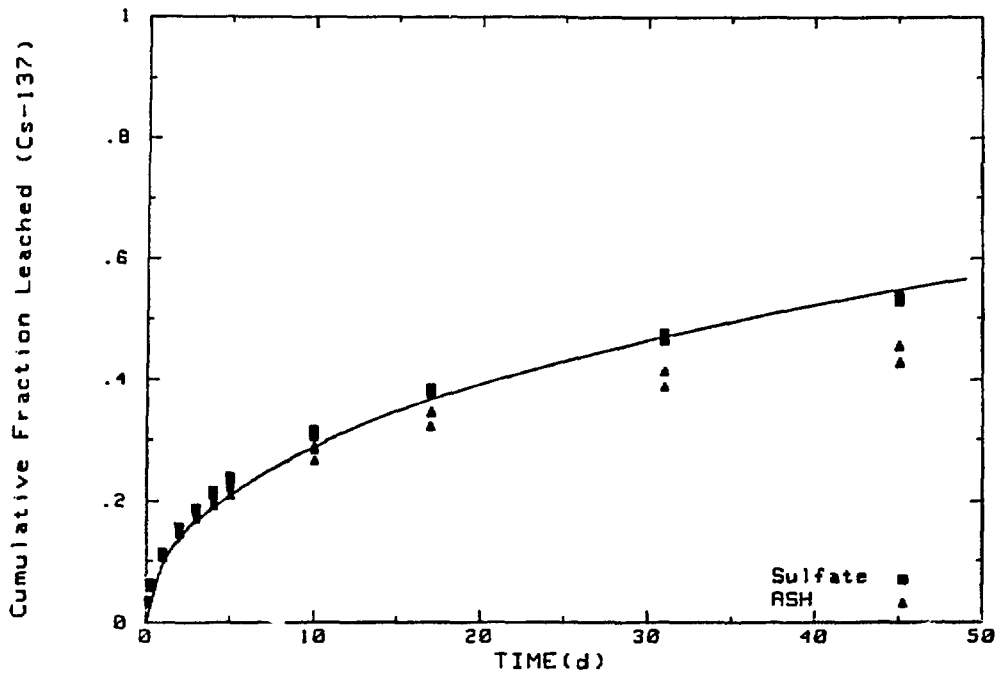


Figure 5.3 Comparison of Cs-137 releases from cement waste forms containing incinerator ash with specimens containing sodium sulfate. The curve is the modeled data for the cement/sulfate specimens.

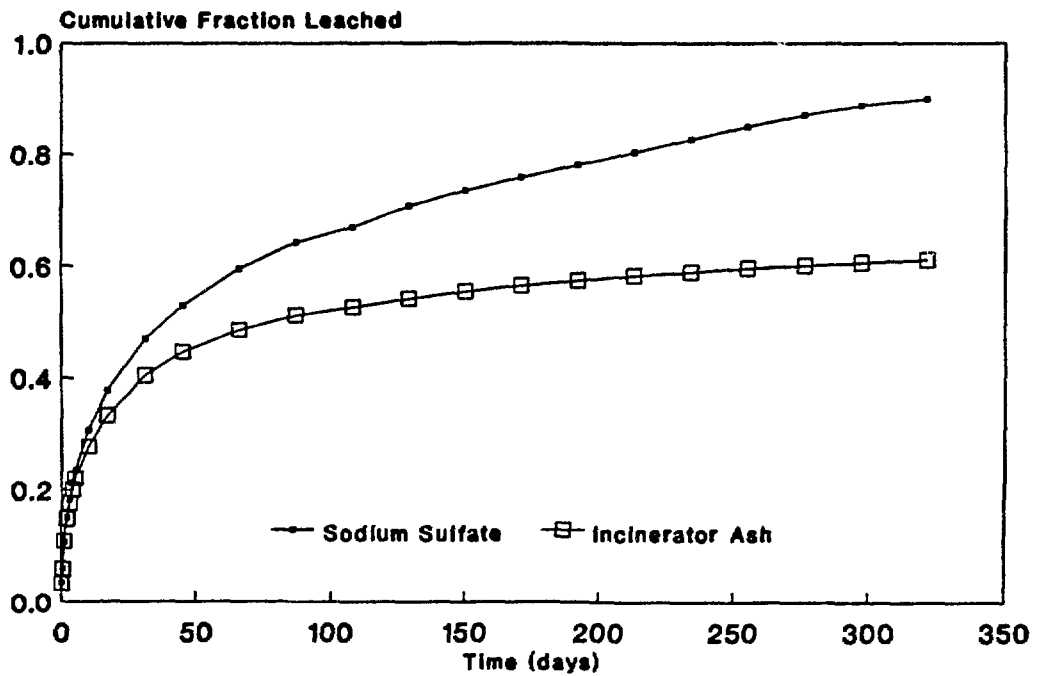


Figure 5.4 Long-term comparison of Cs-137 releases from cement waste forms containing incinerator ash with specimens containing sodium sulfate.

Leaching of Sr-85 from cement/ash wastes is not linear after the daily replacements of the leachant have finished (Figure 5.5). These data are well below CFL=0.2, so depletion is not the cause of this deviation from diffusion.

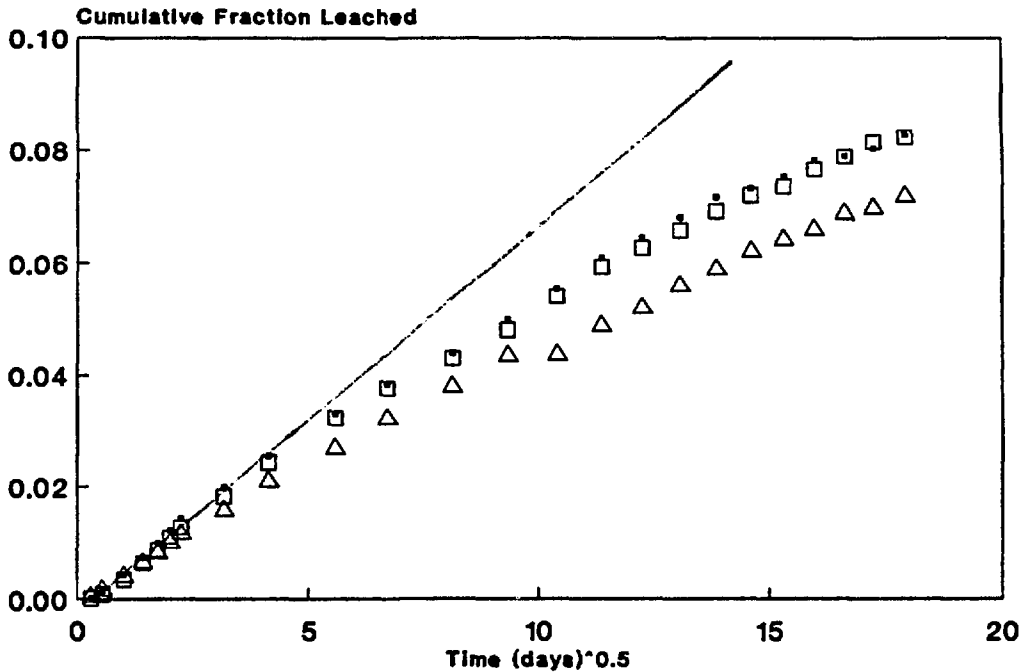


Figure 5.5 Cumulative fraction leached of Sr-85 is plotted against the square root of time for triplicate specimens of portland cement containing incinerator ash.

Applying the finite cylinder model to releases of Sr-85 shows that this model is not appropriate for this type of waste form. A single diffusion coefficient models the data of the first few weeks adequately but then seriously overestimates leaching (Figure 5.6). The latter part of the curve does not conform to the proper shape of the model, even if a second diffusion coefficient is used with adjustments made to the intercept.

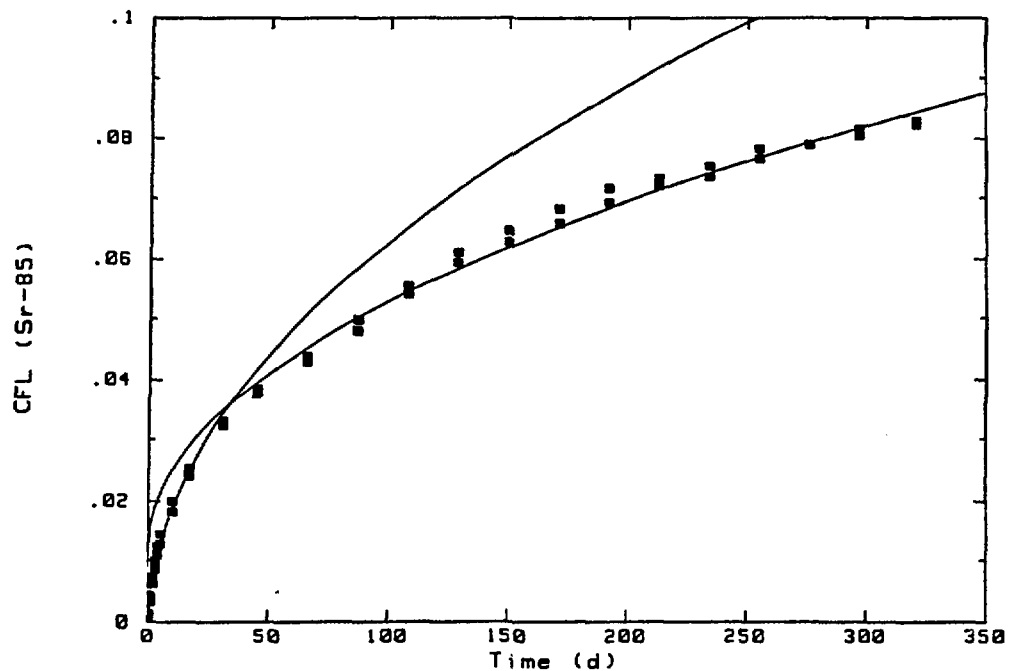


Figure 5.6 The finite cylinder model does not adequately model the Sr-85 data from cement/ash waste forms.

Several possible mechanisms would lead to a reduction in leach rate beyond that observed from depletion. These mechanisms are reactions that reduce the porosity of the solid and adsorption reactions. Electron microscope images of cement/ash waste forms show very large, open pores so the possibility of reducing the size of the pore is doubtful. Adsorption reactions, therefore, appear to be the most reasonable choice. If adsorption is the mechanism, it probably involves a product of the reaction of the ash with the cement which is developing over time. There is indirect evidence for this mechanism in that the reduction of leach rate appears to increase with time.

To confirm the hypothesis that adsorption is acting to limit release rates, we conducted experiments to directly observe sorption of Cs-137, Sr-85 and Co-57 onto incinerator ash and onto a pulverized waste form containing cement and 15 wt% incinerator ash. Other mixtures of cement and ash were used to provide different amounts of ash. Results are shown in Table 5.1.

Table 5.1

**Adsorption of Radionuclides by Incinerator Ash
and Cement/Ash Waste Forms**

<u>Sample Type</u>	<u>Liquid</u>	<u>pH</u>	<u>Percent Adsorption</u>	
			<u>Cs-137</u>	<u>Sr-85</u>
Incinerator Ash	distilled water	11.6	35	56
Incinerator Ash	1M NaOH	13.6	5	81
Cement/Ash (2 g ash)	distilled water	13.1	21	49
Cement/Ash (0.76 g ash)	distilled water	12.9	19	38
Cement/Ash (0.50 g ash)	distilled water	12.8	7	20

Adsorption of Cs-137 by ash alone was 35%. When mixed with cement, uptake was substantially lower but still significant. The percentage of sorbed Cs-137 was related to the amount of ash present. For Sr-85, much more uptake was observed with 49% being adsorbed by the cement/ash waste form. Again, the percentage of uptake was related to the amount of ash present in the system. Adsorption experiments, in combination with the leaching curves, demonstrate that adsorption is an important factor during leaching of cement/ash waste forms. Even though adsorption is contained within the effective diffusion coefficient (D_e), it would not cause the curve to flatten out later in the experiment, as it does, if it were a constant value. Only if adsorption were enhanced with time would the leaching curve respond as it does. This effect could also be the result of high concentrations in the leachant.

5.3 Single Factors that Accelerate Leaching

5.3.1 Temperature. Experiments run at 20°, 40°, 50° and 60°C in 1.3 liters of water indicate little long-term effect of temperature on Cs-137 releases (Figure 5.7). After about 21 days the data for all four temperatures are not separable. However, during the first week, there appears to be an increase in release with increased temperature. The change from a positive response (to elevated temperature) to a lack of difference in leach rate becomes apparent when data from the first weeks are looked at more closely (Figure 5.8). This type of response appears to be related to depletion plus adsorption but may simply be related to the long interval of the leachant replacement. The lack of effect of temperature is shown in the Arrhenius plot (Figure 5.9), where there is no statistically significant difference among the points for the four temperatures tested.

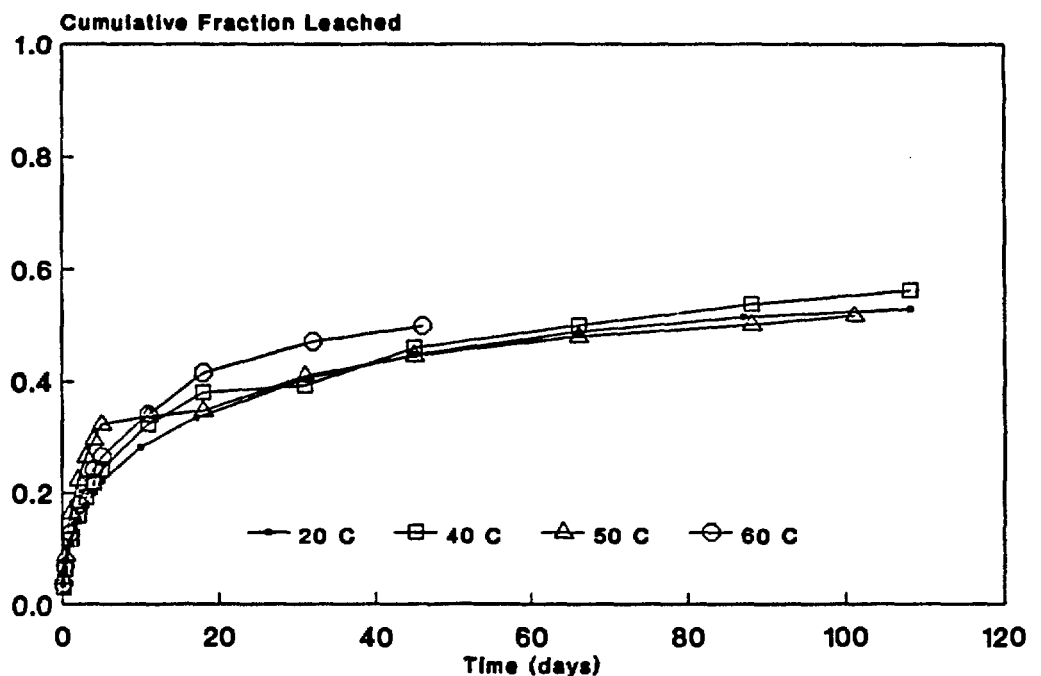


Figure 5.7 Cs-137 cumulative fraction leached vs time from portland I cement containing 15 wt% incinerator ash at 20°, 40°, 50° and 60°C in deionized water.

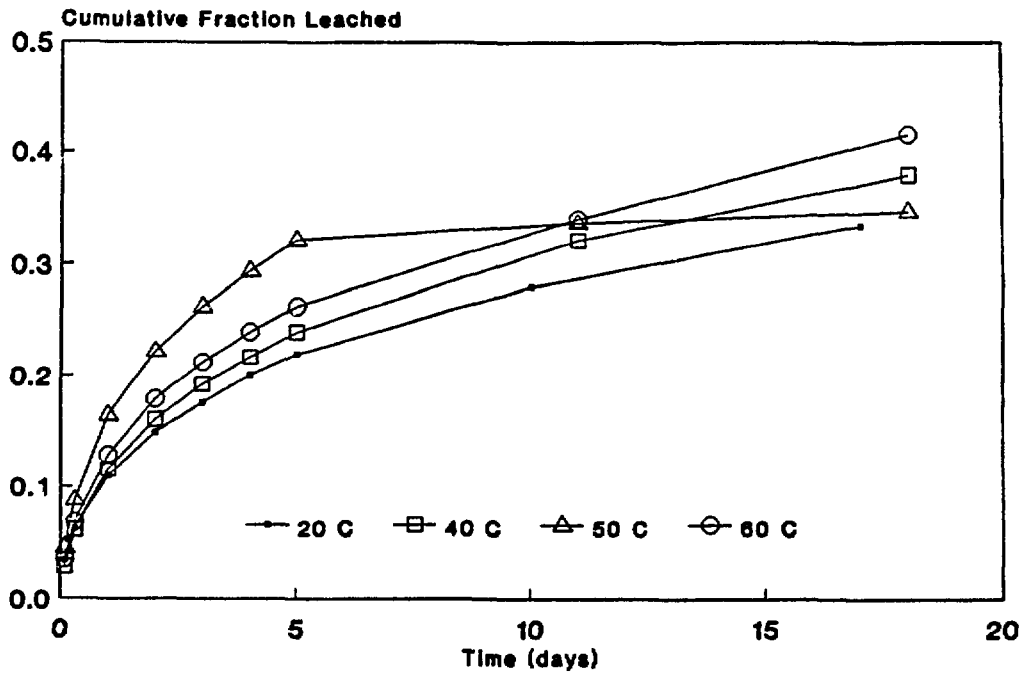


Figure 5.8 Averaged Cs-137 cumulative fraction releases from cement/ash specimens shown for the first nine sampling intervals. While the order of release from the 20°, 40° and 50°C specimens remain unchanged, the releases from the 60°C specimen were anomalous for the last two points.

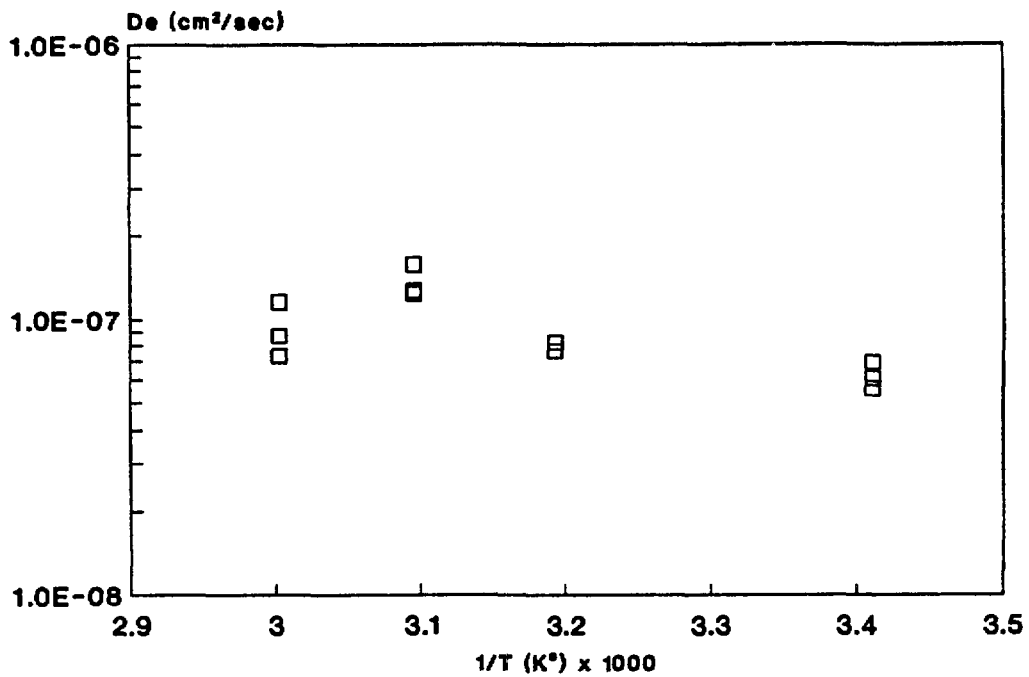


Figure 5.9 An Arrhenius plot of the diffusion coefficient for cement/ash specimens leached at 20°, 40°, 50° and 60°C. There is no statistically significant difference in D_e caused by temperature under these test conditions.

Releases of Sr-85 respond more consistently to elevated temperature. As measured at CFL=0.05, the data at 50°C, in 11 days, gives the equivalent of about 100 days of leaching at 20°C (Figure 5.10). The Arrhenius plot (Figure 5.11) of the diffusion coefficient indicates that the response of leaching to increases in temperature is linear up to 60°C. At 60°C, the leach rate drops below what is expected for that temperature.

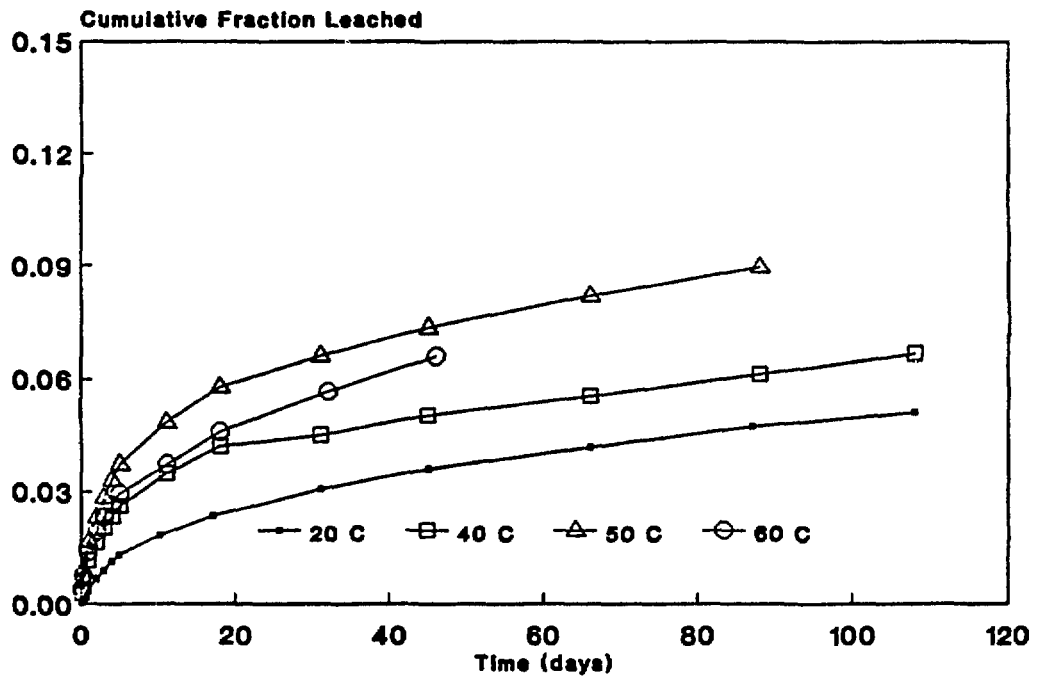


Figure 5.10 Sr-85 cumulative fraction leached vs time from portland I cement containing 15 wt% incinerator ash at 20°, 40° and 50°C in deionized water.

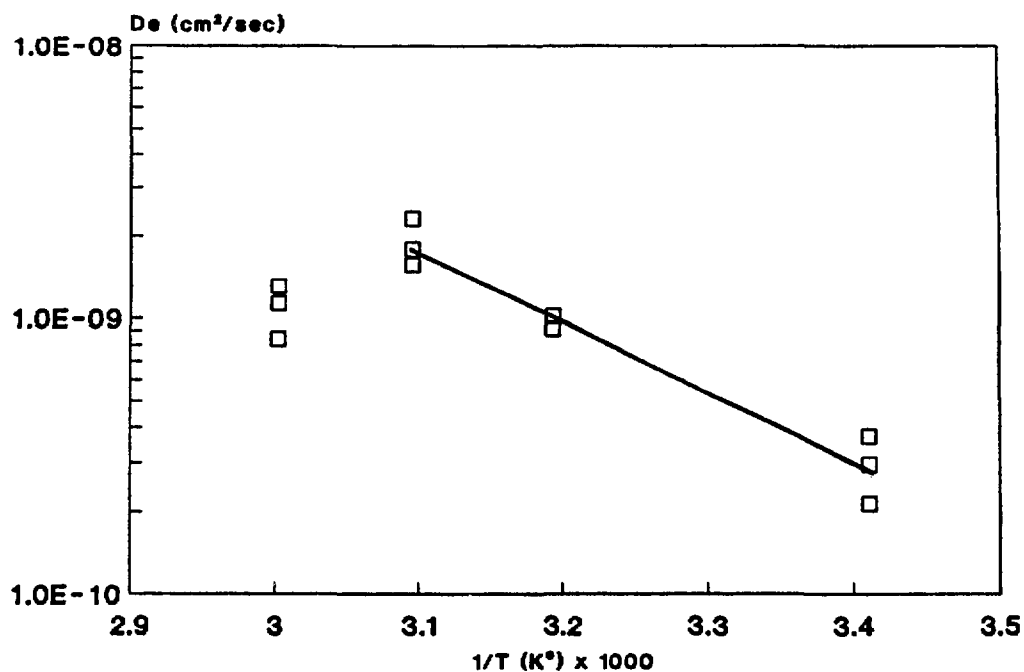


Figure 5.11 An Arrhenius plot of the diffusion coefficient D_e showing that Sr-85 leaching at 60°C is lower than expected.

5.3.2 Size. Reducing the size of waste forms, as expressed by the ratio of volume to surface area, is an effective means of accelerating leaching when diffusion is the mechanism. Releases of Cs-137 (Figure 5.12) from waste forms of several sizes are dependent on size during the first week of leaching. This relationship does not necessarily maintain itself for longer periods of leaching because of depletion. When considering D_e values for these data and their replicates, there first appears to be a dependence of D_e on size. This dependence on size should not be so if diffusion is the mechanism. But on examination of the errors among replicates, they appear to have a broad error band of almost a factor of 10. This factor may be attributable to the heterogeneous nature of ash wastes. Effects of size are also observed for Sr-85.

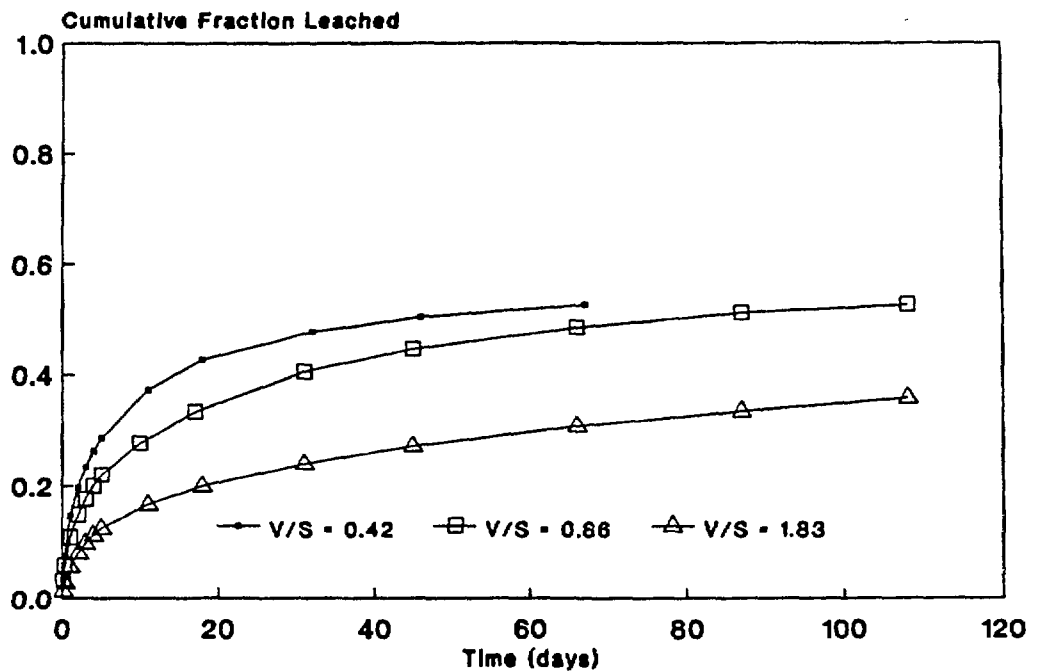


Figure 5.12 Size effect on releases of Cs-137 for cement/ash waste forms. Size is expressed as the ratio of waste form volume to surface area (V/S), with the smaller waste form having the lower ratio.

5.3.3 The Volume of Leachant. As discussed in Section 3, the volume of leachant plays a critically important role in optimizing leach rates. The role of the volumes of leachant or the frequency of the leachant replacement becomes even more important when elevated temperatures are used to increase leach rates so that concentrations in the leachant do not become too high. The earlier work for this acceleration factor will not be reviewed because its effectiveness is highly dependent on other acceleration factors. It will be discussed more in the section on combined acceleration factors.

5.4 Combined Acceleration Factors

As with the study of cement waste forms containing sodium sulfate, the work on individual acceleration factors was used as the basis for investigating combined acceleration factors. Results reported in this section are the product of experiments in which combined acceleration factors were studied to try to maximize leaching.

5.4.1 Cs-137 Results. Average diffusion coefficients for Cs-137 are given in Table 5.2 for experiments in which combined acceleration factors were investigated for cement waste forms containing 15 wt% incinerator ash. The effect of waste loading on the diffusion coefficients for waste forms containing 20 and 30 wt% ash are given in Table 5.3.

Table 5.2

Diffusion Coefficients for Cs-137 from Portland Cement
15 wt% Incinerator Ash Waste Forms

Leach Test	Volume (liters)	Temperature (°C)	Size D x H ¹ (cm)	Average D _e , Cs-137 (cm ² /sec)
Semidynamic	1.3	60	5 x 7	9.2 x 10 ⁻⁸
Semidynamic	6.5	60	5 x 7	9.0 x 10 ⁻⁸
Static	6.5	60	5 x 7	7.0 x 10 ⁻⁸
Semidynamic	3.0	50	2.5 x 2.5	6.8 x 10 ⁻⁸
Static	6.5	50	5 x 7	6.7 x 10 ⁻⁸
Semidynamic	1.3	20	5 x 7	6.2 x 10 ⁻⁸
Static (CO ₂ free)	6.5	50	5 x 7	5.6 x 10 ⁻⁸
Semidynamic	1.3	50	2.5 x 2.5	5.5 x 10 ⁻⁸

1 = right cylinder

D = diameter

H = height

Table 5.3

Effect of Waste Loading on the
Diffusion Coefficients for Cs-137 from Portland Cement
Incinerator Ash Waste Forms

Leach Test	Volume (liters)	Temperature (°C)	Size D x H ¹ (cm)	Average D _e , Cs-137 (cm ² /sec)
Semidynamic (15 wt% ash)	1.3	20	5 x 7	6.2 x 10 ⁻⁸
Semidynamic (20 wt% ash)	1.3	20	5 x 7	5.8 x 10 ⁻⁸
Semidynamic (30 wt% ash)	1.3	20	5 x 7	3.7 x 10 ⁻⁸

1 = right cylinder
D = diameter
H = height

Differences in the rates of release are not particularly large for Cs-137. The test that gives the fastest rate is a semidynamic test run at 60°C in 1.3 liters of water, while the second fastest was a semidynamic test conducted at 60°C but with 6.5 liters of water (Figure 5.13). When comparing data from static and semidynamic tests, as expected, releases of Cs-137 are somewhat higher in the semidynamic test than in the static test, although the data only begins to diverge after several weeks of leaching. Using the finite cylinder model, it is apparent that either the test model is not appropriate for this data or that neither test optimizes releases once longer intervals for the replacement of leachants are used.

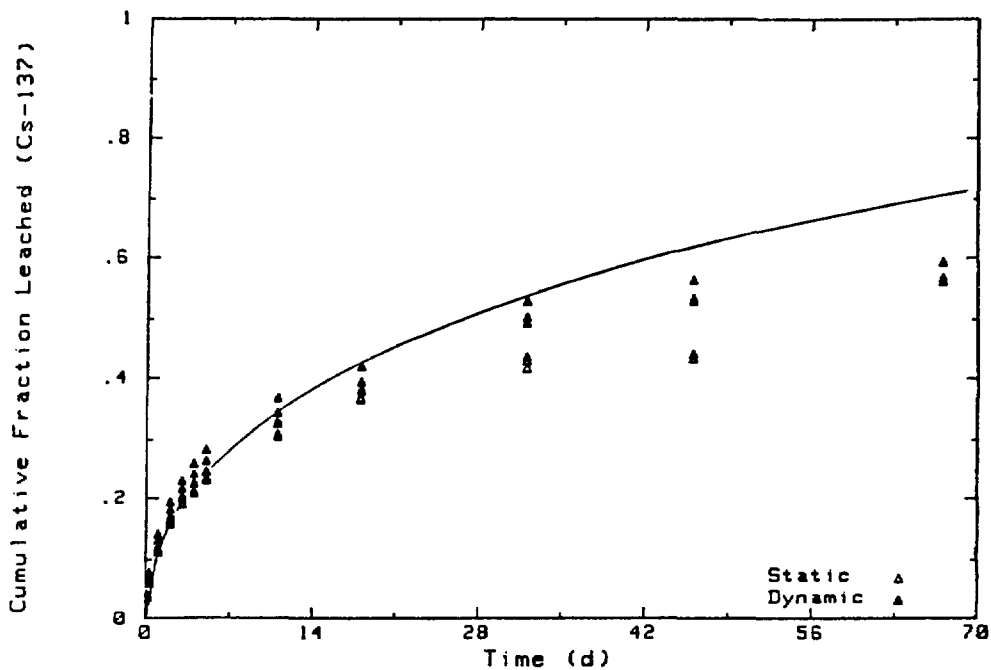


Figure 5.13 Releases of Cs-137 from portland cement containing 15 wt% incinerator ash. Static and semidynamic leach tests were run at 60°C. The finite cylinder model diverges from the data after 12 days.

Cs-137 leaching is insensitive to many factors that could affect leaching. As shown earlier, for temperature alone, a combination of elevated temperature (50° or 60°C) with a static test, also gave no discernible difference in leaching. This difference was true for cement/sodium sulfate specimens, as well. The 50° and 60°C CFL values were significantly higher than those at 20°C although the 50° and 60°C values were almost identical to each other (Figure 5.14).

From the data in Figure 5.12, there is a size effect for Cs-137 leaching from cement/ash wastes even though diffusion is not the only release mechanism. A combination of reduced size, increased leachant volume, increased replacement of leachant and elevated temperature was used to optimize leaching (Figure 5.15). For the 2.5 x 2.5 cm specimens used, the increased volume of water did not cause any increase in Cs-137 leaching over other specimens of the same size that were leached at 50°C and, therefore, no additional water is necessary to accelerate Cs-137. That Cs-137 leaching depends very little on leachant volume is illustrated by the Arrhenius (Figure 5.16) plot which shows that changes in the volume of leachant had no effect in leaching for 5 x 7 cm specimens at 60°C.

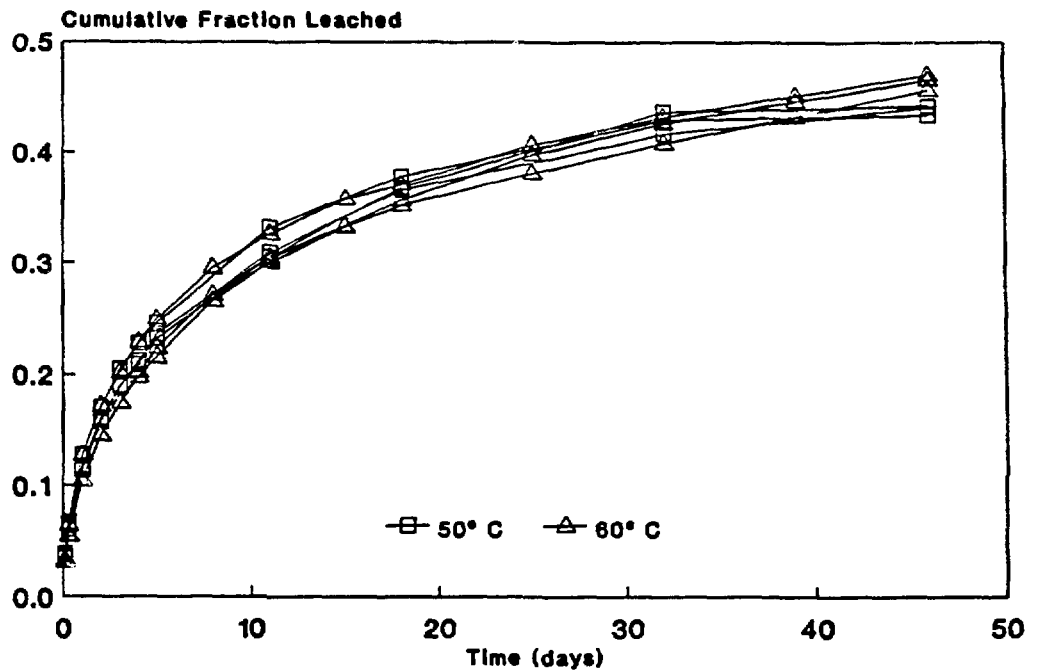


Figure 5.14 Although leaching from a static test at 50° or 60°C is faster than at 20°C, the CFL values taken for tests at 50° and 60°C are almost identical to each other.

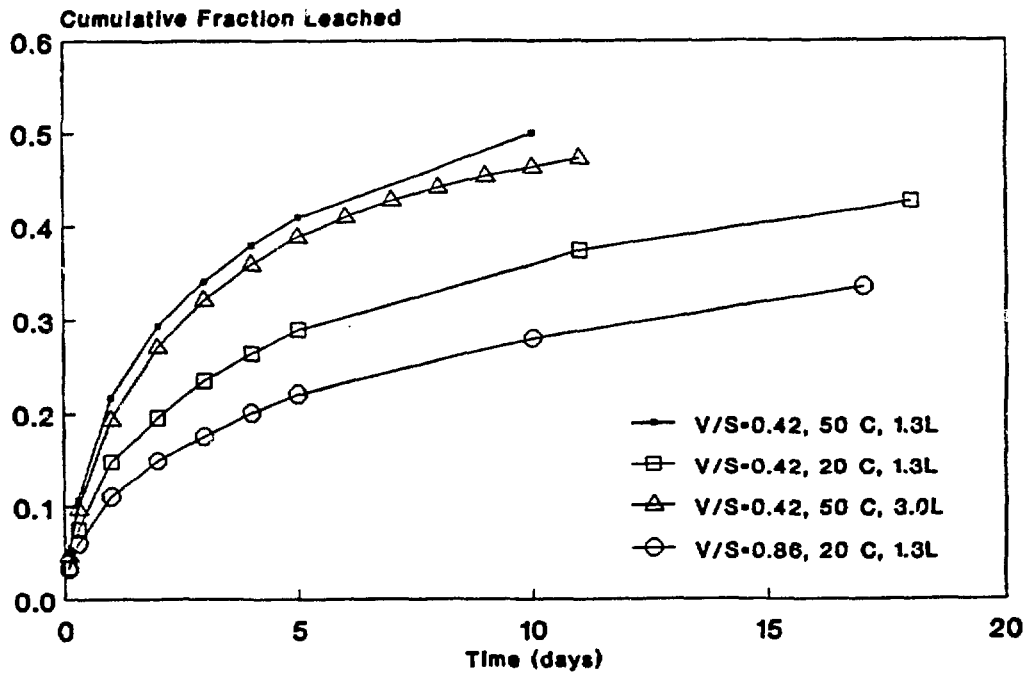


Figure 5.15 The combined effect of small size, elevated temperature, increased volume of leachant, and increased frequency of replacement gave results that were not greater than just small size and elevated temperature. Specimens were portland cement containing 15 wt% incinerator ash.

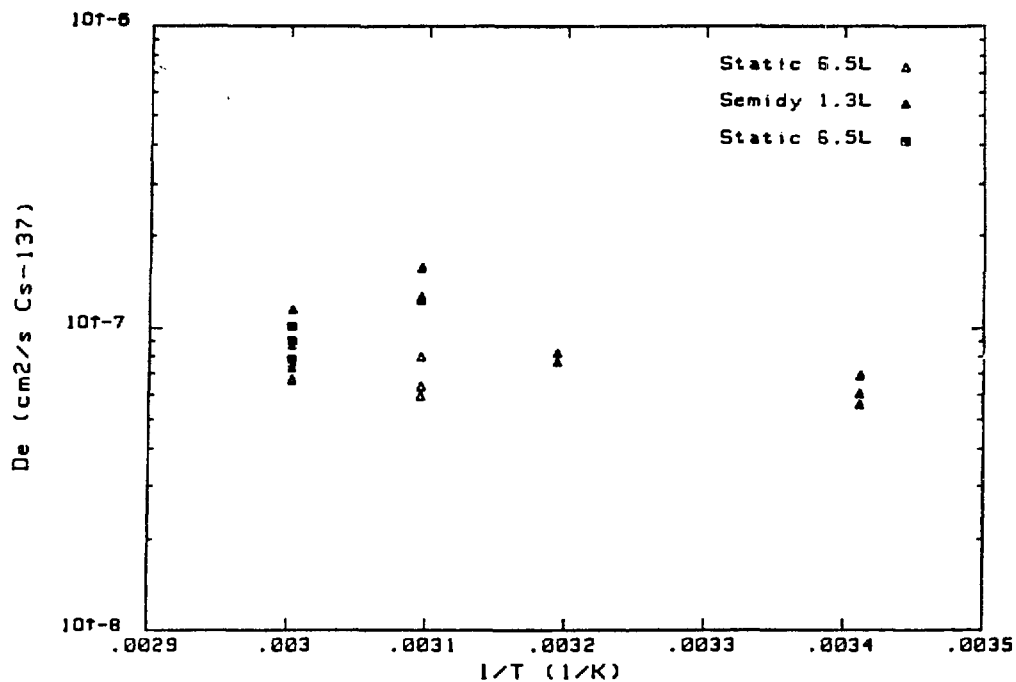


Figure 5.16 Arrhenius plot for Cs-137 releases from cement/ash specimens at 20°, 40°, 50° and 60°C. Changes in the volume of leachant made no difference to leaching at 60°C but smaller volumes (or no leachant replacements) could reduce leaching (at 50°C).

Optimized test conditions of 50°C, 3 liters of distilled water (changed daily) and a 2.5 x 2.5 cm specimen resulted in a diffusion coefficient of $6.8 \times 10^{-8} \text{ cm}^2/\text{s}$. Triplicate data sets for this experiment are shown in Figure 5.17 as are baseline data sets (20°C, 1.3 liters, ANS 16.1 test with a 5 x 7 cm specimen). Comparison of results from the accelerated and baseline experiments gives an acceleration factor of approximately 6.

Since Cs-137 leaching from cement/ash waste forms cannot be modeled by diffusion, an alternate approach can be taken to determine if the leaching mechanisms have changed during the accelerated test. This requires plotting the cumulative fraction leached (CFL) from the baseline experiment against the CFL from the accelerated test. A linear plot should result if the mechanisms have not changed (Figure 5.18). The plot consists of two linear segments with the break in slope being an artifact caused by the change in sampling frequency during the baseline test. The linearity of the two segments indicate that the leaching mechanism does not change during the accelerated test.

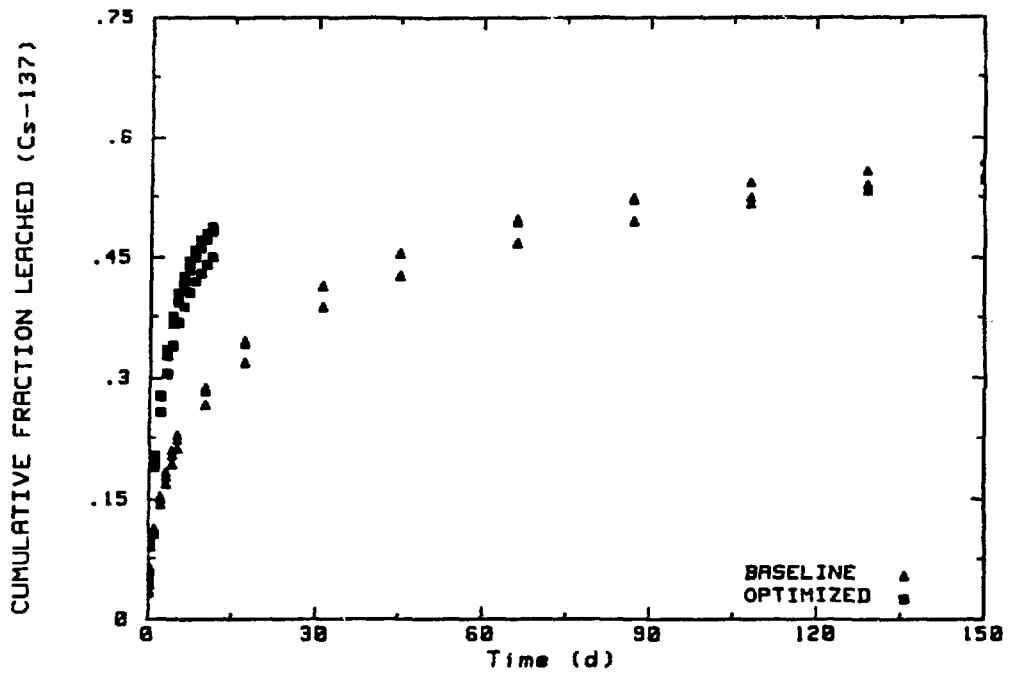


Figure 5.17 Releases of Cs-137 from triplicate specimens of portland cement containing incinerator ash are shown for the optimized accelerated test and for the baseline. The acceleration factor is approximately 6.

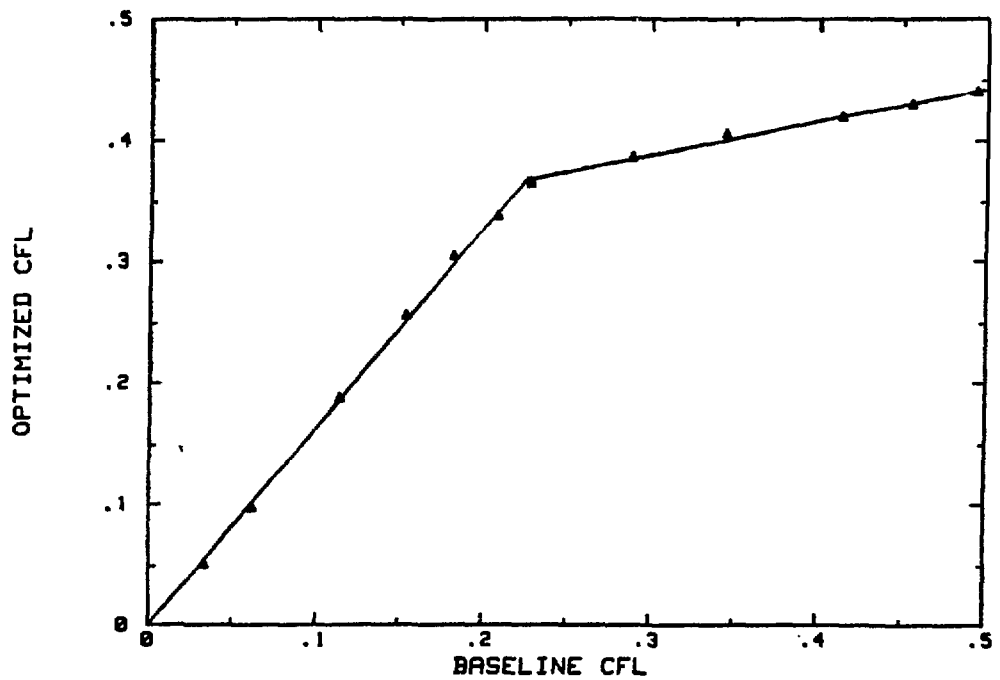


Figure 5.18 Releases of Cs-137 from accelerated tests are plotted against releases from the baseline test. The results produce a linear plot in two segments. The break is caused by the change in sampling interval during the baseline test.

5.4.2 Sr-85 Results. Results of combined acceleration factors for Sr-85 from cement/ash waste forms are shown in Table 5.4. The effect of waste loadings on the Sr-85 diffusion coefficient for waste forms containing 20 and 30 wt% ash are given in Table 5.5. Effects of temperature for Sr-85 are more clearly ordered than are those for Cs-137. This is also true for static experiments during the first week of leaching (Figure 5.19). While the intersample variability of these points looks large compared to Cs-137, note that apparent scatter is an artifact of plot scale. The scatter among triplicate points for Sr-85 is similar to that of Cs-137. These data are contradictory to those discussed earlier (Figures 5.10 and 5.11) in which Sr-85 releases at 60°C is lower than at 50°C. The earlier data are from semidynamic tests and have 10 to 20% higher CFL values in general, so this discrepancy may be a result of the type of test used.

Table 5.4

Diffusion Coefficients for Sr-85 from Portland Cement/
15 wt% Incinerator Ash Waste Forms

Leach Test	Volume (liters)	Temperature (°C)	Size D x H ¹ (cm)	Average D _e , Sr-85 (cm ² /sec)
Semidynamic	6.5	60	5 x 7	2.3 x 10 ⁻⁹
Semidynamic	3.0	50	2.5 x 2.5	1.0 x 10 ⁻⁹
Static	6.5	60	5 x 7	9.9 x 10 ⁻¹⁰
Static	6.5	50	5 x 7	5.9 x 10 ⁻¹⁰
Static	6.5	50	5 x 7	4.8 x 10 ⁻¹⁰
Semidynamic	1.3	60	5 x 7	4.5 x 10 ⁻¹⁰
Semidynamic	1.3	20	5 x 7	2.9 x 10 ⁻¹⁰

1 = right cylinder
D = diameter
H = height

Table 5.5

Effect of Loading on the Diffusion Coefficient for Sr-85
from Portland Cement plus Ash

Leach Test	Volume (liters)	Temperature (°C)	Size D x H ¹ (cm)	Average D _e , Sr-85 (cm ² /sec)
Semidynamic (15 wt% ash)	1.3	20	5 x 10	2.9 x 10 ⁻¹⁰
Semidynamic (20 wt% ash)	1.3	20	5 x 10	2.4 x 10 ⁻⁹
Semidynamic (30 wt% ash)	1.3	20	5 x 10	1.2 x 10 ⁻⁹

1 = right cylinder
D = diameter
H = height

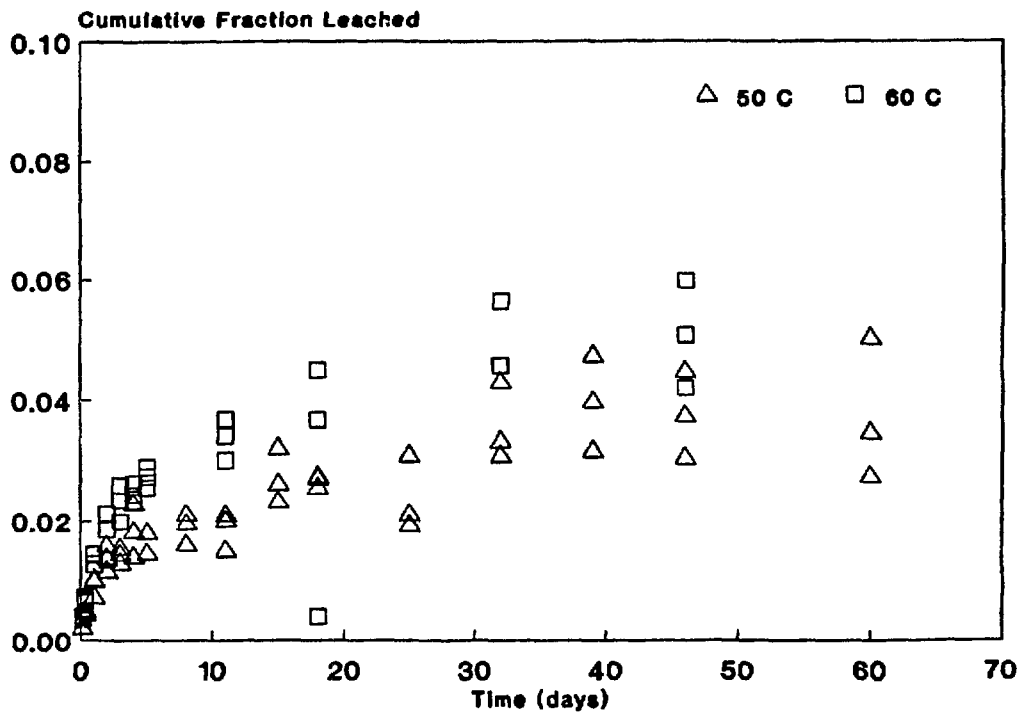


Figure 5.19 Sr-85 releases from cement/ash specimens during static tests run at 50° and 60°C.

Comparing the static and semidynamic results of leaching shows that Sr-85 responds more to the frequency of the replacement of leachant than does Cs-137. The finite cylinder model fits the data for one week very well, as it does for Cs-137, but rapidly overestimates releases after one week (Figure 5.20).

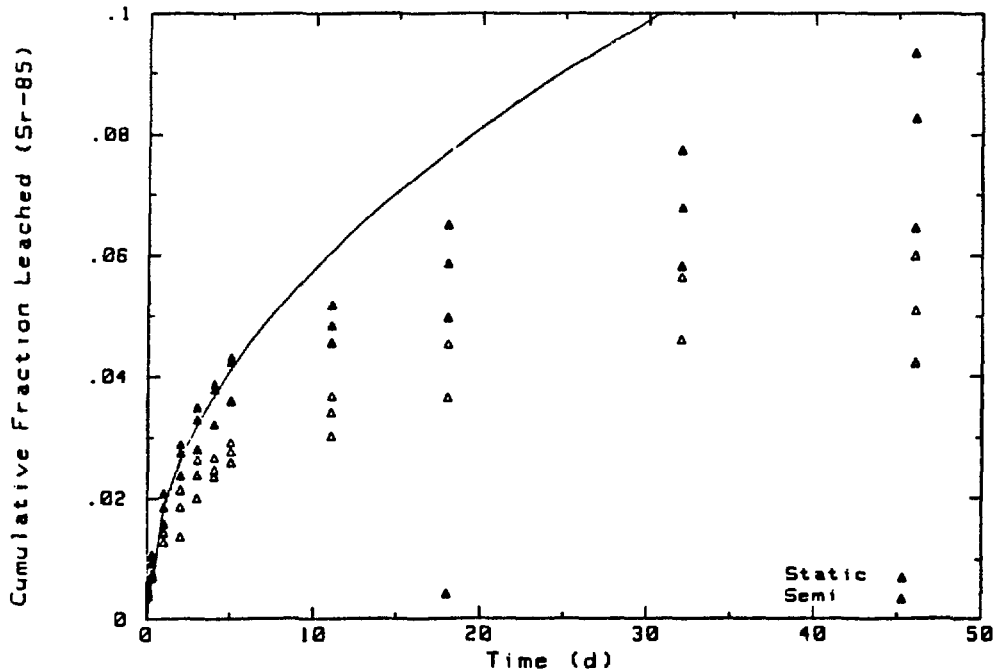


Figure 5.20 Releases of Sr-85 during static and semidynamic tests at 60°C. The finite cylinder model fits the data during the daily leachant replacement intervals, but overestimates it for longer intervals.

An Arrhenius plot (Figure 5.21) illustrates that by using 6.5 liters of water at 60°C instead of 1.3 liters, the data points are brought closer to the expected value (indicated by the line). Nevertheless, the data are still below the line and could mean a change in the mechanism of leaching.

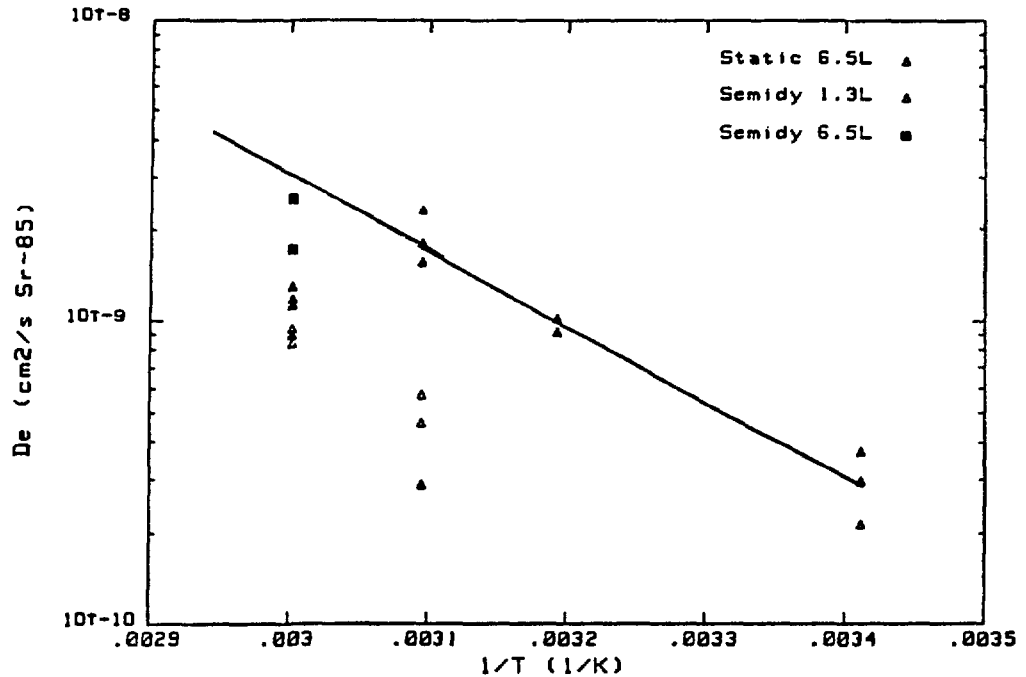


Figure 5.21 Arrhenius plot of Sr-85 diffusion coefficients for cement/ash specimens showing that increasing the leachant volume to 6.5 liters increased releases at 60°C.

From this evidence, optimized accelerating conditions were determined to be the same for cement/ash specimens as they are for cement/sulfate. Specifically, 2.5 x 2.5 cm specimens are run at 50°C in 3 liters of water that are changed daily. These conditions give an effective diffusion coefficient of $1 \times 10^{-9} \text{ cm}^2/\text{s}$ for Sr-85. Faster leaching of Sr-85 was obtained at 60°C, but this temperature was not acceptable for Cs-137 and is mechanistically questionable for Sr-85 as well. Figure 5.22 shows data from an optimized accelerated test and from the baseline test. The acceleration factor as measured at CFL=0.02 is about 17. Figure 5.23 shows all of the replicates from the two experiments. Data from one specimen of the accelerated test is modeled with the finite cylinder model and the curve is also shown in Figure 5.23. The model curve is not a good match of the data sets, implying that the diffusion model alone is not appropriate for this material.

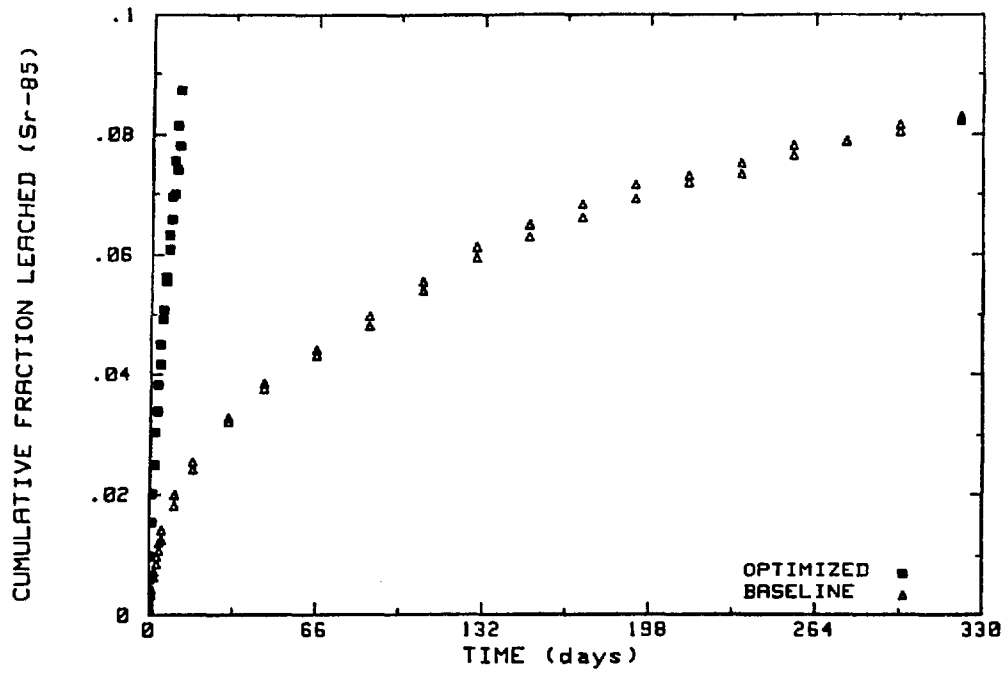


Figure 5.22 Data from the accelerated test and from the baseline test are plotted together. The acceleration factor is approximately 17.

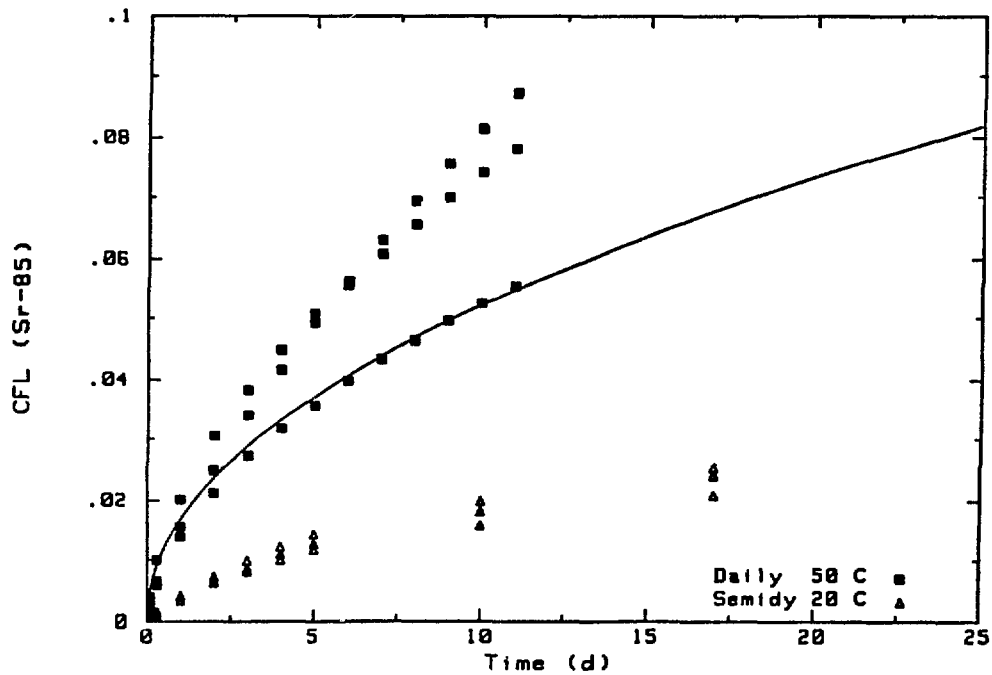


Figure 5.23 Triplicate data sets from the optimized accelerated test and the baseline test. One specimen is modeled with the finite cylinder model but none fit the model very well.

As with Cs-137 data, an alternative method was used to determine if the accelerated test altered the leaching mechanism. The scatter plot of CFL for Sr-85 from the accelerated test versus CFL from the baseline is shown in Figure 5.24. Like the Cs-137 plot, it is broken into two linear segments, indicating by their linearity that leaching mechanisms have not changed under accelerating conditions.

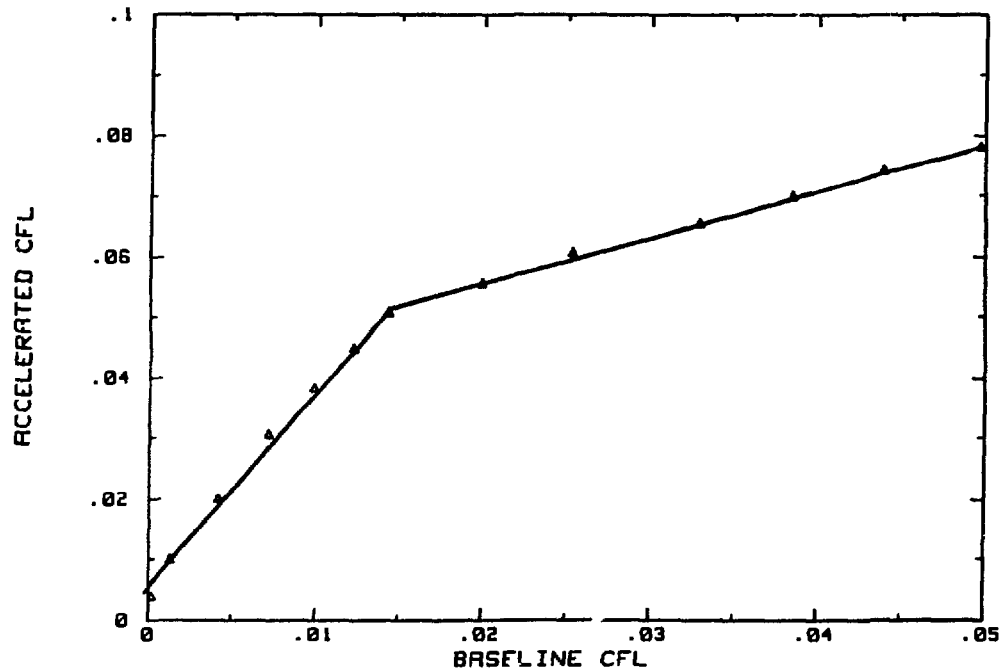


Figure 5.24 Plotting the CFL data from the baseline experiment against the CFL data from the accelerated test, a linear plot should result if the leaching mechanism has not changed. The break in slope is caused by a change in sampling intervals during the baseline test, but each segment is linear.

One extraneous effect that could have a significant impact on Sr-85 leaching from cement waste forms is that of carbonation of the surface of waste forms. This effect is of particular concern at elevated temperatures because of the increased rate of reaction. A set of static experiments were run at 50°C in which atmospheric carbon dioxide was excluded from the container. This experiment was done by welding the top on the container and using valves to control inlets and sampling ports. An air vent was required; therefore, an Ascarite trap was included to sorb carbon dioxide.

Results show that the presence or absence of carbon dioxide from the air had no observable impact on Sr-85 release (Figure 5.25). These results also are true for Cs-137 as well as for nonradioactive elements leached from the waste form.

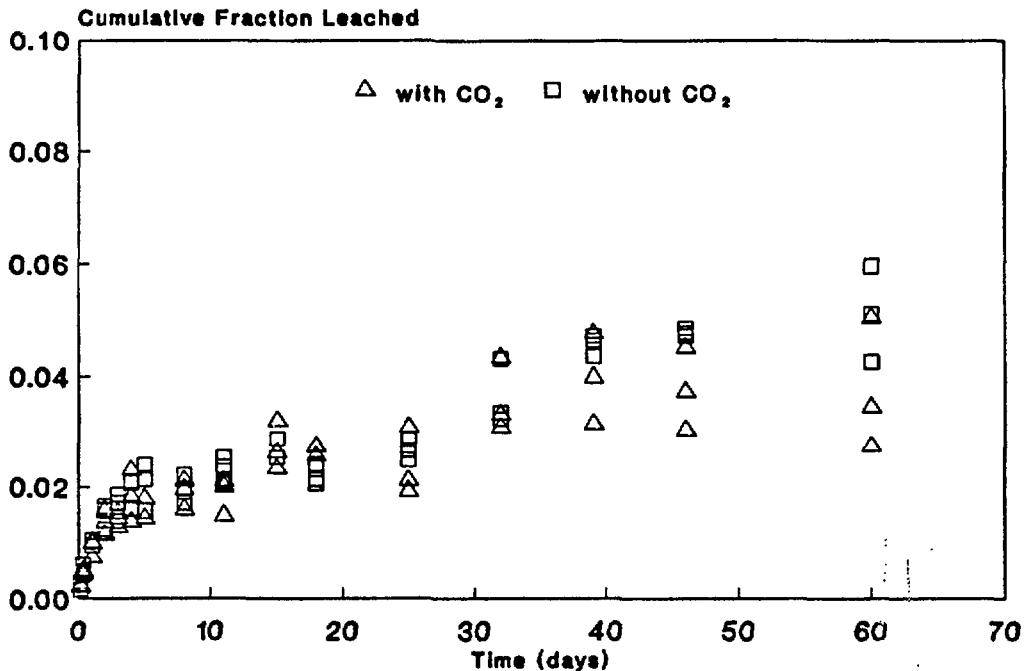


Figure 5.25 Sr-85 releases from cement/ash waste forms were no different for specimens exposed to atmospheric carbon dioxide than they were for specimens from which carbon dioxide was excluded.

Releases of stable strontium (Figure 5.26) from static tests are influenced only slightly by temperature and not at all by the presence of carbon dioxide. Releases of calcium (Figure 5.27) are higher in the 20°C experiment that is carbon dioxide free than in the others, possibly implying an effect of carbonation on calcium concentrations. While there was CaCO₃ precipitation observed in experiments that were exposed to air, there was no removal of Sr-85 or Cs-137 as a result. The Sr-85 content of the precipitated CaCO₃ was determined by acidifying the entire volume of leachant until no CaCO₃ was left undissolved. A sample was then taken and counted with no additional activity being detected.

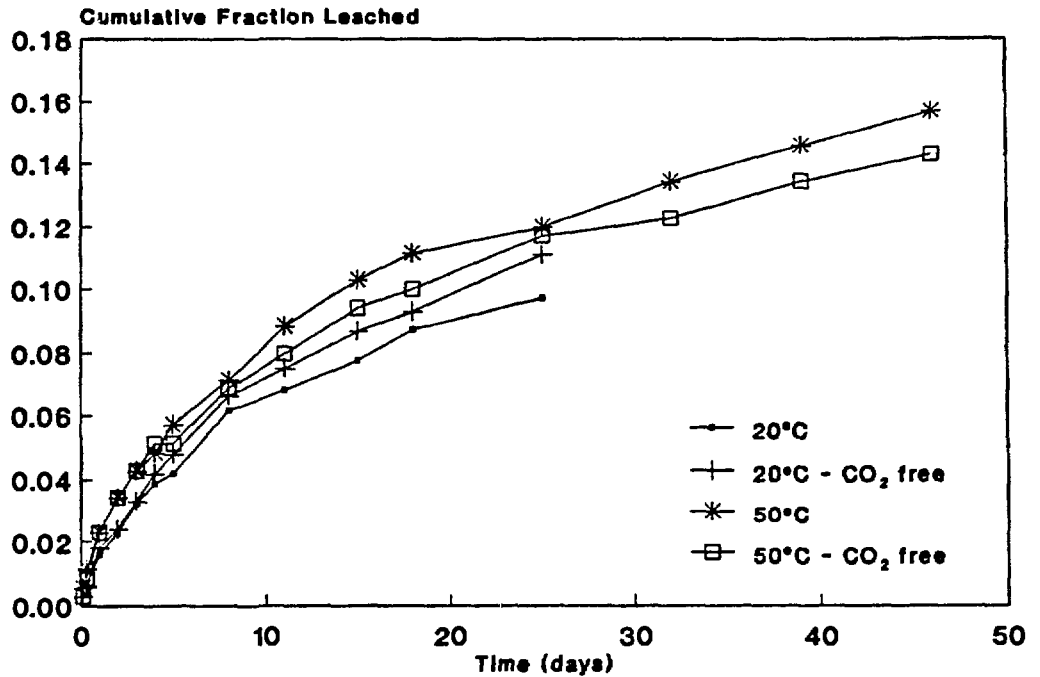


Figure 5.26 Dissolved strontium released from cement/ash waste forms in static leach tests shows no effect of carbonation at 20° or 50°C.

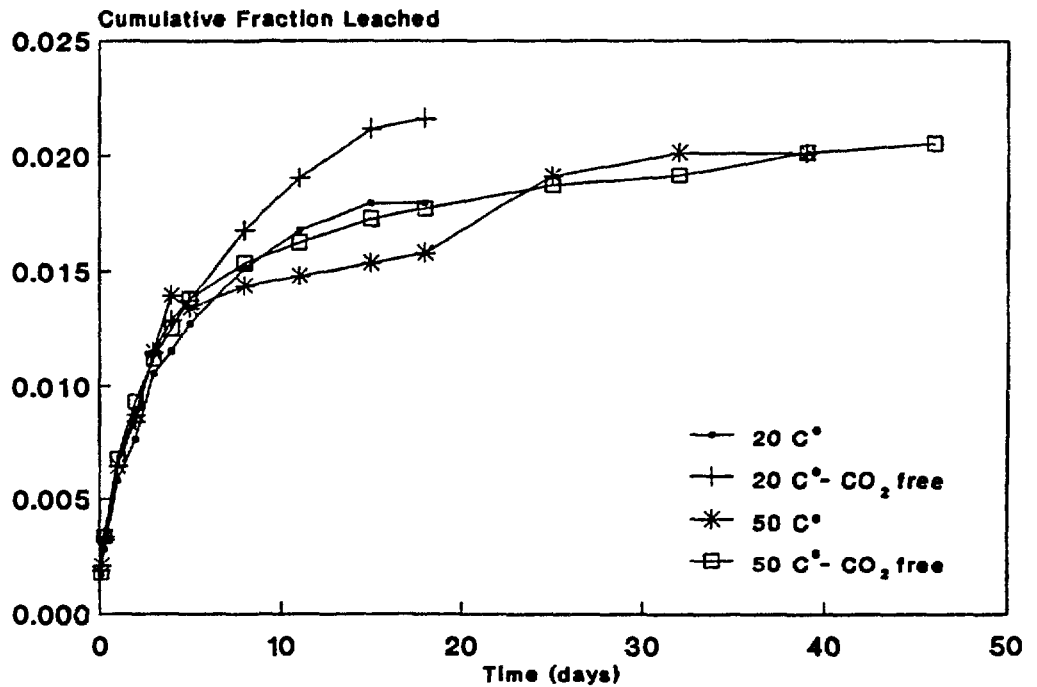


Figure 5.27 Dissolved calcium released from cement/ash waste forms in static leach tests shows no effect of carbonation, although the 20°C CO₂-free experiment did have slightly higher calcium concentrations.

5.5 Conclusions

Conditions for leaching Cs-137 for cement/ash waste forms were optimized. The greatest acceleration of Cs-137 occurs at 50°C (60°C provides no faster release rate) in a semidynamic test with 1.3 liters of water. Increasing the volume of the leachant or increasing the frequency of the replacement of leachant serves no useful purpose. Smaller sizes provide additional increase in leaching. An optimized leach test run at 50°C with a 2.5 x 2.5 cm specimen leached in 3 liters of water that is changed daily provides an acceleration factor of 6.

The finite cylinder model does not adequately describe processes of leaching from cement/ash waste forms. A model that uses an adsorption term that is a function of time is required.

Sr-85 releases are accelerated by elevated temperatures up to 50°C. With the optimized test conditions described above, the acceleration factor for Sr-85 was approximately 17. At 60°C the leach rate decreases although an increased volume of leachant (6.5 liters) appears to bring the leach rate up slightly. At 50°C the presence of atmospheric carbon dioxide has no effect on the leaching of radionuclides.

Leaching of Sr-85 cannot be modeled adequately during the entire process of leaching by the finite cylinder model. Although the data and the model agree during the first 5 days of leaching, the model overestimates releases after that time. Consequently, as with Cs-137, a model that contains an adsorption term that is a time function is required.

For both Cs-137 and Sr-85, linear correlations exist for CFL data taken at 50°C with CFL data at 20°C. These data imply that elevated temperatures do not change the leaching mechanism.

6. ASPHALT (BITUMEN)

6.1 Introduction

The use of asphalt for the solidification of low-level radioactive waste relies upon its thermoplastic properties. Asphalt processes solidify wet wastes by first evaporating the water in the waste while it is in direct contact with hot liquid asphalt. The asphalt then coats the particles that remain and the solids are mechanically held in the solid asphalt matrix upon cooling.

As discussed in Section 2, the asphalt waste forms used in this study were made with Witco Chemicals Pioneer 321 asphalt. This type of oxidized asphalt meets ASTM Standard D312-71, Type III, and is used at several waste generation sites in the United States for solidification of evaporator sludges.

The specimens for the test were made by mixing dry, powdered sodium tetraborate ($\text{Na}_2\text{B}_4\text{O}_7$) with molten asphalt to give waste forms with loadings of 20, 30 and 40 wt% salt. When required, radioactive tracers were added along with the waste.

Because no clear acceleration of leach rate was observed for any individual accelerating factor, no major experimental effort was made to investigate combined factors using bitumen specimens. Instead, we developed a synthesis that describes the leaching behavior of bitumen waste forms. From this, the major components of the process of leaching can be described empirically (albeit rather roughly) based on the loading of waste, and a conceptual model of mechanisms can be described.

6.2 Effect of Single Factors on the Leaching of Bitumen

Data presented in the topical report on factors that affect leaching [1] led to the conclusion that none of the factors investigated caused a useful increase in leaching from

bitumen waste forms. In some experiments, acceleration was observed but it was accompanied by other undesirable phenomena. For example, elevating the temperature to 40°C provided a slight increase in the rates of release of radionuclides from bitumen specimens, but the increase was not large compared to the intersample variability typical of this solidification agent. This increase can be seen in Figure 6.1 which shows the CFL plotted against time for bitumen specimens containing 40 wt% sodium tetraborate leached at 20°, 40°, and 50°C. Triplicate specimens containing salt can have greater than 20% spread in CFL values even at room temperature. This variability is due to fabrication problems that are inherent to bitumen, such as shrinkage cracks and settling of salt in the molten bitumen. Increasing the temperature to 50°C caused a decrease in the leach rate that will be discussed later.

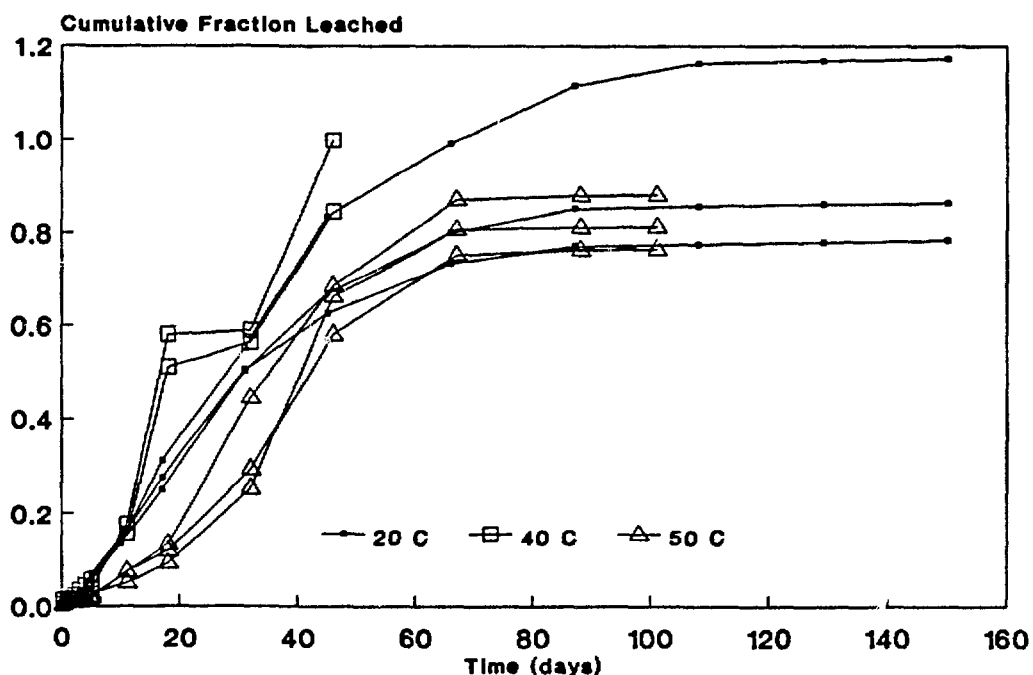


Figure 6.1 Cs-137 cumulative fraction leached vs time from bitumen containing 40 wt% sodium tetraborate at 20°, 40° and 50°C leached in deionized water.

The leach rate of Co-57 was increased by the presence of 100 ppm EDTA (disodium ethylenediamine tetraacetate hexahydrate salt, a strong complexing agent) as shown in Figure 6.2. Similarly, Co-57 leaching was enhanced in groundwater containing natural complexing

agents. However, in these same experiments, the leaching of Cs-137 and Sr-85 was suppressed by the increased ionic strength of the leachant. Increased leachability of Co-57 was caused by the formation of a strong Co-EDTA complex. The incongruent leaching of complexed Co-57 relative to Cs-137 and Sr-85 makes this method of increasing leaching invalid.

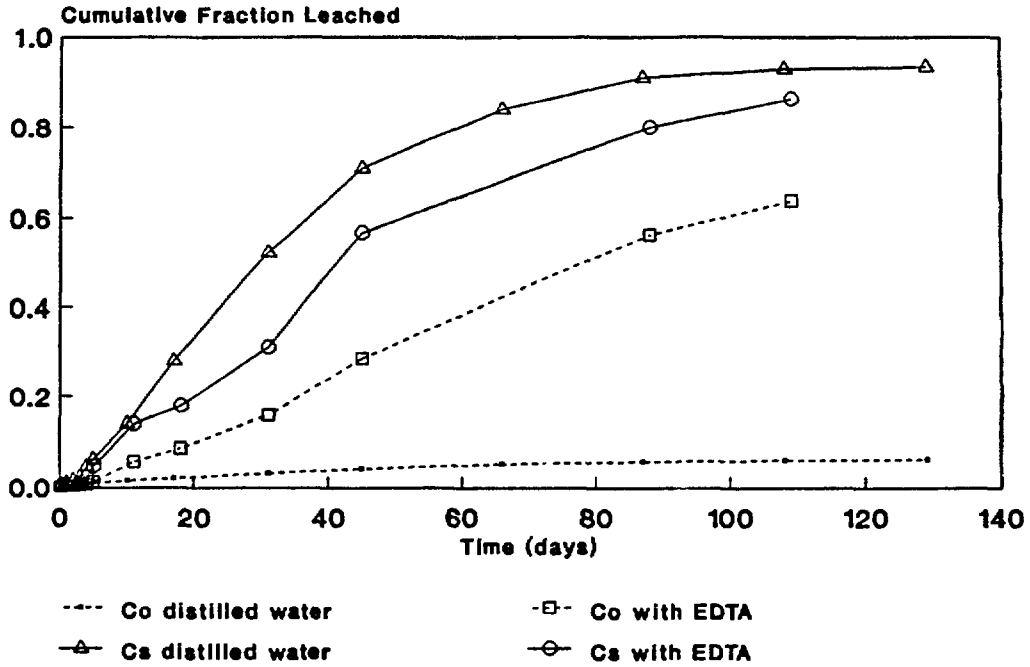


Figure 6.2 Leaching of cobalt is enhanced in a leachant containing 100 ppm EDTA. The cesium releases are slightly suppressed by the presence of additional sodium.

Neither increasing the volume of leachant, nor increasing the sampling frequency (along with changes of leachant) (Figure 6.3) provided acceleration of leaching. Releases from bitumen specimens with high salt loadings (40 wt%) are governed more by the physical condition of the specimen than by suppression caused by increased concentrations of dissolved salt.

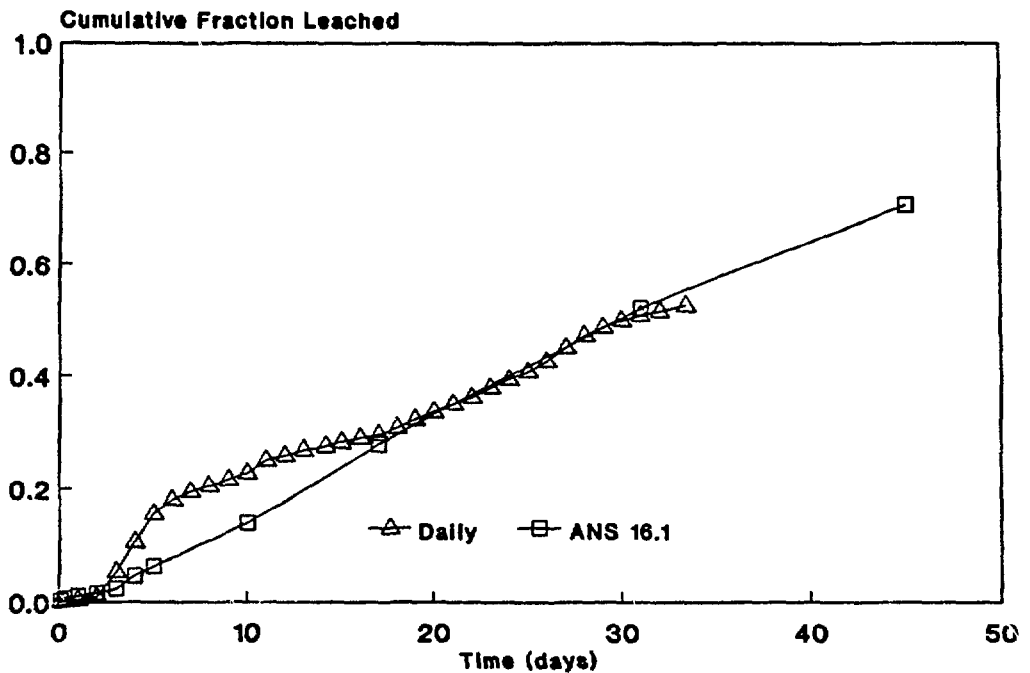


Figure 6.3 Average values of Cs-137 cumulative fraction leached from experiments with daily replacements of leachant and with less frequent replacements.

6.3 Waste Loading

Although waste loading is not an accelerating factor, by investigating leaching as a function of loading, certain facets of the process become apparent. Figure 6.4 shows the cumulative fraction leached of Cs-137 for averages of triplicate specimens with loadings of 0, 20, 30 and 40 wt% of sodium tetraborate. Releases at 0 wt% salt loading were very low; they are barely detectable. At 20 wt%, there was a long period of low release, lasting about one year, followed by a rapid increase in leaching. By 550 days, these specimens leached about 65% of their Cs-137 and were leaching at a very low rate.

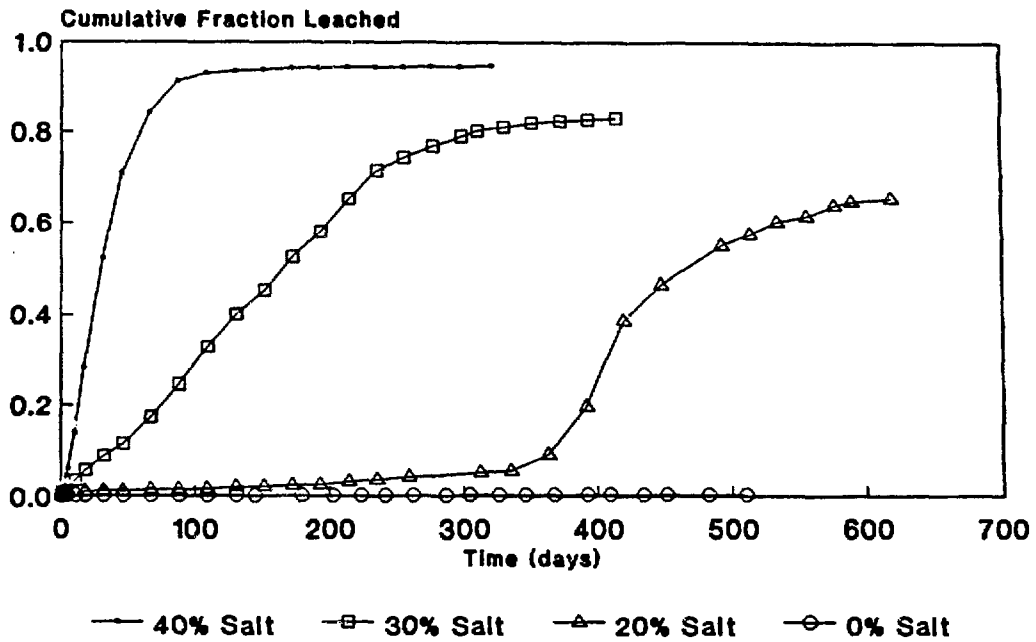


Figure 6.4 Release of Cs-137 from bitumen is related to the amount of salt loading.

Specimens containing 30 wt% salt leached at a low rate for 5 or 6 days (Figure 6.5) and then released Cs-137 in a manner that was linear with time, indicating control by dissolution. These samples stopped leaching at about 80% release. Those specimens containing 40 wt% sodium tetraborate also had an initial period of low leach rate, lasting three days. This period was followed by rapid leaching during which 90% of the activity was leached in about 75 days. No activity was leached after 95% had been released. The rapid phase of leaching, from 4 days to about 50 days, was characterized by a linear release with time.

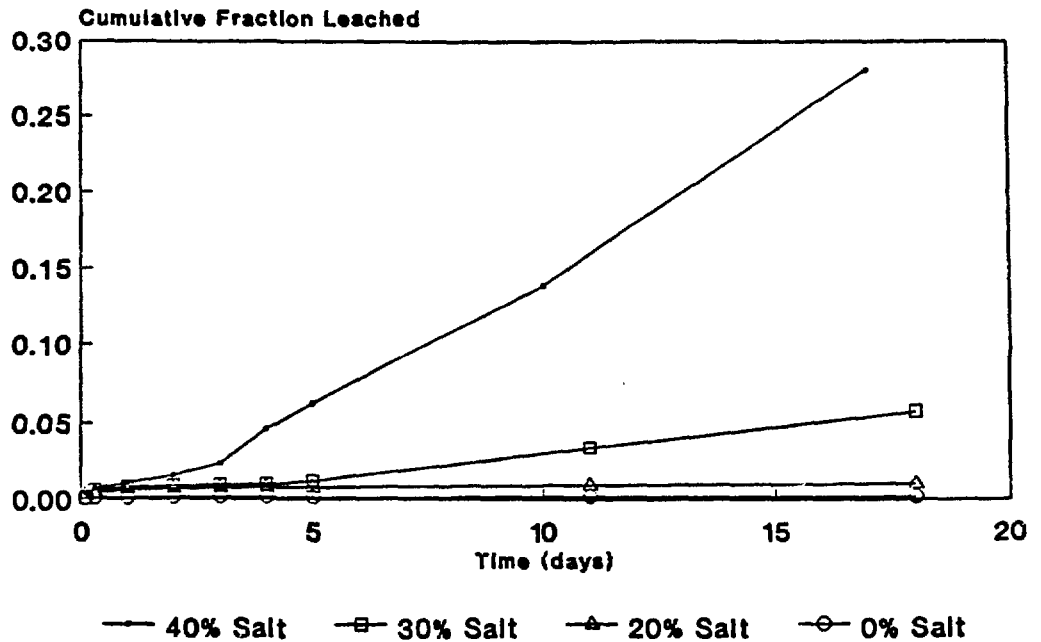


Figure 6.5 Releases of Cs-137 from specimens with various waste loadings during the early portion of the leaching experiment.

Some of this information is condensed in Table 6.1. The duration of the slow leaching is inversely related to leaching as is the time required to reach 50% release of activity. Each loading also has a characteristic fraction release where leaching appears to level off which can be interpreted as the fraction of activity that is not available to leaching. This relationship of loading to CFL also has an approximate inverse proportionality to loading.

Table 6.1

Effect of Salt Loading on Leaching of Cs-137 from Bitumen Waste Forms

Waste Loading (wt%)	Duration of the Slow Leaching Phase (days)	Time to 50% Release (days)	% Cs-137 Retained
0	> 510	> 510	> 95
20	185, 350, 410*	450	35
30	5, 5, 6*	170	20
40	3, 3, 3*	30	6

*Data from triplicate specimens

Leaching behavior of Sr-85 and Co-60 is quite different than that of Cs-137. Sr-85 leaching is limited to about 200 days because of radioactive decay of this short-lived isotope ($t^{1/2}=65$ days). While Sr-85 releases from the 40 wt% loaded specimens were comparable to those of Cs-137, releases at 20 and 30 wt% were much lower (Figure 6.6). Releases of Co-60 are much lower than for Cs-137. The 40 wt% specimens leached Co-60 the fastest for 100 days and then stopped leaching at CFL=0.05 (5% release). After 400 days, cobalt from the 20 wt% specimens began to leach rapidly but leveled off at about CFL=0.22. None of the specimens at other loadings had similar behavior (Figure 6.7)

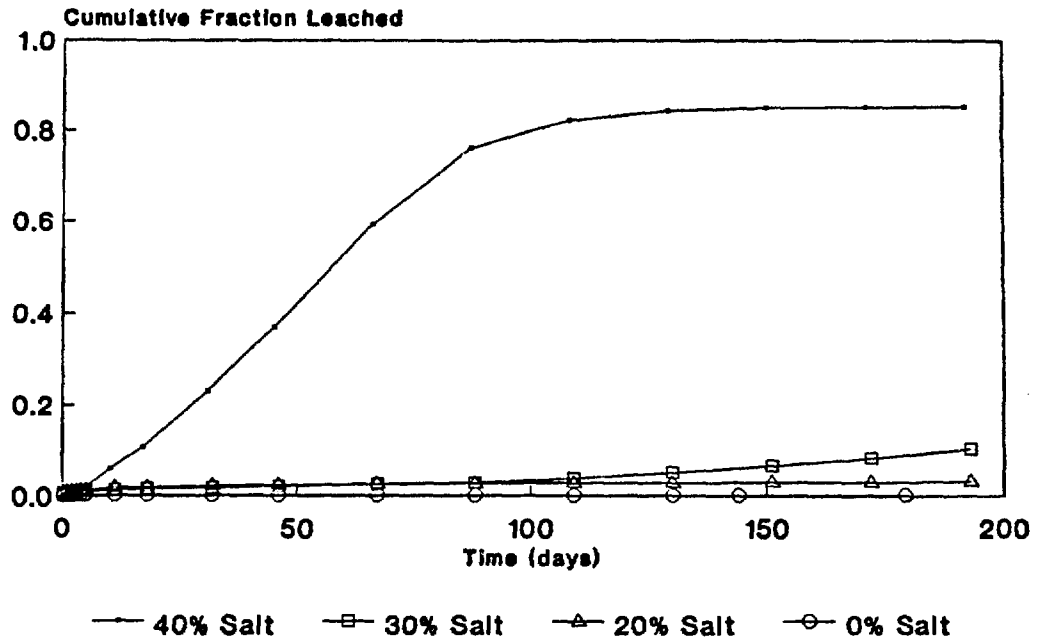


Figure 6.6 While leaching of Sr-85 from specimens containing 40 wt% salt was comparable to Cs-137, releases from the 20 wt% and 30 wt% specimens was lower.

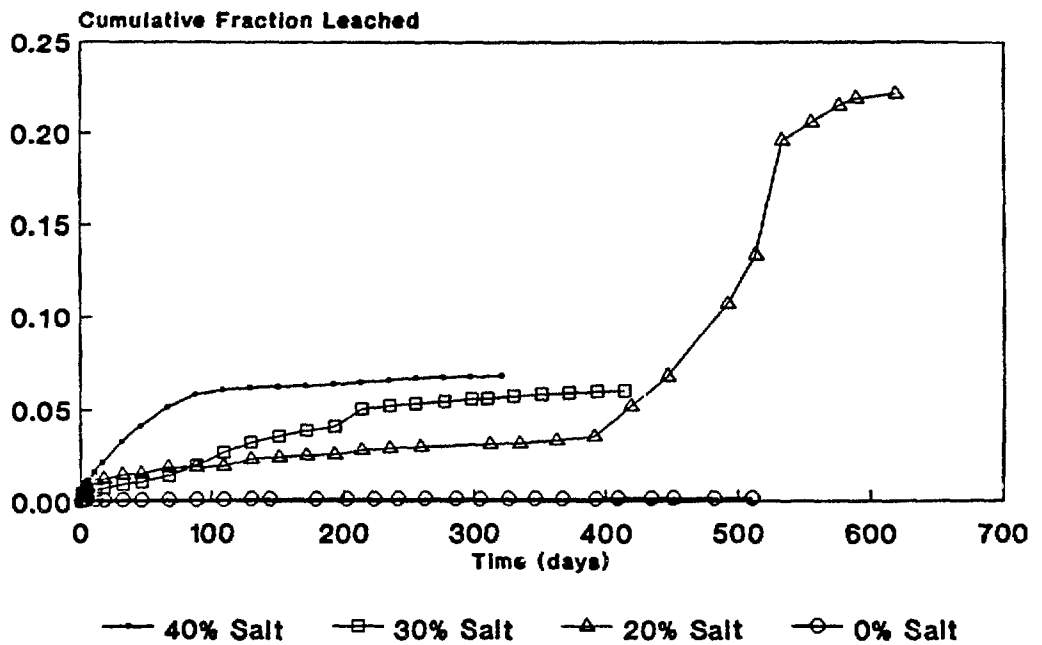


Figure 6.7 Releases of cobalt are much lower than for Cs-137 and Sr-85, but are systematic with loading up to 400 days.

There are several possible explanations for this type of behavior. One may be poor mixing of radionuclides into the molten bitumen, but this is unlikely; because of checks made during production of the specimens. The most likely explanation is that cobalt and strontium are reacting with the bitumen. This could be an ion exchange mechanism, but other researchers have shown that ion exchange is not a significant process for bitumen. Another possibility is that at the elevated temperatures of the melt, organic degradation products of heated bitumen are reacting with the tracers and inhibiting their release into water. This would not be the case for Cs-137, which is less likely to form organic associations. The pH of bitumen leachates averages around 9 (Figure 6.8), which is too low for cobalt to form the hydroxide.

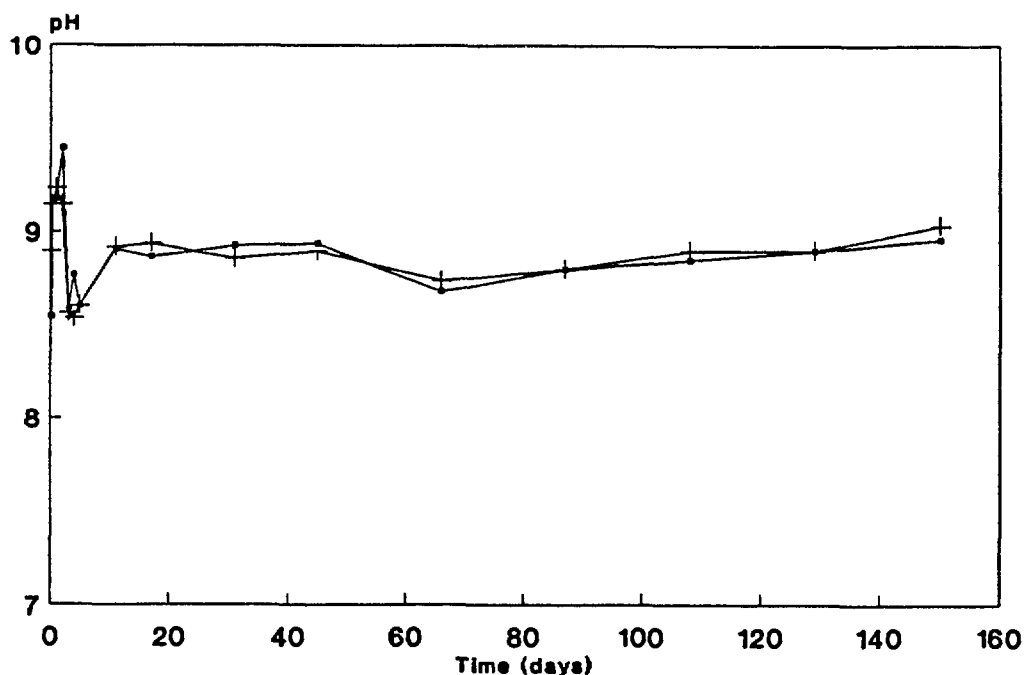


Figure 6.8 Values of pH of leachates are typically around 9 at 20°C. Data is for bitumen containing 30 wt% sodium tetraborate.

6.4 Mechanisms of Leaching

Mechanisms of leaching of bitumen waste forms are described by several authors in various ways based on leaching results and on solid phase analysis. In one early report, leach rates from sodium nitrate wastes solidified in bitumen were described as being a function of the solubility of the solids in water [38]. This interpretation was based on the steady state leach rate that developed after about 140 days. In another paper, the mechanism of leaching was interpreted as being diffusion-controlled [39]. More recently, the leaching behavior of bitumen waste forms was described in terms of diffusion plus a time-dependent absorption term [40]. In this case, however, sorption of the radionuclide species of interest was attributed to uptake by the condensate waste that was solidified by the bitumen. Other work with thin films of plain bitumen, in classical diffusion experiments, showed that ion-exchange is of minor importance to transport of radionuclides through bitumen [41]. Although there may be some adsorption of cobalt, this work also demonstrated that migration of ions through bitumen is very slow or does not take place at all. However, water movement, as indicated by tritiated water, is relatively rapid and is characterized by two stages. The first is described by a low diffusion coefficient of $5 \times 10^{-11} \text{ cm}^2/\text{sec}$, which lasts about one week. After that, the coefficient increases to $1.3 \times 10^{-9} \text{ cm}^2/\text{sec}$.

The physical structure of bitumen waste forms must be considered in developing any discussion of the mechanisms of leaching. Bitumen waste forms typically consist of dried particles (typically dried salts) that are encapsulated by a matrix of bitumen. The low thermal conductivity of this material keeps the center of waste forms molten for hours after they are cast. Consequently, some waste forms exhibit settling of particulates, shrinkage cracks and cavities and other defects that can significantly alter the rate of water penetration and radionuclide release. For these reasons, the intersample variability among leached specimens is often high.

A conceptual model of radionuclide releases from concentrated sodium nitrate wastes that were solidified in bitumen was proposed by Brodersen [42] and is described below and depicted in Figure 6.9. Salt grains are assumed to be thoroughly coated with bitumen. As water diffuses

into the waste form, the salt particles it contacts begin to dissolve, forming cells in the bitumen matrix that contain saturated salt solution and solid salt. The salt itself may change to the hydrated form (e.g., $\text{Na}_2\text{SO}_4 \rightarrow \text{Na}_2\text{SO}_4 \cdot 10\text{H}_2\text{O}$) with a volume increase. From this expanding cell, water diffuses to other adjacent salt grains. As water continues to move into the cells containing saturated solutions, the cells expand and the salt concentration decreases. Expansion causes the bitumen layer to stretch around each cell, becoming thinner and eventually rupturing, releasing its dissolved salt.

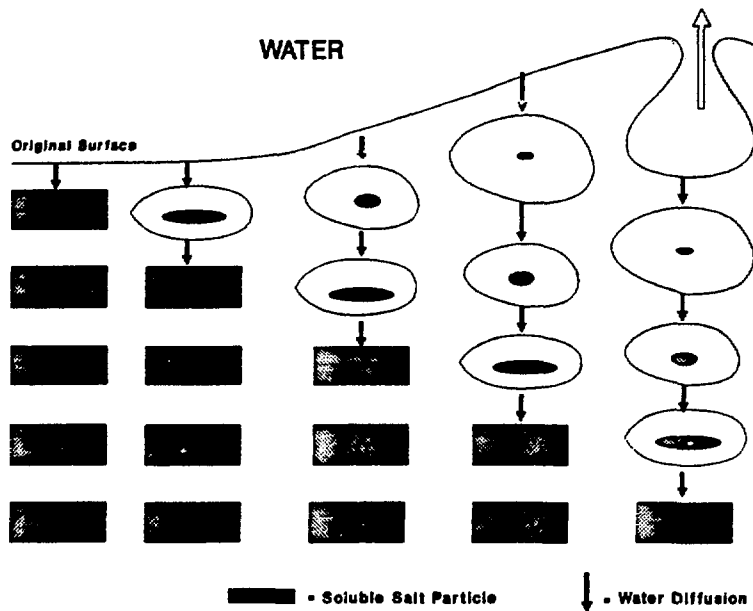


Figure 6.9 Schematic showing the mechanism of leaching of a soluble salt incorporated in bitumen.

Solid phase analysis performed for the accelerated leach tests program confirmed this mechanism, even though our specimens consist of a different salt and a different type of bitumen than those used in the Danish studies. An SEM image (Figure 6.10) shows the surface of an unleached bitumen specimen containing 40 wt% sodium tetraborate. It is smooth and

numerous salt grains show through the bitumen. On careful examination, a few small cracks are visible. After leaching for 320 days in distilled water, the surface is characterized by a blistered appearance caused by the swelling of salt grains (Figure 6.11). In many cases, the blisters burst leaving holes with diameters of 2 to 5 μm . A single, ruptured bitumen blister is also shown at higher magnification (Figure 6.12). A sample from the interior of the same specimen shows a similar morphology (Figure 6.13). The specimen itself failed catastrophically (Figure 6.14).

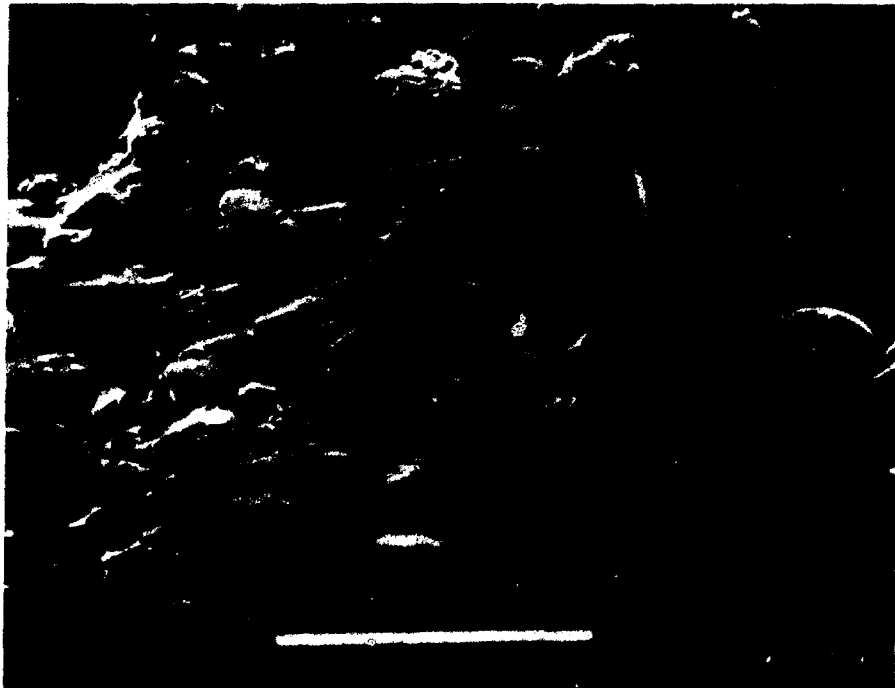


Figure 6.10 An unleached surface of a bitumen specimen containing 40 wt% sodium tetraborate. Outlines of salt grains can be seen.

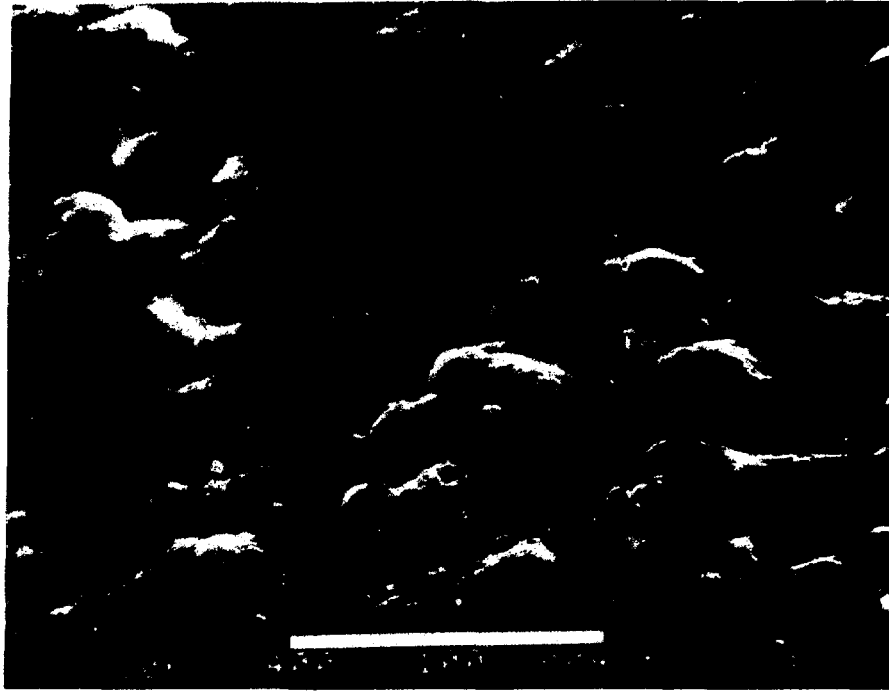


Figure 6.11 After leaching, the surface of a 40 wt% loaded bitumen specimen is characterized by swelling and burst blisters where the saturated salt solution broke through the bitumen.

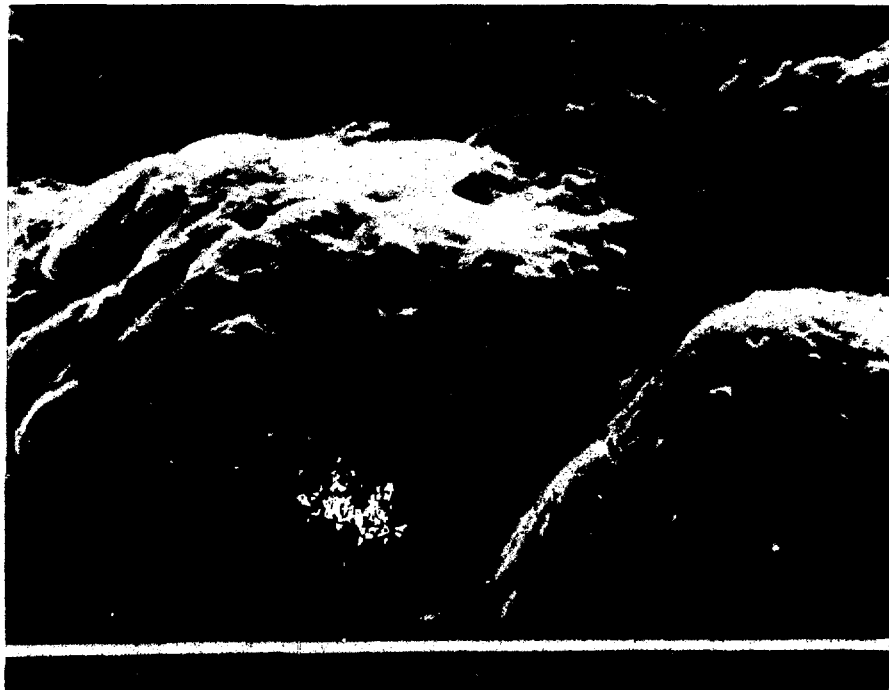


Figure 6.12 At a magnification of 1000 times, a single blister with numerous holes illustrates how saturated salt solution is leached.



Figure 6.13 An interior sample from the same leached specimen (Figure 6.10) shows that the same process operates inside the form. It is not just a surficial phenomenon.

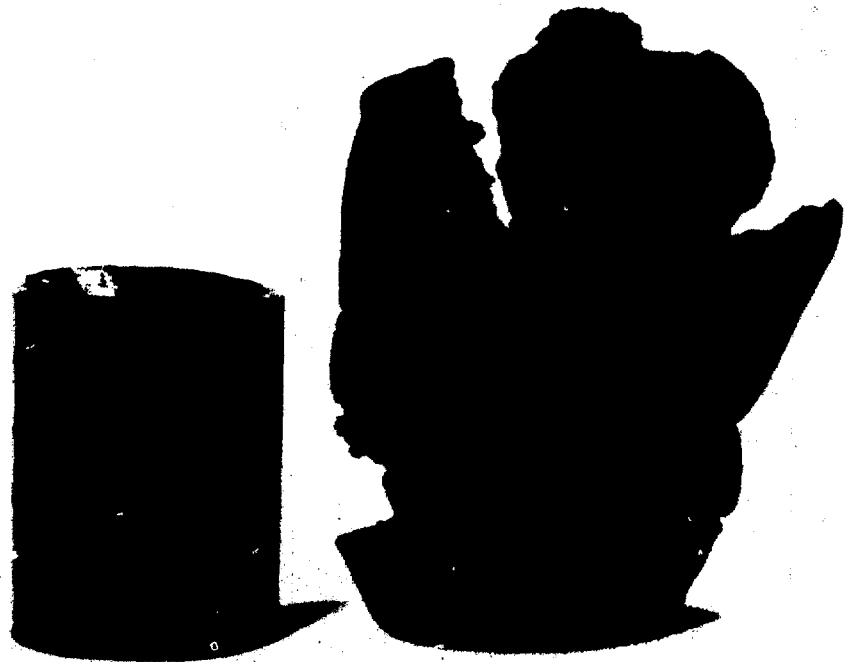


Figure 6.14 Bitumen forms containing 40 wt% sodium tetraborate. The one at left is as fabricated. The one at right was leached for 320 days in deionized water at 20°C. Samples were 4.8 cm diameter by 6.5 cm high right cylinders.

Bitumen is a thermoplastic material that becomes quite fluid as temperatures of about 110°C are approached. Even at 50°C, bitumen specimens deform slightly. The decrease in leachability at 50°C, discussed earlier, can be explained as a self-sealing process. With its increased flow at elevated temperatures, the bitumen around the swelling salt tends to fall back into a few of the holes that open up. This restricts some of the conduits that would be open at lower temperatures. The processes described above result in a two-step form for typical leaching curves showing cumulative fraction release versus time. The two leaching regimes of bitumen (shown in Figure 6.15) are A) a slow release and B) a later, more rapid release.

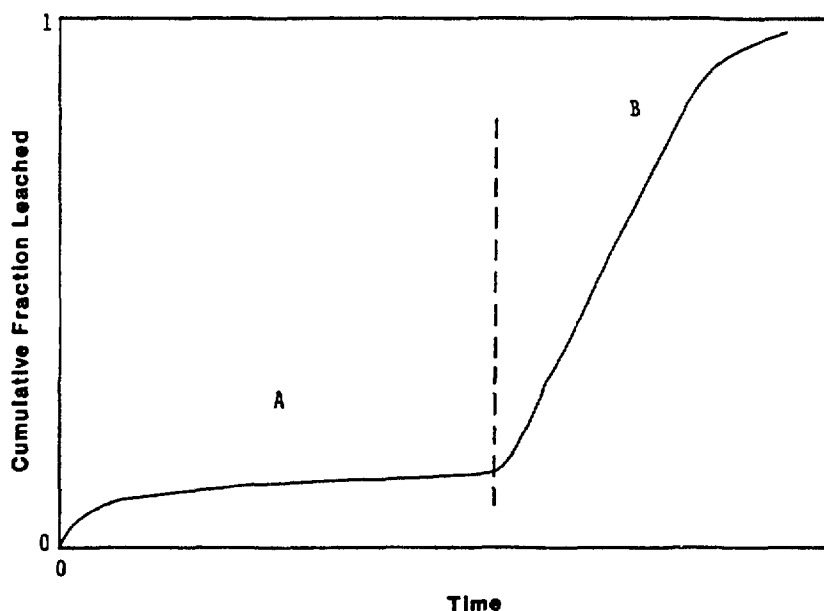


Figure 6.15 Schematic model of expected leaching behavior of bitumen waste forms incorporating soluble waste and/or waste which swells upon hydration. The dashed vertical line separates Region A, in which no swelling has occurred, and Region B, in which there has been enough water uptake to cause swelling. The leach rate increases markedly with swelling.

The slow release regime is not necessarily characterized by a diffusion mechanism but is dependent on the rate that water penetrates the bitumen itself. This rate, expressed as an effective diffusivity, is in the order of 10^{-8} cm²/sec [41] or 3×10^{-4} cm/day when expressed as a penetration rate. The duration of the slow leaching regime is controlled by the thickness of the bitumen layer at the surface of the waste form and by the physical characteristics of that layer, such as microcracks and voids due to shrinkage. There is an approximate relationship between the length of time that this slow leaching period lasts and the waste loading of the specimen. This data is given in Table 6.1.

The second leaching regime typical of bitumen waste forms is characterized by a distinct increase in leach rate. This increase is initiated over a short time period: less than one day at higher waste loadings and continues until the specimen is depleted. The form of this portion of the leaching curve is quite linear with time, indicating that dissolution may be the operative mechanism.

This two-step process was observed by other researchers who have leached bitumen waste forms [40,41]. Although some authors have explained the mechanisms of leaching of bitumen differently, work in this program and in others show that swelling of the waste within the bitumen matrix is critical in describing release from bitumen specimens.

Brodersen [42] gives an equation for calculating the smallest distance between adjacent particles (h) distributed in a tetrahedral unit cell as:

$$h = d \sqrt[3]{\pi \frac{(1-w) \cdot \frac{P_w}{P_{bit}}}{4.242} - 1}$$

where w is waste loading as described by g waste/g product, and P_w and P_{bit} are the densities of the dry waste particles and the bitumen, respectively. For the sodium tetraborate used to

produce specimens for this program, the grain size was found to average between 20 and 50 μm . Based on the equation given above, a set of curves were generated for particles of 10 to 50 μm diameter, describing the thickness of the bitumen layer as a function of waste loading (Figure 6.16). Leaching becomes very rapid at waste loadings between 20 and 30 wt%, which corresponds to layer thicknesses of about 30 μm . Water penetration rates of 3×10^{-4} cm/d were measured for mexphalte 40/50 [43]. At this rate, water would require 10 days to penetrate a typical layer, but we observed that the onset of rapid leaching occurs in half that time (4 to 6 days). This amount of time, however, is appropriate if one considers that the average layer thickness at the surface of the waste forms is about half the thickness between grains that are within the specimen. If the intergrain film thickness of bitumen is a critical factor, then the diameter of the waste particles is also important and these calculations show that small diameter (>10 or $20 \mu\text{m}$) particles are more detrimental to a waste form than larger particles.

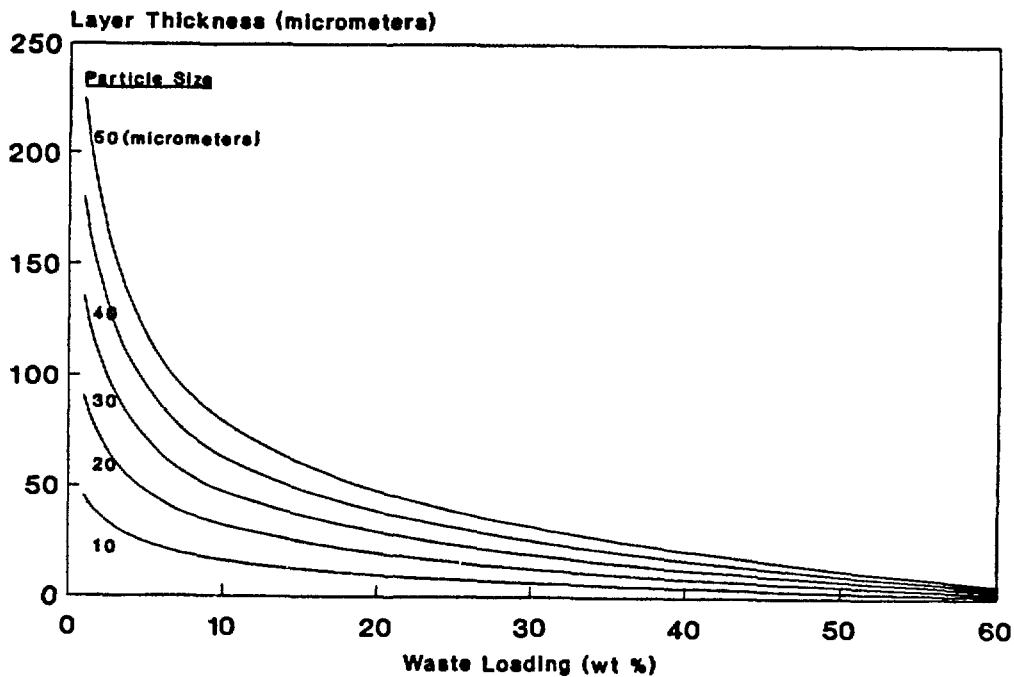


Figure 6.16 Layer thickness between salt particles is shown as a function of waste loading and particle size. Specimens with loadings of 30 wt% and 40 wt% begin the rapid leaching phase within 4 to 6 days of the start of an experiment indicating that a layer thickness of $30 \mu\text{m}$ is critical to waste form performance in the short term.

6.5 Modeling

Leaching of Cs-137 from bitumen that contains no soluble salt, just bitumen and radioactive tracers, can be modeled by the finite cylinder model starting about 30 days following the beginning of a leaching experiment (Figure 6.17). The diffusion coefficient for this curve is $1.6 \times 10^{-14} \text{ cm}^2/\text{s}$ and is used to fit data taken at 3-week intervals. When a soluble salt is mixed with bitumen, the leaching curves cannot be modeled by simple diffusion. The type of leaching behavior exhibited in Figures 6.4 through 6.7 is non-Fickian in nature (see Section 3). Consequently, modeling approaches other than diffusion are required. A model that employs a moving boundary may be useful and needs to be explored further. In addition, as discussed earlier in this section, there is some evidence that reactions with bitumen are affecting the leaching of Sr-85 and Co-57. If this is so, another factor must be considered in the model.

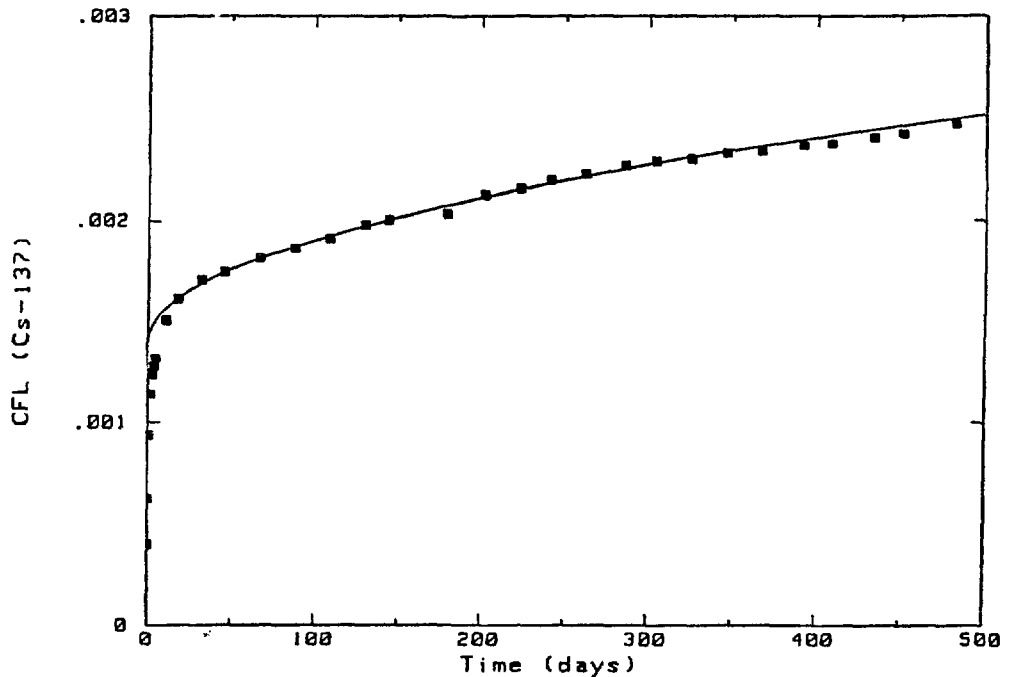


Figure 6.17 CFL versus time for Cs-137 leached from neat bitumen in deionized water at 20°C. The solid line represents the finite cylinder calculation for a D_e of $1.6 \times 10^{-14} \text{ cm}^2/\text{s}$.

6.6 Conclusions

Leaching from bitumen waste forms, by the physical nature of the solidification agent, cannot be accelerated in a systematic way. Releases from bitumen containing radioactive tracers but no salts can be modeled by the finite cylinder model. However, leaching from bitumen waste forms containing sodium tetraborate is non-Fickian and cannot be modeled in the same way. The leaching mechanism of bitumen is related to waste loading, and electron microscopy has confirmed the hypothesis from the literature regarding the physical manner in which leaching takes place.

7. VINYL ESTER-STYRENE CONTAINING SODIUM SULFATE SALT

7.1 Introduction

A proprietary vinyl ester-styrene has been used at nuclear power plants to solidify radioactive waste. This material, known as the Dow Binder (a product of Dow Chemical Company), is a thermosetting polymer that immobilizes the waste by encapsulating it in a plastic matrix. The solidification process includes three or four components such as the binder, a catalyst, a promoter, and (in some processes) an emulsifier or a wetting agent. The latter component is used when a liquid waste is processed. Polymerization is started by adding a catalyst to the waste/binder mixture. A promoter is later added and polymerization is complete in approximately one hour. The waste does not take part in the reactions, although polymerization is sometimes inhibited by certain waste components.

7.2 Modeling and Mechanisms of Leaching

The polymer matrix itself has a very low leachability. Vinyl ester-styrene specimens containing only radioactive tracers have such a low leach rate that no statistically significant releases were observed, corresponding to a diffusion coefficient less than 10^{-14} cm²/s. Electron microscope images show no porosity in this material down to about 1 μm. Therefore, transport presumably takes place by diffusion through the solid.

When waste is added to the system in the form of a solid salt, the process of leaching changes. For example, by adding 40 wt% sodium sulfate, the leach rate increases by a factor of 200-300. The salt forms a network through which water can enter as the salt is dissolved. The presence of salt changes the leaching mechanism from diffusion through a solid to diffusion through a porous medium. In this case, leaching behavior should be related to waste loading. This is demonstrated in Figure 7.1 where releases of Cs-137 are greater for higher waste loadings.

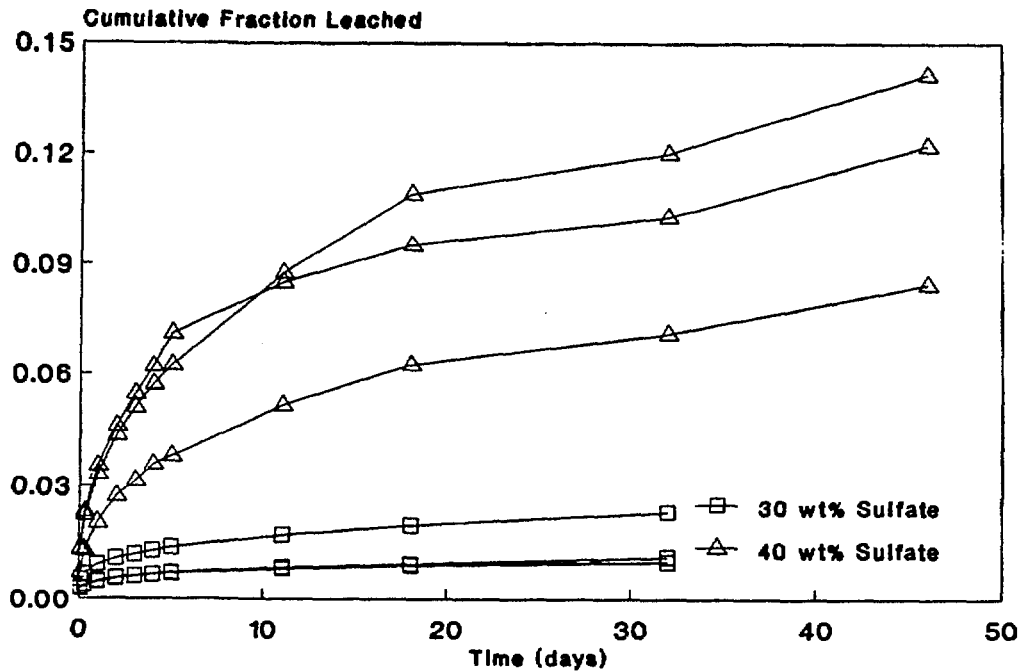


Figure 7.1 Releases of Cs-137 from VES are related to the loading of a sodium sulfate salt, with significant scatter in leaching data for higher loadings.

Leaching results for VES containing 20 wt% salt can be modeled very well by the finite cylinder model (Figure 7.2), as can specimens containing 40 wt% sodium sulfate (Figure 7.3). However, the latter specimens show an effect caused by the interval of leachant replacement in which the cumulative fraction leached is suppressed below the modeled curve. In these experiments, where the frequency of replacement becomes as long as three weeks, the data must be modeled by using two diffusion coefficients (Figure 7.4). The first describes leaching during the daily replacements, while the second describes long-term leaching. When replacements were performed daily, the effect of interval was eliminated, and the data and model fit closely (Figure 7.5).

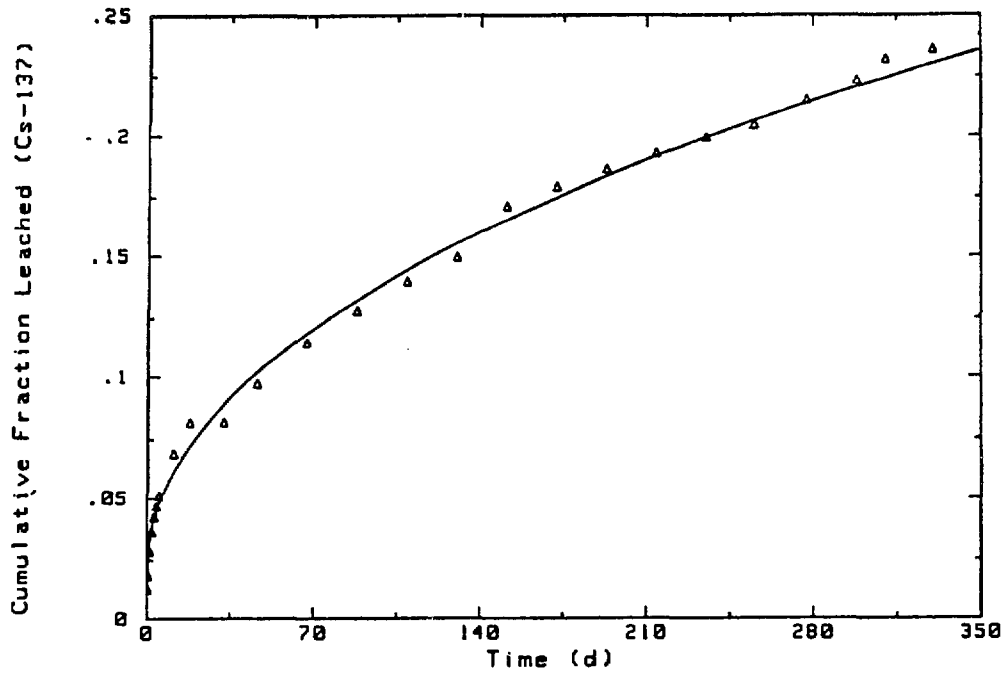


Figure 7.2 Releases from VES containing 20 wt% salt can be modeled by a single diffusion coefficient and the finite cylinder model.

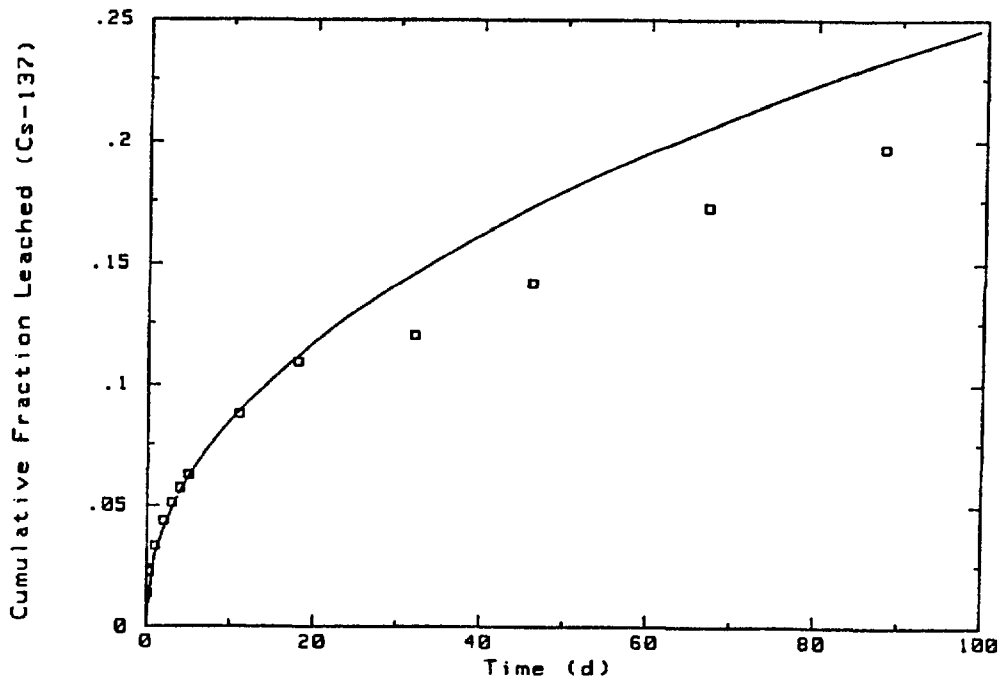


Figure 7.3 Releases from VES containing 40 wt% sodium sulfate can be modeled by the finite cylinder model and a single diffusion coefficient for the first 20 days of the experiment only. After that, the interval of increased leachant replacement appears to inhibit releases.

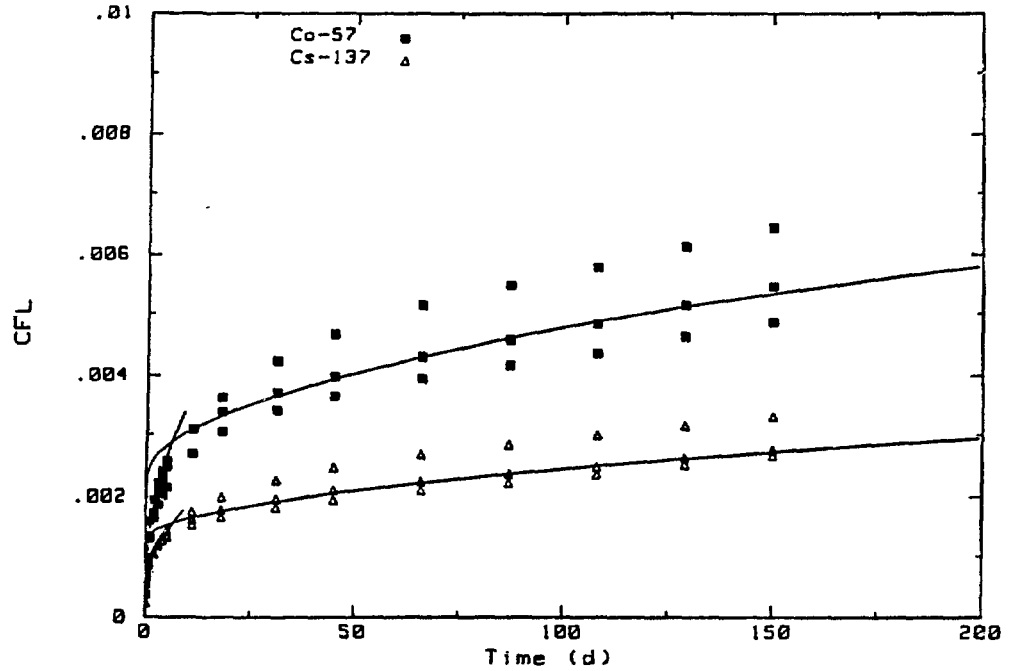


Figure 7.4 Cs-137 releases from specimens that are 10 cm in diameter and 13 cm in height, showing that the finite cylinder model and two diffusion coefficients can accurately model the data.

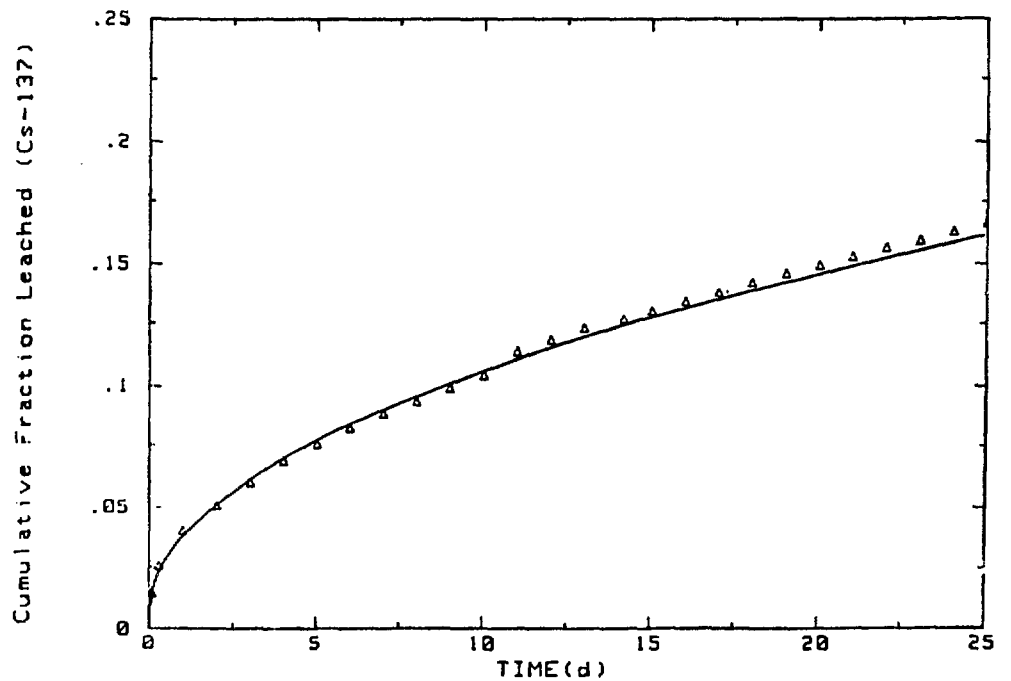


Figure 7.5 Cs-137 releases from VES containing 40 wt% salt during an experiment with daily replacements of the leachant. The finite cylinder model fits the data accurately.

7.3 Single Factors that Accelerate Leaching

7.3.1 Temperature. Leaching of vinyl ester-styrene wastes is accelerated by elevated temperatures. Releases of Cs-137 at 20°, 40°, and 50°C (Figure 7.6) show significant increases with higher temperatures. The Arrhenius plot of diffusion coefficients calculated from this data (Figure 7.7) shows a linear response to increased temperature. Conducting the tests at 50°C gave an acceleration factor of 11 over results at 20°C.

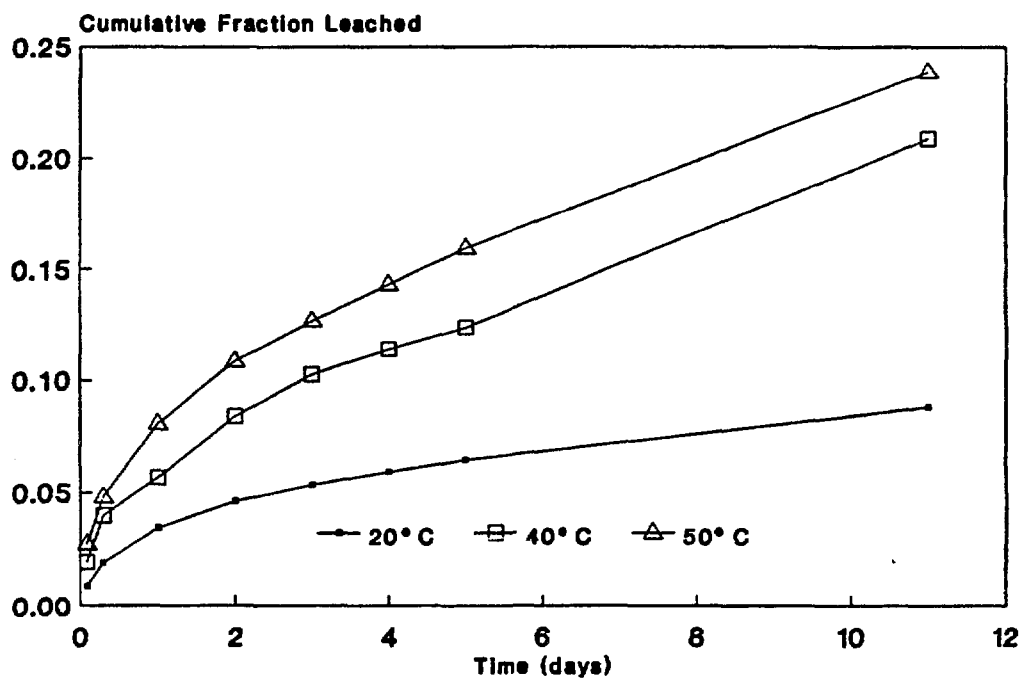


Figure 7.6 Average releases of Cs-137 at 20°, 40°, and 50°C during the first 11 days of leaching for VES waste forms containing 40 wt% sodium sulfate.

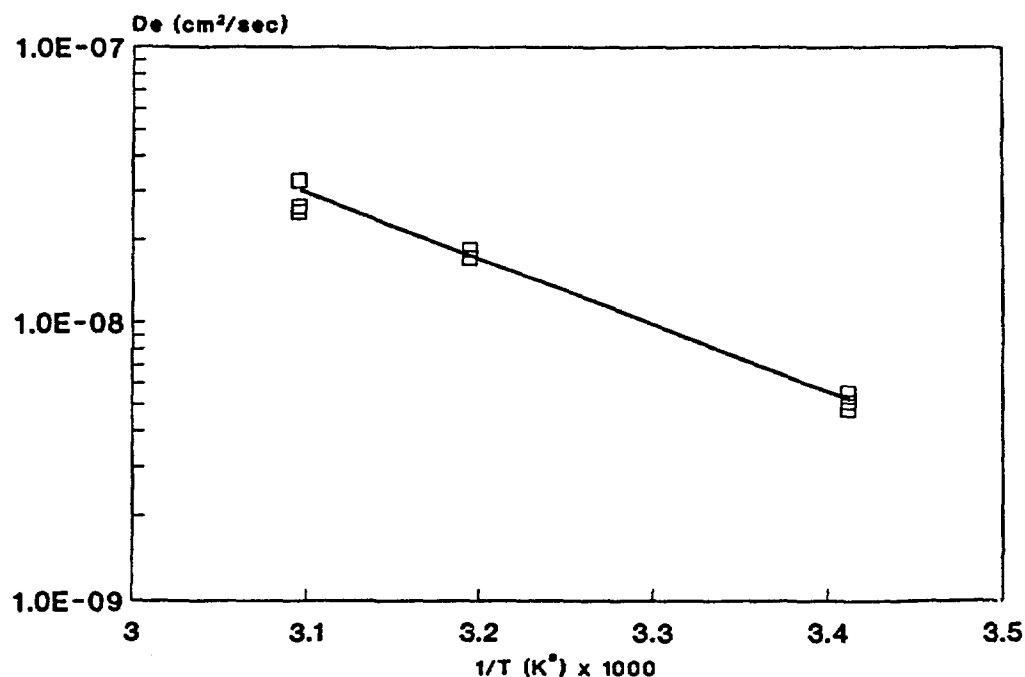


Figure 7.7 Arrhenius plot of diffusion coefficients for VES leached at 20°, 40° and 50°C. These specimens contained 40 wt% sodium sulfate.

7.3.2 Size. With any material that leaches by diffusion, leaching is more rapid from a small specimen than from a large one. The ratio of waste form volume to surface area (V/S) can be used to normalize releases from specimens of various sizes. Figure 7.8 shows the cumulative fraction leached for specimens of several sizes with the smallest leaching the fastest. As with the effects of temperature, the results from the early part of the test are the most ordered. When the intervals of leachant replacement become longer, the data becomes more scattered.

7.3.3 Volume of Leachant. Increased volume of leachant has a small but significant effect on leaching. As can be seen by comparing Figure 7.3 with Figure 7.5, increased leachant replacement provided about 25% increase in release. More importantly, the data that was not suppressed by experimental conditions fit the finite cylinder model.

Releases at 20°C do not require much larger volumes of leachant, but at elevated temperatures this factor must be included.

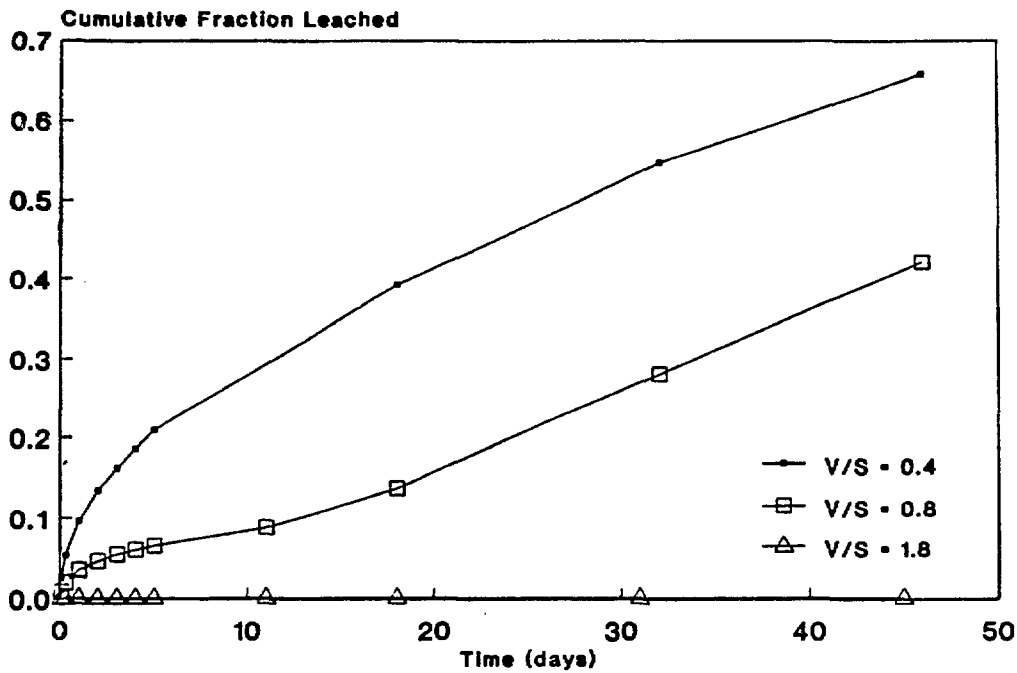


Figure 7.8 Average releases of Cs-137 from three different sized specimens of VES containing 40 wt% sodium sulfate.

7.4 Combined Acceleration Factors

Several combinations of acceleration factors were experimentally investigated and the diffusion coefficients are reported in Tables 7.1, 7.2 and 7.3 for each isotope studied.

Table 7.1

Diffusion Coefficients for Cs-137
for Vinyl Ester-Styrene + 40 wt% Sodium Sulfate

Leach Test	Volume (liters)	Temperature (°C)	Size D x H ¹ (cm)	Average D _e , Cs-137 (cm ² /sec)
Semidynamic	1.3	20	5 x 7	5.2 x 10 ⁻⁹
Semidynamic (daily)	1.3	20	5 x 7	5.8 x 10 ⁻⁹
Semidynamic	6.5	20	5 x 7	3.6 x 10 ⁻⁹
Semidynamic	6.5	60	5 x 7	2.0 x 10 ⁻⁸
Semidynamic	0.3	50	2.5 x 2.5	1.6 x 10 ⁻⁸
Semidynamic	1.3	60	5 x 7	1.2 x 10 ⁻⁸
Static	6.5	60	5 x 7	1.7 x 10 ⁻⁸

1 = right cylinder
D = diameter
H = height

Table 7.2

Diffusion Coefficients for Sr-85
for Vinyl Ester-Styrene + 40 wt% Sodium Sulfate

Leach Test	Volume (liters)	Temperature (°C)	Size D x H ¹ (cm)	Average D _e , Sr-85 (cm ² /sec)
Semidynamic	1.3	20	5 x 7	2.9 x 10 ⁻⁸
Semidynamic (daily)	1.3	20	5 x 7	7.1 x 10 ⁻⁹
Semidynamic	6.5	20	5 x 7	3.4 x 10 ⁻⁹
Semidynamic	6.5	60	5 x 7	7.7 x 10 ⁻⁸
Semidynamic	0.3	50	2.5 x 2.5	9.7 x 10 ⁻⁹
Semidynamic	1.3	60	5 x 7	4.1 x 10 ⁻⁸
Static	6.5	60	5 x 7	5.6 x 10 ⁻⁸

1 = right cylinder

D = diameter

H = height

Table 7.3

Diffusion Coefficients for Co-57
for Vinyl Ester-Styrene + 40 wt% Sodium Sulfate

Leach Test	Volume (liters)	Temperature (°C)	Size D x H ¹ (cm)	Average D _e , Co-57 (cm ² /sec)
Semidynamic	1.3	20	5 x 7	1.3 x 10 ⁻⁸
Semidynamic (daily)	1.3	20	5 x 7	4.3 x 10 ⁻⁹
Semidynamic	6.5	20	5 x 7	2.6 x 10 ⁻⁹
Semidynamic	6.5	60	5 x 7	2.4 x 10 ⁻⁸
Semidynamic	0.3	50	2.5 x 2.5	1.0 x 10 ⁻⁸
Semidynamic	1.3	60	5 x 7	1.5 x 10 ⁻⁸
Static	6.5	60	5 x 7	2.7 x 10 ⁻⁸

1 = right cylinder

D = diameter

H = height

By combining elevated temperatures with different volumes of leachant, the effect and sensitivity of these two factors can be investigated. Releases of radionuclides at 60°C were identical for static and semidynamic tests (Figure 7.9). The static experiment used 6.5 liters while the semidynamic test used a total of 71.5 liters, with results that cannot be distinguished from each other. Similar results are seen for Sr-85 and Co-57. Semidynamic tests using small quantities of leachant (1.3 liters instead of 6.5 liters) gave similar results. The data from the two experiments overlapped each other.

Comparing the data from the semidynamic experiment run at 60°C and 6.5 liters of water used at each replacement with a similar experiment run at 20°C, a clear difference is seen (Figure 7.10). These data show an acceleration factor of 17.

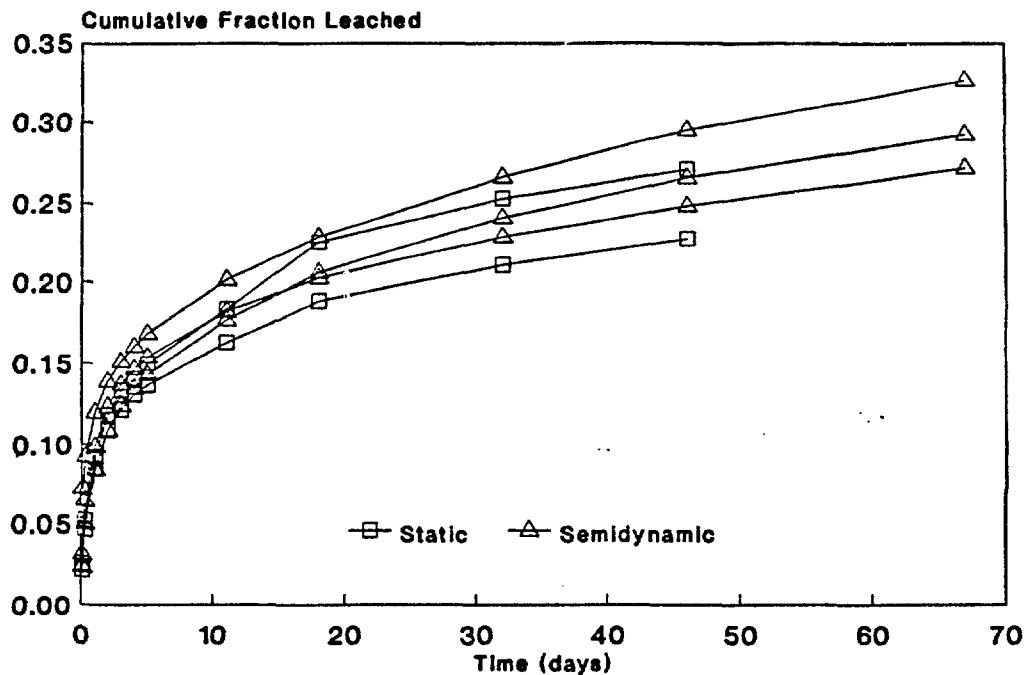


Figure 7.9 Releases of Cs-137 from VES/sodium sulfate at 60°C from static and semidynamic tests are not statistically different from each other.

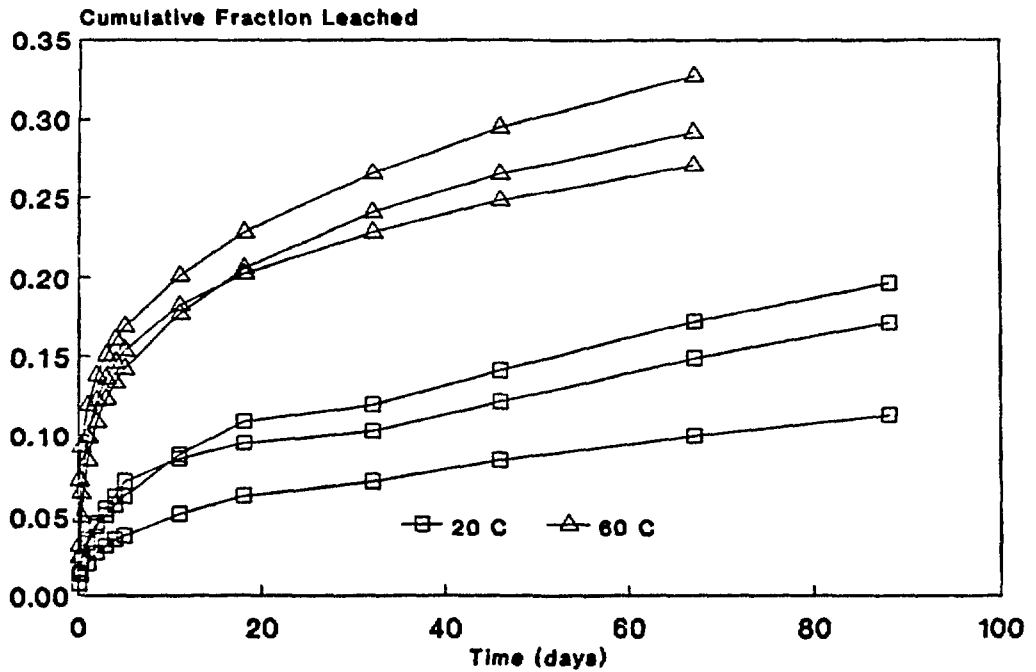


Figure 7.10 Leaching of Cs-137 in semidynamic tests using 6.5 liters of water at each interval showed relatively uniform behavior and a definite temperature effect.

Releases from the experiments run at 20°C and 60°C using 6.5 liters of water are diffusion controlled. The finite cylinder model fits this data during intervals of daily replacement (Figure 7.11), but overestimates releases during the longer intervals of replacement. This deviation probably can be corrected by daily replacements of leachant. Consequently, diffusion appears to be the release mechanism for these two sets of data up to at least 7 days.

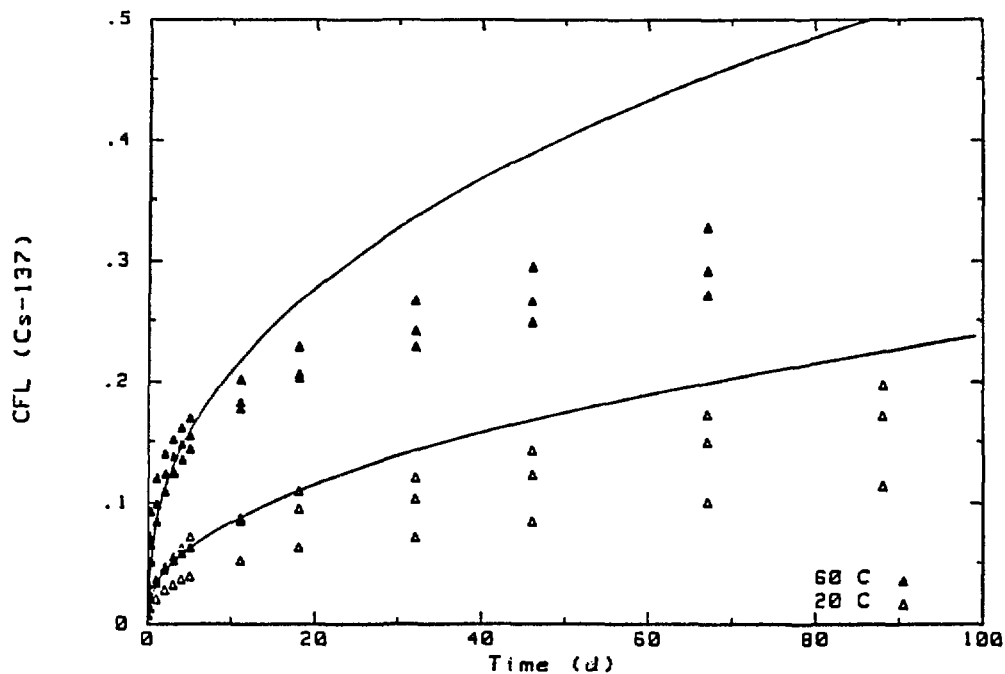


Figure 7.11 The finite cylinder model fits data from experiments run at 60° and 20°C, during the daily replacements of leachant. When the intervals of replacement are longer, the model overestimates releases.

7.5 Conclusions

Leaching of 5 x 7 cm VES/sodium sulfate waste forms can be accelerated by increasing temperature to 60°C and by using 6.5 liters of water for each interval of leachant replacement. This combination of acceleration factors gives a seventeenfold increase in leach rate as measured at 15% release. Leaching from VES waste forms during the initial daily phase of leachant replacement (at loadings of 20, 30 and 40 wt%) is diffusion controlled. This is true at 20°C and at 60°C. Additional experimental evidence is required to determine what factors will provide optimized leaching.

8. CONCLUSIONS

The overall conclusions of the work presented in this topical report are that: 1) accelerated leaching can be achieved for low-level waste forms with acceleration factors as high as 17, 2) the results can often be modeled by diffusion from the finite cylinder, and 3) leaching mechanisms do not change as a result of the accelerated test conditions. These conclusions apply to cement and thermosetting polymer-based waste forms but not to bitumen waste forms. Specific conclusions for each of the materials studied are given below.

8.1 Leaching Cement Containing Sodium Sulfate

Leaching from portland cement containing 5 wt% sodium sulfate as a simulated waste can be optimized by the following conditions: 2.5 x 2.5 cm cylindrical specimen, 50°C and 3 liters of water replaced daily. These conditions give an acceleration factor for both Cs-137 and Sr-85 of approximately 17. Above 50°C, releases of some elements decline, apparently due to changes in the structure of the cement. The large volume of leachant and daily leachant replacement is required to maximize the release of Sr-85. Leaching of Cs-137 and Sr-85 from cement containing sodium sulfate can be modeled by diffusion theory.

8.2 Portland Cement Containing Incinerator Ash

Releases of radionuclides from portland cement containing 15 wt% incinerator ash as a simulated waste can be accelerated and leaching conditions for this material were optimized. The greatest acceleration for Cs-137 occurs at 50°C (60°C provides no faster release rate) in a semidynamic test with 1.3 liters of water. Increasing the volume of leachant or increasing the frequency of the leachant replacement serves no useful purpose. Smaller sizes provide additional increase in leaching.

The finite cylinder model does not adequately describe leaching processes of Cs-137 from cement/ash waste forms. A model that uses an adsorption term that is a function of time is

required. However, a linear correlation exists between releases at 50°C and at 20°C, indicating that the leaching mechanism is not altered by accelerated leaching.

Sr-85 releases are accelerated by elevated temperatures up to 50°C. At 60°C the leach rate decreases although an increased volume of leachant brings the leach rate up slightly. Leaching of Sr-85 cannot be modeled during the entire leaching process by the finite cylinder model. Although the data and the model agree during the first 5 days of leaching, the model overestimates releases after that time. Linear correlations indicate that the leaching mechanism does not change with accelerated leaching. Consequently, as with Cs-137, a model that contains an adsorption term that is a function of time is required.

Optimum conditions are similar to those for cement containing sodium sulfate: 2.5 x 2.5 cm specimen, 50°C and 3 liters of water replaced daily. With these conditions, acceleration factors for Cs-137 and Sr-85 were 6 and 17, respectively.

8.3 Bitumen Containing Sodium Tetraborate

Leaching of bitumen waste forms cannot be accelerated in any way that provides uniform results. However, the study of this material has provided significant information on the mechanisms of leaching of bitumen containing a soluble salt. Physical processes of leaching were confirmed by Electron Scanning Microscopy. In addition, a complex relationship between waste loading and leaching was observed and discussed in this report.

8.4 Vinyl Ester-Styrene Containing Sodium Sulfate

Leaching of vinyl ester-styrene (VES)/sodium sulfate waste forms can be accelerated by increasing the temperature to 60°C and by using 6.5 liters of water for each interval of leachant replacement. This combination gives an acceleration factor of 17 as measured at 15% release. Leaching of VES containing various loadings of sodium sulfate can be modeled by diffusion theory.

The work presented in this report will lead to the development of an accelerated leach test that is useful for cement-based waste forms and for thermosetting polymers as well. In addition, the combined use of models for leaching and experimental efforts has led to a better understanding of the mechanisms of leaching for cement, polymer and bitumen waste forms.

REFERENCES

1. Dougherty, D.R., R.F. Pietrzak, M. Fuhrmann and P. Colombo, "An Experimental Survey of Factors that Affect Leaching from Low-Level Radioactive Waste Forms," BNL-52125, Brookhaven National Laboratory, Upton, NY, 11973, June 1987, in press.
2. American Nuclear Society, "Measurement of the Leachability of Solidified Low-Level Radioactive Wastes by a Short-Term Test Procedure," ANSI/ANS-16.1, April 1986.
3. McKercher, B.B., C.C. Miller and M.D. Naughton, "Operation Experience of the Palisade Station Volume Reduction System-The First Two Months," from Post (editor) Waste Management 84, Volume 2, Tucson, AZ Symposium, 1984.
4. American Society for Testing and Materials, "Standard Practices for the Measurements of Radioactivity," ASTM Standard D-3648 in 1982 Annual Book of ASTM Standards, Part 31, Water.
5. American Society for Testing and Materials, "Standard Practices for Gamma-Ray Spectrometry," ASTM Standard D-3649, in 1982 Annual Book of ASTM Standards, Part 31, Water.
6. American Society for Testing and Materials, "Standard Practice for Flame Atomic Absorption Analysis," Standard E663, in 1982 Annual Book of ASTM Standards, Part 42, Analytical Methods-Spectroscopy; Chromatography; Computerized Systems.
7. Perkin-Elmer, Analytical Methods for Atomic Absorption Spectroscopy, Perkin-Elmer Corporation, 1982.
8. Greenberg, A.E., J.J. Connors and D. Jenkins, editors, "Alkalinity, Method 403," in Standard Methods for the Examination of Water and Waste Water, 15th edition, American Public Health Association, Washington, DC, 1981.
9. American Society for Testing and Materials, "Standard Test Methods for pH of Water," Standard D-1293 in 1982 Annual Book of ASTM Standards, Part 3, Water.
10. Goldstein, J.I. and H. Yakowinz (editors), Practical Scanning Electron Microscopy, Electron and Ion Microprobe Analysis, Plenum Press, 1975.
11. Dougherty, D.R. and P. Colombo, "Leaching Mechanisms of Solidified Low-Level Waste, The Literature Survey", BNL-51899, 1985.
12. Bowerman, B.S., K.J. Swyler, D.R. Dougherty, R.E. Davis, B.S. Siskind, and R.E. Barletta, Brookhaven National Laboratory, "An Evaluation of the Stability Tests Recommended in the Branch Technical Position on Waste Forms and Container Materials", NUREG/CR-3829, BNL-NUREG-51784, 1984.

REFERENCES - continued

13. Godbee, H.W. and D.S. Joy, "Assessment of the Loss of Radioactive Isotopes from Waste Solids to the Environment. Part I: Background and Theory," ORNL-TM-4333, Oak Ridge National Laboratory, Oak Ridge, TN, 1974.
14. Côté, P.L., T.W. Constable and A. Moreira, "An Evaluation of Cement-Based Waste Forms Using the Results of Approximately Two Years of Dynamic Leaching," Nuclear and Chemical Waste Technology, Volume 7, pp. 129-139, 1987.
15. Crank, J., "The Mathematics of Diffusion", Clarendon Press, Oxford, 1975.
16. Carslaw, H.S. and J.C. Jaeger, "Conduction of Heat in Solids", Clarendon Press, Oxford, 1959.
17. Godbee, H.W., E.L. Compere, D.S. Joy, A.H. Kibbey, J.G. Moore and C.W. Nestor, Jr., O.U. Anders, R.M. Neilson, Jr., "Application of Mass Transport Theory to the Leaching of Radionuclides from Waste Solids", Nuclear and Chemical Waste Management, Vol. 1, pp 29-35(1980).
18. Nestor, Jr., C.W., "Diffusion from Solid Cylinders", ORNL CSD/TM-84, Oak Ridge National Laboratory, Oak Ridge, TN, 1984.
19. Fuhrmann, M. and P. Colombo, "Leaching Induced Concentration Profiles in the Solid Phase of Cement," in: Symposium Volume on Environmental Aspects of Stabilization/Solidification of Hazardous Wastes: American Society for Testing and Materials, 1987, in press.
20. Kienzler, B., E. Korthaus and R. Koster, "Modellrechnungen zum Korrosions-Und Auslanguerhalten Von zementierten Abfallprodukten," KFK 3612, November 1983.
21. Nimnual, S., Application of Multi-Group Diffusion Theory to Mechanistic Modeling of Leaching Behavior of Solidified Low-Level Radioactive Waste Forms, Dissertation, The University of Arizona, 1986.
22. Amarantos, S.G. and J.H. Petropoulos, Certain Aspects of Leaching Kinetics of Solidified "Radioactive Wastes" - Laboratory Studies, Greek AEC, DEMO 81/2, January 1981.
23. Jantzen, C.M., "Radioactive Waste-Portland Cement Systems: II, Leaching Characteristics," Journal of the American Ceramic Society, 67(10), 674-78, 1984.
24. Hespe, E.D., "Leach Testing of Immobilized Radioactive Waste Solids, A Proposal for a Standard Method," Atomic Energy Review, Volume 9, pp. 195-207, 1971.

REFERENCES - continued

25. Croney, S.T., "Leachability of Radionuclides from Cement Solidified Waste Forms Produced at Operating Nuclear Power Plants", NUREG/CR-4181, EGG-2355, EG&G Idaho, Inc., 1985.
26. Arora, H. and R. Dayal, "Solidification and Leaching of Boric Acid and Resin LWR Wastes, Topical Report", NUREG/CR-3909, BNL-NUREG-51805, Brookhaven National Laboratory, 1984.
27. Matsuzura, H., "Effect of Dimensions of Specimen in Amounts of Cs-137, Sr-90, Co-60 Leached from Matrix of Hardened Cement Grout", Journal of Nuclear Science and Technology, 15,4, April 1978, pp 296-301.
28. Double, D.D. and A. Hellawell, "The Solidification of Cement," in Scientific American, Volume 237, No. 1, p. 82-90, July 1970.
29. Brunauer, S. and L.E. Copeland, "The Chemistry of Concrete," Scientific American, Vol. 210, pages 81-92, April 1964.
30. Fuhrmann, M., R. Pietrzak, D. Dougherty and P. Colombo, "Progress in Development of an Accelerated Leach Test for Low-Level Radioactive Waste Forms," in: Proceedings of the Ninth Annual DOE Low-Level Waste Management Conference, Session III, Performance Assessment, CONF-870859, February 1987.
31. Fuhrmann, M. and P. Colombo, "Radionuclide Releases from Cement Waste Forms in Seawater," in Interim Oceanography Description of the Atlantic Disposal Site for Radioactive Waste, Volume 3, Nuclear Energy Agency, Paris, France, in press.
32. Barth, E.J., Asphalt Science and Technology, Gordon and Breach Science Publishers, NY, 1962.
33. ASTM P312-78, Standard Specification for Asphalt Used in Roofing, in Annual Book of ASTM Standards, Part 15, American Society for Testing and Materials, 1986.
34. International Atomic Energy Agency, Conditioning of Low- and Intermediate-Level Radioactive Wastes, Technical Report Series No. 222, Vienna, Austria, 1983.
35. International Atomic Energy Agency, Bitumenization of Radioactive Wastes, Technical Report Series No. 116, Vienna, Austria, 1970.
36. Organization for Economic Cooperation and Development, The Bitumenization of Low and Medium-Level Radioactive Wastes, Proceedings of a Seminar, May 18-19, 1976.

REFERENCES - continued

37. Fuhrmann, M., R.M. Neilson, Jr., and P. Colombo, "A Survey of Agents and Techniques Applicable to the Solidification of Low-Level Radioactive Wastes, BNL-51521, Brookhaven National Laboratory, Upton, NY 11973, Dec. 1981.
38. Blanco, R.E., et al., "Recent Developments in Treating Low- and Intermediate-Level Radioactive Wastes in the United States, ORNL-TM-1289, 1965.
39. Dejonghe, P., et al., "Asphalt Conditioning and Underground Storage of Concentrates of Medium Activity," Proc. Int. Conf. Peaceful Uses of Atomic Energy, UN, NY, 1964, 14:343.
40. Burney, S.G., "Comparative Evaluation of α and γ Radiation Effects in a Bitumenisate," Nuclear and Chemical Waste Management, Vol. 7, pp. 107-127, 1987.
41. Brodersen, K. and K. Nilsson, "Mechanisms and Interaction Phenomena Influencing Release in Low- and Medium-Level Waste Disposal Systems," in: Characterization of Radioactive Waste Forms, Progress Report, 1986, EUR 11354 EN.
42. Brodersen, K., "The Influence of Water Uptake on the Long-Term Stability of Conditioned Waste," 1984.
43. Brodersen, K., "Leaching of Bitumenized and Cemented Waste Forms," in: Characterization of Low- and Medium-Level Radioactive Waste Forms, edited by Vejmelka, P. and R.A.J. Sambell